COMPARATIVE STUDY FOR EARTHQUAKE PERFORMANCE OF STEEL BUILDINGS WITH SEISMIC ISOLATOR AND FIXED BASED STEEL BUILDINGS WITH DAMPER

ABDULLAHI ABDIAZIZ ABDI

IŞIK UNIVERSITY
JANUARY, 2022

COMPARATIVE STUDY FOR EARTHQUAKE PERFORMANCE OF STEEL BUILDINGS WITH SEISMIC ISOLATOR AND FIXED BASED STEEL BUILDINGS WITH DAMPER

ABDULLAHI ABDIAZIZ ABDI
Işık Üniversity, School of Graduate Studies Civil Engineering Master Programme
2022

Submitted to the Graduate School of Science and Engineering In partial fulfillment of the requirements for the degree of Master of Science in Civil Engineering

IŞIK UNIVERSITY
JANUARY, 2022

IŞIK UNIVERSITY
LİSANSÜSTÜ EĞİTİM ENSTİTÜSÜ
İNŞAAT MÜHENDİSLİĞİ YÜKSEK LİSANS PRPOGRAMI

COMPARATIVE STUDY FOR EARTHQUAKE PERFORMANCE OF STEEL BUILDINGS WITH SEISMIC ISOLATOR AND FIXED BASED STEEL BUILDINGS WITH DAMPER

ABDULLAHI ABDIAZIZ ABDI

APPROVED BY:

Ass.Prof. Dr.Onder Umut (Thesis advisor)	Işık Üniversitesi
Ass Prof. Dr. Bora Akşar (Member)	Işık Üniversitesi
Ass Prof. Dr. Fatma İlknur Kara (Member)	Gebze Teknik Üniversitesi

APPROVAL DATE 28/01/2022

COMPARATIVE STUDY FOR EARTHQUAKE PERFORMANCE OF STEEL BUILDINGS WITH SEISMIC ISOLATOR AND FIXED BASED STEEL BUILDINGS WITH DAMPER

ABSTRACT

Earthquake causes huge loss of lives and enormous damages to properties every year. In order to understand and avoid such damages, different types of seismic isolators have been used. To get the optimal and effective types of seismic isolators, a comparison study of three same-sized 12-storey steel buildings with conventional steel braced frames, and lead rubber bearing (LRB) fixed-based with fluid viscous dampers (FVD) is conducted and their seismic performance enhancements are evaluated using SAP2000 software.

Researchers suggest that the seismic isolator building can survive seismic agitation behaviors such as uplifts, stress against ruptures, shears, cracking and displacements.

In the study, three same-sized steel structures with different seismic isolator models, special moment and concentric moment frames of all three structures (SMF and SCBF) respectively, earthquake location (Kocaeli Turkey, Yarimca, 8/17/1999) have been selected, performing non-linear time history analysis, non-linear evaluation of dynamic behavioral building response spectrum analysis under load varying time function and design parameters are conducted.

As a result of this study, conventional buildings, lead rubber bearing buildings and fluid viscous damper building storey displacement, inter-storey drifts, mode shape, shear force, axial force, base shear, and time history analysis for nonlinear dynamic structural responses are evaluated and compared with the conventional, lead rubber bearing and fluid viscous damper building, according to American Institute of Steel Construction (AISC 360-16).

Keywords; Lead Rubber Bearing, Conventional Structure, Fluid Viscous Damper, Fixed Base, Response Spectrum, and Nonlinear Time History Analysis; SAP2000

COMPARATIVE STUDY FOR EARTHQUAKE PERFORMANCE OF STEEL BUILDINGS WITH SEISMIC ISOLATOR AND FIXED BASED STEEL BUILDINGS WITH DAMPER

ÖZET

Deprem her yıl önemli can kayıplarına ve maddi hasarlara neden olmaktadır. Bu tür hasarları anlamak ve önlemek için yıllardır farklı tipte sismik izolatörler icat edilmiş ve mevcuttur. Optimum ve etkili sismik izolatör türlerini elde etmek için, geleneksel çelik çapraz çerçeveli üç adet aynı büyüklükteki 12 katlı çelik bina ve akışkan viskoz damperli (FVD) sabit tabanlı kurşun kauçuk mesnetli (LRB) bir karşılaştırma çalışması yapıldı ve sismik performans iyileştirmeleri SAP2000 yazılımı kullanılarak değerlendirilmektedir.

Araştırmacılar, sismik izolatör binasının yükselmeler, yırtılmalara karşı stres, kesme, çatlama ve yer değiştirme gibi sismik ajitasyon davranışlarına dayanabileceğini öne sürüyorlar.

Bu çalışmada bina seçim aşaması, yapısal sistemlerin (SMF ve SCBF) kararı, deprem yerinin seçimi (Kocaeli Türkiye, Yarımca, 8/17/1999), doğrusal olmayan zaman tanım alanı analizi yapılması, dinamik davranışın doğrusal olmayan değerlendirilmesi ele alınmaktadır. yük değişen zaman fonksiyonu ve tasarım parametreleri altında yapı tepki spektrumu analizi dikkate alınmıştır.

Bu çalışmanın sonucunda, doğrusal olmayan dinamik yapısal tepkiler için konvansiyonel binalar, kurşun kauçuk taşıyan binalar ve akışkan viskoz sönümleyici bina kat deplasmanı, katlar arası ötelenmeler, mod şekli, kesme kuvveti, eksenel kuvvet, taban kesme ve zaman alanı analizleri değerlendirilmiştir. ve Amerikan Çelik Konstrüksiyon Enstitüsü'ne (AISC 360-16) göre geleneksel, kurşun kauçuk yataklı ve akışkan viskoz damper binası ile karşılaştırıldığında.

Anahtar Kelimeler; Kurşun Kauçuk Yatak, Konvansiyonel Yapı, Akışkan Viskoz Sönümleyici, Sabit Taban, Tepki Spektrumu ve Doğrusal Olmayan Zaman Alanı Analizi; SAP2000

ACKNOWLEDGEMENTS

Thanks to God, Whose allowed me to complete my graduate study and the thesis work I properly completed, He has given me the power and the strength throughout my study! Thank God. Most profound appreciation goes to my thesis Advisor, Prof. Dr. Onder Umut, for the prompt support, professional guidance, kind advice, with tireless efforts even in the late night by receiving help messages and sending me back responses at the same time and this will not be forgotten forever!!

His guidance helped me a lot in order to accomplish and reach my goals, particularly my thesis work. I'm so grateful for his support, and without you, this accomplishment wouldn't be possible for me.

I also would like to thank all my advisors Ass, Prof Dr. Ali Sercan Kesten and Dr. Esin INAN and as well as Işık Üniversitesi and their administrations, due to the fact that they allowed me to become part of the student member and facilitate me to complete the master's degree here in this university.

I would like to express my gratitude to my beloved mother, Ruqiya Adde Hassan, and father, Prof. Abdiaziz Abdi Hussein, for their handful-support, prayer, and encouragement in my entire study! I can't imagine how they helped me during my entire life. Especially my father, who gave me enormous encouragement, proper counselling, and valuable help in various ways during my whole study.

Finally, I would like to thank my friends, classmates, colleagues for helping each other. And as well as Turkey's government, who’s facilitated me to get this opportunity.

ABDULLAHI ABDIAZIZ ABDI

TABLE OF CONTENTS

LIST OF TABLES

LIST OF FIGURES

LIST OF ABBREVIATIONS

AISC = American Institute of Steel Construction

ASCE = American Society of Civil Engineering

EERI = Earthquake Engineering Research Institute

ECC = Expected Connection Capacity

IED = Inelastic Demand

LFRS = Lateral Force-Resisting System

LRFD = Load Resistance Factor Design

MCE = Maximum Considered Event

MRF = Moment-Resisting Frame

LRB = Lead Rubber Bearing

FVD = Fluid Viscous damper

SCBF = Special Concentrically Braced Frame

SMF = Special Moment Frame

SDC = Seismic Design Category

UBC = Uniform Building Code

NTHA = Nonlinear Time History Analysis

ECT = Turkish Earthquake code

FEMA = Federal Emergency Management Agency

PGA = Peak Ground Acceleration

DBE = Design Based Earthquake

LIST OF SYMBOLS

A = Area (m^2)

A_f = Area of flange (m^2)

B_D = Coefficient effective damping (βD)

B_M = Coefficient effective damping (βM)

B1, B2 = Moment magnification factors (MMF)

C = Demand over capacity (D/C) ratio

C_d = Deflection amplification factor (DAF)

C_{RS} = Mapped risk coefficient at short periods

Cs = Coefficient seismic response

Ct = Fundamental period coefficient approximate

Cu = Coefficient for upper limit period

C_v = Shear web coefficient

C_{vx} = Vertical distribution of seismic forces

D = Demand over capacity (D/C) ratio

DD = Design displacement of the isolation system (m)

DM = Maximum displacement of the isolation system (m)

E = Modulus of elasticity (KN)

Fa = Short-period site coefficient

FPGA = Site coefficient for PGA

F_R = Residual member strength (KN-m)

F_U = Ultimate member strength (KN-m)

F_v = Coefficient long period site

F_x = Lateral seismic force (KN)

F_Y = Yield member strength (KN-m)

F_y = Yield strength of steel

K = Stiffness (KN-m)

Keff = Effective stiffness of isolation bearing (KN/m)

R_I = Response isolation modification coefficient

R_t = Minimum tensile strength ratio

R_y = Minimum yield stress ratio

Sa = Spectral response acceleration (g)

Ss = Short period (Ss)

T = Period of building (sec)

T_0 = 0.2SD1/SDS

Ta = Fundamental period (sec)

T_D = Effective period of the isolated building at the design

T_{eff} = Effective period of bearing (sec)

T_L = Long period transition period (sec)

T_M = Effective period of the isolated structure at the maximum

T_o = Period of the original conventional structure (sec)

T_S = SD1/SDS

T_1 = First mode period

V = Base shear (KN)

V_b = Seismic design shear force below the isolation system (KN)

V_n = Nominal shear strength (KN)

V_{nx} = Strong-axis shear force (KN)

V_{ny} = Weak-axis shear force (KN)

V_s = Seismic design shear force above the isolation system (KN)

V_t = Base shear from the required modal combination (KN)

V_x = Seismic design story shear (KN)

α = Design philosophy factor (1.0 for LRFD)

f_i = Floor lateral force (KN)

g = gravitational acceleration (m/sec^2)

Δ = Story drift

CHAPTER 1

1. INTRIDUCTION

1.0 General

Developing structural engineering must be taken into consideration on how such structures stand up to the extreme prevalence of different natural and earthquake forces in order to overcome structural failure, loss of lives, and as well as investments. So, engineers predict and pre-plan properly in order for the buildings to resist all kinds of forces, save lives and investments as well.

When developing structural engineering, important key infrastructures to be projected are proper base isolation systems and special concentrically braced steel frames (SCBF) as the primary lateral force-resisting system (LFRS) in low- to mid-rise structures. They are characterized by a high elastic stiffness-to-weight and strength-to-weight ratio that allows for strength and stiffness design requirements to be met with minimum steel tonnage [1].

In general, the design of (SCBF) is less complex than other (LFRS), such as special concentrically braced frames (SCBF) and special moment frames (SMF) because members are designed as axially loaded members with limited interaction with flexural stresses. The simplified design coupled with the more in-depth and costly member and connection detailing requirements of (SMF) makes them frequently used to resist lateral forces from wind and seismic events. The seismic performance of (SCBF), however, is generally considered to be inferior to (SCBF) and (SMF) because of the drastic and potentially unsafe nature through which braced frames dissipate energy during a severe ground shaking event making them popular to resist seismic forces only in regions of low to moderate seismicity.

For the earthquake forces exceeding the elastic limit of the frames, the brace will dissipate most of the energy through cycles of inelastic deformations designed for such behavior. The most used configuration of braces in a (SCBF) called chevron or inverted-v arrangement because it minimizes impact to architectural components.

Structural seismic manipulate is to alternate or regulate the dynamic characteristic or dynamic movement thru with the assist of putting in devices which include a seismic isolation bearing, a few mechanisms which include energy-dissipation braces and joints, fluid viscous damper in a certain segment of structure [2]. Requiring no additional energy to operate, these devices create controlled pressure or provide additional strength dissipation in the structural design. Hence for the protection of the structure, there is a need to dissipate the energy imparted to the frame, which can be made through earthquake safety systems. Two vibration management systems such as lead rubber bearing (LRB) and fluid viscous damper (FVD) are used as main essential components to dissipate and overcome seismic energy [3].

In regards of my thesis study in general, those two vibration management systems are applied and conducted comparative study of overall performance of steel building with seismic isolator and fixed-based steel building with a damper.

Finally, more calculations have been done considering the earthquake location time history analysis, non-linear evaluation of dynamic structural behavior from database record in Kocaeli Turkey, 8/17/1999, Yarimca, Thus, modal design and analysis of steel framed buildings are extremely important in understanding the behavior of steel framed buildings under applied dynamic loads.

1.1 Background

Many years significant volume of research on conventional steel building, lead rubber bearing, and fluid viscous dampers has been done in many different forms when it comes to the behavioral and structural steel design of conventional, seismic absorbing and seismic damping structures. Figure 1.1.

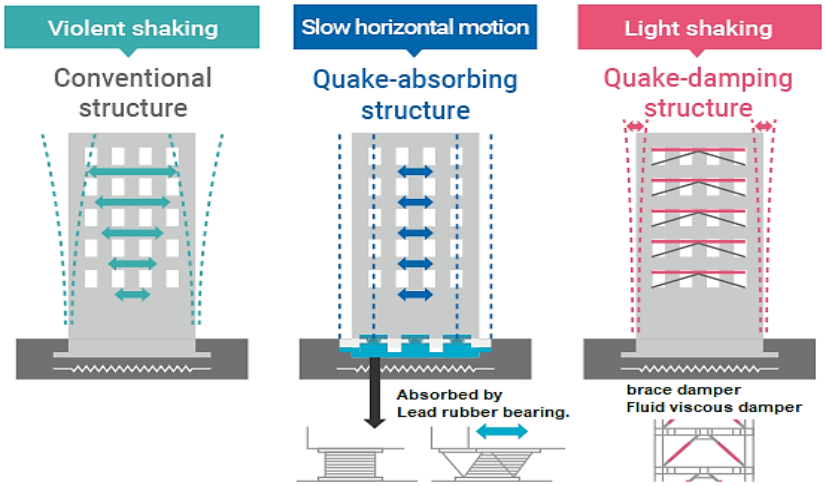

Figure 1. 1 Comparing three structures conventional building, lead rubber bearing, and fluid viscous damper.

1.1.1 Conventional steel structure

Steel braced frames (SBF) are widely recognized as one of the most efficient, cost-effective, and adaptable structural solutions in the face of seismic excitations. However, when confronted to enormous earthquake stresses, most traditional steel braced systems no longer exhibit remarkable overall performance, particularly owing to the focus of deformations in a single story, which leads to premature dynamic instability of the structure.

This one so soft-storey failure process affects both concentrically braced frames (CBFs) and special moment frames (SMFs), which range in height from mid to high-rise. Sap2000 was used to study the failure process of steel braced frames. In CBFs, input energy is meant to be dissipated through brace inelastic behavior such as yielding and buckling. Even though conventional CBFs lack the functionality to redistribute inelastic demand over the constructing height, brace inelastic movement typically provides a soft in terms of every stiffness and energy in the structure, resulting in an awareness of deformation and eventually collapse of the structure, as shown in Figure 1.2.

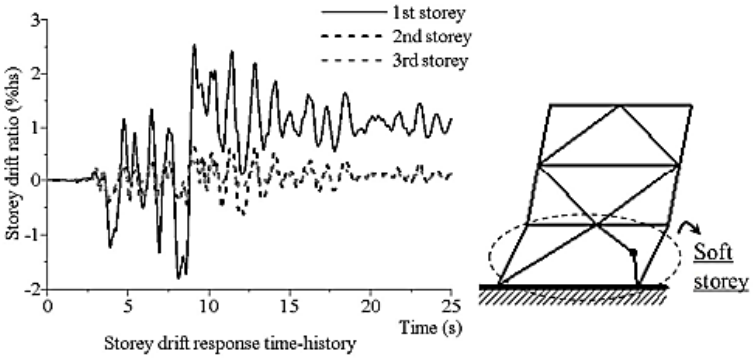

Figure 1. 2 Standard soft storey reaction (CBFs).

Large research has been conducted from Northridge, Japan and Mexico earthquakes especially how the exposure was and how was the performance's design for concentrically braced frames (SCBFs). Collections and reviews of existing experimental results as well surveys of damaged structures have also been conducted to understand and improve the behavior of SCBFs.

1.1.2 Lead rubber bearing isolation system

Dr. Bill Robinson from New Zealand during the 1970s had invented base isolator systems. It is among the most effective earthquake resistant techniques against structural vibration process control to mitigate damages of structural and non-structural components during earthquakes. He used layers of rubber and steel called lead rubber bearings. This method is so-called "detach" or "isolate" a building structure from its ground using flexible devices, referred to as an isolator Figure 1.3 below. The mechanical power transmitted by high-frequency seismic waves to the isolated structure completely diminishes the isolators themselves.

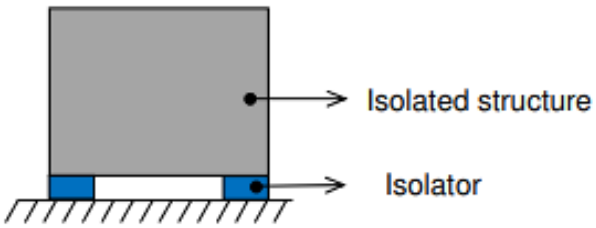

Figure 1. 3 Lead rubber bearing (LRB) isolation system.

Figure 1.4 below, compares regular base and isolated base building structures. In order to isolate buildings from horizontal masses such as wind and earthquakes, creating considerably horizontal displacements thus, isolators spontaneously generate stiffness to the extent to resist deformation in response to an applied horizontal force-displacement.

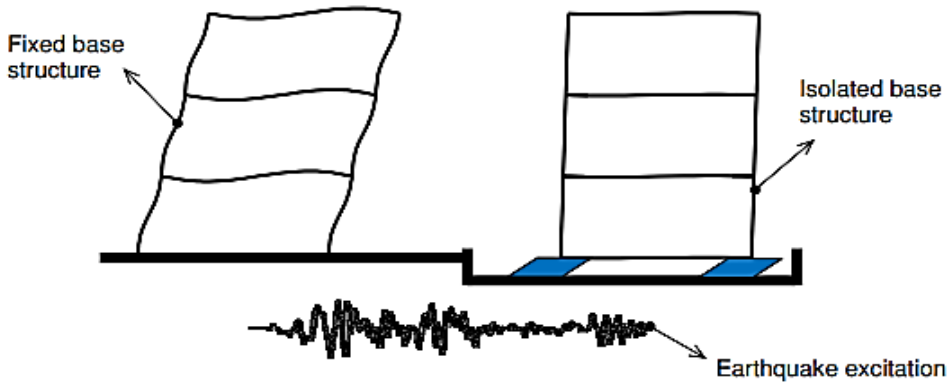

Figure 1. 4 Deformation in fixed base caused by earthquake excitation.

Typical idealized unidirectional hysteresis conduct (force vs. deformation) in the horizontal route of an isolator is proven in Figure 1.5. The isolator hysteresis loop suggests that mechanical strength is dissipated, which affords damping to the isolated structure.

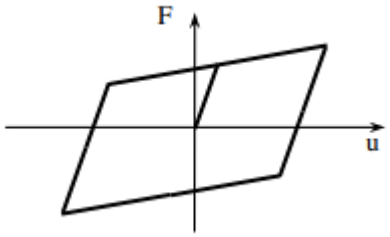

Figure 1. 5 Typical idealized unidirectional hysteresis behavior of isolators in horizontal direction.

In earthquake engineering language, an isolation device lengthens the natural duration of the isolated structure, moving it to a decreased spectral acceleration area of the design spectrum Figure 1.6 (a). The reduction in spectral acceleration reduces the inertia force on the superstructure, and as a result, reduces the damage. However,

the flexibility will increase the displacement relative to the floor of the isolated building for the duration of an earthquake Figure 1.6 (b). Another essential issue of lead rubber bearing is that the modal properties of the isolated building are modified so that the contribution of greater modes to the reaction of the isolated building due to horizontal seismic excitation is small (Naeim and Kelly, 1999).

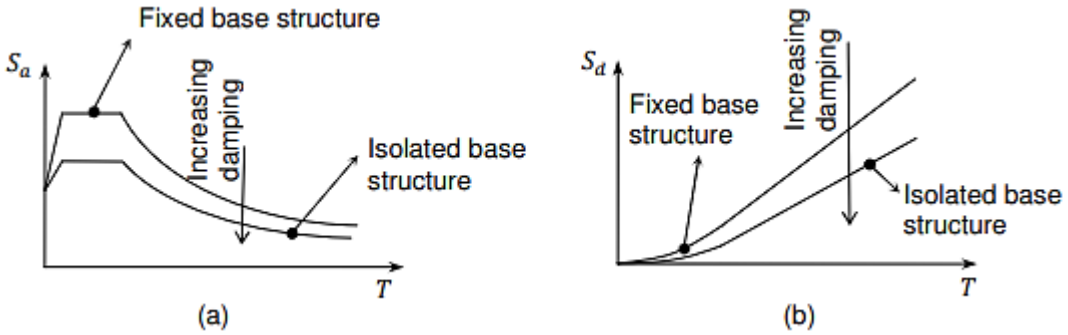

Figure 1. 6 Typical design spectral acceleration and displacement. a) Spectral acceleration. b) Spectral displacement.

Current isolators are categorized into two basic types (Kelly, 1997; Naeim and Kelly, 1999): elastomeric bearings and friction bearings. An elastomeric bearing consists of alternating steel and rubber layers to supply flexibility in the horizontal axis while rigidity in the vertical axis. Lead plugs are typically installed into elastomeric bearings to provide damping and initial horizontal stiffness [4]. An elastomeric bearing with a lead plug is (LRB), as shown in Figure 1.7.

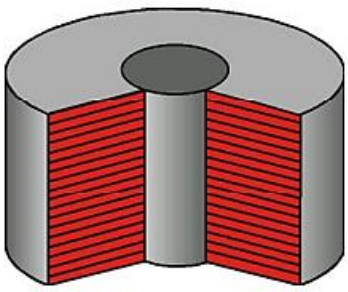

Figure 1. 7 Lead rubber bearing (LRB).

1.1.3 Fluid viscous damper

The most regularly utilize passive damping systems, a fluid viscous damper (FVD) was once used to reduce the throwback artillery rifle in 1897 [5]. It became sizeable to all military equipment's to some nations in the 1900-1945. However, it used to be no longer extensively publicized due to the fact of its secretive nature [6]. Most fluid viscous dampers operates between inside the damper, metallic plates are submerged in fluid, as shown in Figure 1.8. The damping effects are determined by the fluid's viscosity, which varies significantly with temp, the initial fluid viscous dampers were sensitive to temperature and operating environment with the end of the Cold War in the late 1980s, the completely established fluid viscous damping (FVD) technological know-how was once recognized and made available to consumers [7].

The high-potential fluid viscous dampers decided a number of commercial functions in civil structures and bridges subjected to seismic and wind excitations. Soong and Constantine created a modern fluid viscous damper in 1994, which is now widely employed in the safety of mechanical and civil engineering structures [8], as shown in Figure 1.9. A type of (FVD) reduced the vibration strength by pushing the compressible silicone fluid to flow through orifices and imposing a stress differential to generate the resistance force. The modification of the damping principle of advanced (FVDs) significantly reduced the damping devices' extent and multiplied their steadiness in complex working settings, accelerating the development and functions of (FVDs) in realistic mechanical and civil engineering processes.

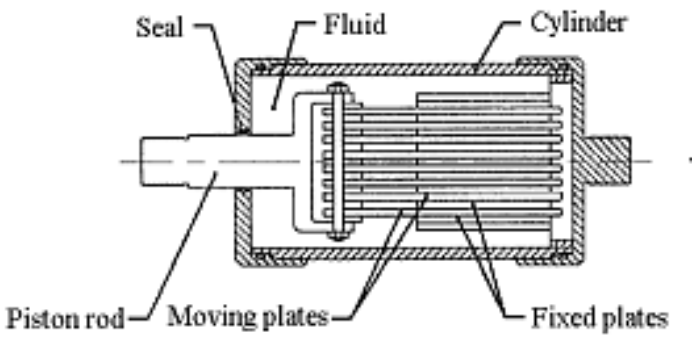

Figure 1. 8 Early fluid viscous damper (FVD).

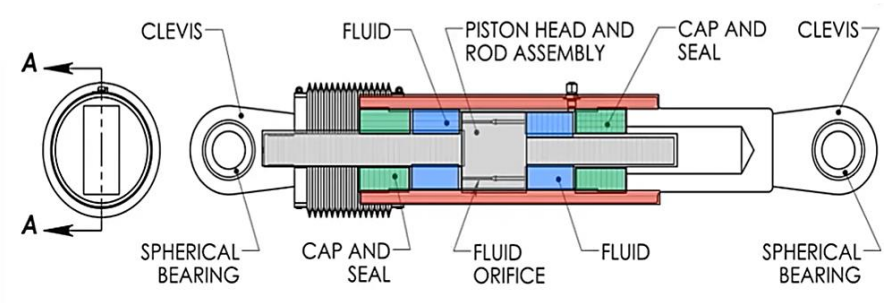

Figure 1. 9 Modern or recent fluid viscous damper (FVD).

Until recently, several theoretical and practical research have shown (FVDs) are the least costly and leased space intensive in device vibration stabilization design. Compared with different sorts of vibration manage systems, (FVDs) have various intrinsic and considerable benefits:

1. The damping pressure is actually out of the section with the most important flexing and shear strength in building imply that a fluid viscous damper (FVD) can be utilized to reduce each inner applied load and deflection in the building.
2. (FVD) are self-contained, requiring no additional tools or energy.
3. Modern (FVDs) operate at a massive fluid stress level, allowing the dampers to be tiny, compact, and simple to install.
4. (FVDs) are often less costly, easier to install, and require less maintenance than other passive damping devices, which help to reduce the typical cost of a realistic building.
5. The efficiency of passive (FVDs) has been demonstrated throughout time, with over a century of large-scale economic usage in the most harsh settings by the army and aerospace sectors.

Fluid viscous damper (FVDs) for the protection of corporate and government buildings under earthquake and wind loadings have been widely used since the 1990s and have seen significant improvements as a result of pressing needs for the safety of structural installations, nuclear reactors, mechanical components, and sensitive devices from seismic shaking, horrifies, and actually impact masses. To meet these criteria, engineers and scientists have devised a variety of setup modes for (FVD) devices, as seen in Figure 1.10.

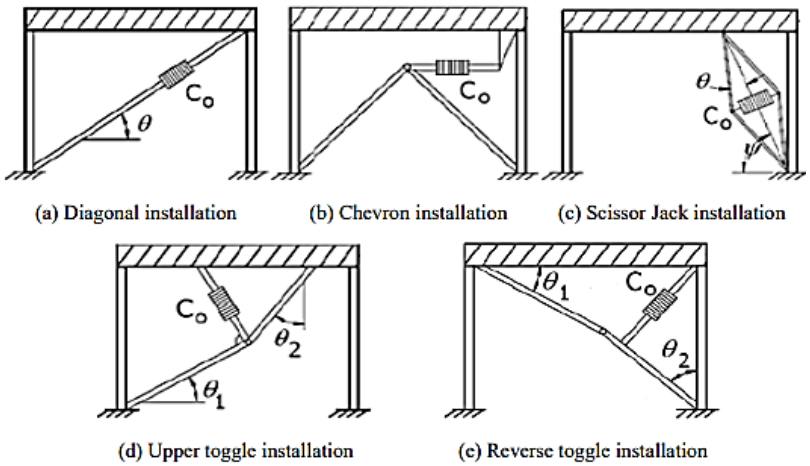

Figure 1. 10 Typical installation modes of fluid viscous damper devices.

1.2 Objectives of the study

The following are the project thesis objectives:

1. The comparison between earthquake performance of three 12-storey steel buildings of:

a. Conventional steel structure

b. Base isolation with lead rubber bearing system (LRB)

c. Fixed base with fluid viscous damper.

2. Structural models analysis to predict building behavior in the case of deformations, stresses, dynamics nonlinear, and vibration from horizontal seismic forces.
3. To determine the validity of the project model, inter-drift, axial load, combined axial and shear loads based on seismic requirement standards.
4. To analyze the structural model and estimate its horizontal stiffness in the event of seismic loading, responses from nonlinear isolated and un-isolated model structures with dampers, lead rubber bearing, viscous dampers, and braces, all subjected to lateral loads providing simplified (RSA) and (THA), storey displacement, inter-storey drifts, shear force, acceleration of all project model using SAP2000.

1.3 Main scope

The main scope emphasis on the analysis and design of the fixed-base, lead rubber bearing, and fluid viscous damper of all three 12-storeys steel buildings. Each structure steel frame has a lateral system of special moment frame (SMF) oriented in the x-axis, and special concentrically braced frame (SCBF) in the y-axis. For each design basis earthquake (DBE), and maximum considered earthquake (MCE) earthquake requirement level, earthquake performance against of each building is examined and contrasted in each other. In order to conduct non-linear time-history analysis (THA), studies on three buildings, one seismic ground motion is selected to each structure building. Outcome result has been obtained ofter used Sap2000 v22 software program.

1.4 Overview procedure/ Thesis outline

The thesis dissertation are classified into six chapters.

Chapter 1 presents a general introduction to steel structures with fixed base, lead rubber bearing, and fluid viscous damper, and their types with their limitations given by the American institute of steel construction (AISC 360-16) and ASCE 7-16 seismic code. Describes the background of the conventional steel building, lead rubber bearing, fluid viscous damper during the past background advances technology devices up to now and beneficial of the resist seismic behavior structure response under load. The final part states the thesis's primary objective and thesis scope.

Chapter 2 introduces a literature review of previous studies titled comparative steel structures with conventional building, lead rubber bearing, and fluid viscous damper of seismic performance. Scientific studies related to this study are presented in this section.

Chapter 3 presents the numerical and structural modeling analysis. The modeling of three models of three-dimension steel buildings with twelve storeys are selected the fixed base, lead rubber bearing, fluid viscous damper of the steel frame structures. The model has been analyzed using SAP2000 v22. The first part of this chapter defines the general description of the structure model has material properties, steel details, and load combinations. Secondly, describes the formulation of the constrained optimization problem to calculate the optimal parameters of the devices to achieve

certain performance objectives in an optimal manner. Finally, the earthquake location was taken from Kocaeli, Turkey, on August 17, 1999.

Chapter 4 this chapter describes the design structures phase using building code requirements for both R=8 (SMF) and R=6 (SCBF). The general procedure for designing each structure involves the use of load and resistance factor design (LRFD) load combinations to check the structure's ability to withstand static, life, and seismic loads.

Chapter 5 presents analysis results and a discussion of the case study buildings. That it includes storey displacement, inter-storey drifts, mode shape, shear force, axial force, base shear, and time history analysis are mainly used for nonlinear analysis dynamic structural responses are evaluated of building for comparison of the conventional building, lead rubber bearing, and fluid viscous damper was presented in terms of tables and graphs more details.

The chapter 6 includes a conclusion and recommendation of the thesis with a note on understanding the complexity of the studying the steel structures with seismic isolators and fixed base steel buildings with dampers were compared for earthquake performance.

CHAPTER 2

2. LITERATURE REVIEW

2.0 Introduction

Elaborative studies and analysis on the works carried out a literature review of different researchers. Hence, we analyze that the various effects for structure models with the fixed base, base isolation system, and fluid viscous damper to their strength, stiffness, their measures, slenderness ratios, and their performance studies. As the study is based on a comparative analysis of rigid base, base isolation system, and fluid viscous damper are mainly formed by two materials, concrete, and steel which are far and broadly utilized in the manufacture of multi-storey high-rise buildings bridges. Their process provides remarkable stagnant and earthquake-resisting properties, such as high strength, high flexibility, high stiffness, and huge energy-assimilation capacity.

The models developed in the study will be utilized in future exploration to investigate the fixed base, base isolation system, and fluid viscous damper research will furthermore continue with the use of contact elements positioned at the boundary of the two materials, which are steel and concrete.

The scope of this study was to develop high-rise buildings with a fixed base structure, base isolation system, and fluid viscous damper that accurately define which of the structure models responses is better under seismic action. The models developed in this study will be customized in a future study to seem to be particularly at the structure behavior at the steel-concrete of material which is used in a multi-storey building under seismic condition for their better performance.

2.1 Review of previous studies

Around many researchers carried on the fixed base structure, base isolation system, and fluid viscous damper for investigating its behavior. A significant data over the past 40 years. It has been intended that for superior consideration and the observable advantages of the conventional structure, base isolation system, and fluid viscous damper. These models attracted the interest of research workers all over the world. On the origin of this research, it has resulted that different design codes are utilized by different countries, which can be generated by their engineers. The present intended principles and provisions have originated either from the steel or concrete design approach of that time.

A. N. Lin, et.al and H. W. Shenton III (1992). Studied the earthquake results of conventional structure and base isolation special concentrically brace steel frames and moment frame are introduced. Refer to different codes to design base isolation and fixed base framework. The Structural Engineering Association of California (SEAOC) designed the fixed foundation frame in 1990 and used it for the recommended design foundation shear. The basic isolation building is designed to withstand 100%, 50%, and 25% of the lateral force recommended by SEAOC. Fifty-four different ground motion records are used for research purposes. Perform nonlinear time history analysis dynamic of different results such as roof displacement, and the collapsed frame was carried out, along with these yield frames, yield units, and total relative roof displacements were found. The results obtained in this way under different conditions show that 50% of the SEAOC recommended lateral forces have better compatibility than certain combinations. A comparison analysis was conducted to generate the peak response achieved the conventional structure and isolation moments of the supporting brace steel frame [9].

Donato Concellara et.al (2013). Assessed on his study it was described the comparison of the (LRBs) and (FS). The seismic isolator consists of (LRB) combined with (FS) called a high-damping hybrid seismic isolator. The earthquake response of a high-damping hybrid isolator is compared with (LRB). Examine the identical structure under different earthquake occupation in the form of frequency and intensity. This article mainly attentive on (HDHSI) and compares it with (LRB). These two other vibration isolators are fixed in the building, and a nonlinear time history analysis has been performed. Various seismic activities are considered. The results are compared

in the form of foundation shear force, bottom motion, and base shear of the structural frames. A comparison results show that HDHSI is better than other methods in protecting severe seismic activity [10].

Minal Ashok Somwanshi (2015). Earthquake performance evaluation and investigation are carried out on conventional structure and base separation independent structures. In two situations, this study entails the modeling and analysis of 13-story flexibly coupled planar frameworks. The conventional structure is the first situation, while the base isolation is the second. Use ETABS software to model and analyze Bhuj seismic ground shaking records. The analysis in the ETABS program yields the reaction's greatest vertical. The complete mass of the structure results in rubber when this vertical reaction is used. The bearings are made by hand, during ground shaking, (THA) is used to measure storey response, acceleration, and displacement. This research aims to show how to efficiently isolate the system and assess its efficacy on the building, Shear force, bending moment, base shear, inter-drift, and floor displacement are all minimized. According to the analytical results, the base isolation approach is highly crucial in order to lower the earthquake response of each regular as well as asymmetric models in comparison to conventional buildings and manage the damages within the structure during intense ground shaking [11].

Win and Htun (2017). Studied the steel building performance with (LRBs) and conventional structure. The study's aim was to evaluate the utilization of (LRB) as an isolation system, and then correlate various criteria between conventional structure and isolated base conditions. The modeling performed the analysis by using non-linear time history analysis. The analysis results were compared using different parameters such as storey displacement, storey acceleration, and inter-storey drift ratio. The analysis model was an 8-storey building having conventional structure and base isolator. However, a study result shows that the storey acceleration is decreased crucially in the base structure compared to the conventional structure. Moreover, the isolated base structure period is more compared to the conventional building [12].

Abdelouahab Ras et al (2013). The study carried out the 3D 12-storey steel structure building by analyzing and numerically observing. The non-linear FVD is installed diagonally in the frame. Use SAP2000 software to conduct a comparative study using two models. One model is without braced, and the second one with braced FVD. Fast non-linear time history performed for analysis. Model FVD using mathematical expressions with different values of velocity exponent. It was found that

for alpha values less than 1, a decrease in the amplitude value will increase the value of the damping ratio. Finally, it is concluded that, compared with the unbraced model, the diagonal will not transmit any unwanted axial force but will reduce the damping [13].

H.kit Miyamoto et al, (2013). Studied the (FVD) are added to the structure to protect it is structural and non-structural components, as well as its content. The dampers are built to withstand the forces caused by the most powerful earthquakes. The efficiency of dampers in providing earthquake safety, as well as the process of designing similar devices, are well known, as evidenced by the outstanding performance of structures with dampers in previous earthquakes. The analysis model of the steel structure building with viscous dampers, including the limit state of the dampers, has been produced, and progressive analytical model on it has been done to assess the failure efficiency. So far, when confronted to significant earthquakes, the performance of structures employing (FVD) has been found to be satisfactory. However, the results of SMRFs are used to provide strength; dampers are used to control storey drift. The demand for building and non-structural components is reduced. Designers will be supplied with important information to aid in earthquake design utilizing the fluid viscous damper technique as one of the study findings. Research on the use of four-storey commercial buildings. For the 3D mathematical model, SAP2000 software was used. Non-linear FVD is used to control storey drift. Perform a non-linear time history to determine performance. The first studied two levels of earthquake disaster (MCE) and the second (DBE). Finally, the maximum response of displacement, acceleration and floor shear was evaluated [14].

D.Lee et al (2001). Observed the viscous dampers can protect the structure from wind, explosions, and seismic. (FVD) technology originated in army and aeronautical uses. About ten years ago, people discovered. The similar (FVD) technology that shields missiles from nuclear strikes and submarines from underwater near-explosions may also protect buildings, bridges, and other buildings from damaging shocks and vibrations. Therefore, Summarized in detail the working method, installation method, and future scope of FVD. This paper studies the role and relationship of nonlinear dampers. It is recommended to use various software for damping modeling, such as SAP2000 and ETABS, to reduce the seismic response. Various bracing support methods for installing dampers are also described [15].

Y. Rajesh Kumar (2018). Through vibration control systems and technologies, such as providing Base isolation and dampers in the structure, the structure can be made to resist seismic activity. Base isolation is a method that isolates buildings from the ground in order to lessen the impact of earthquakes. The base isolator also enhances the building's flexibility and minimizes the force imparted to the building. Seismic dampers, on either side, absorb energy delivered to the building by seismic ground motion. The purpose of the research is to use base isolation and fluid viscous dampers as the vibration control system in order to comprehend the seismic reaction of reinforced concrete buildings on different floor levels when subjected to earthquake ground motion (such as El Centro) and to compare the two vibration control systems. Therefore, models of 5, 8, 12, and 15 floors are considered in the study. These models are basic structures and use ETABS software for modal time history analysis. All structures were modeled with base isolators and fluid viscous dampers, and changes in seismic response were observed. The parameters considered in the study are foundation shear, lateral roof displacement, and basic time period. According to observations, in the basic isolation structure, the foundation shear force has been reduced by 96%, and the lateral roof displacement has increased by 45%. As the foundation shear force has been reduced by 38%, the roof displacement has been reduced by 71%. Compared with the bare frame structure, the Ina structure with viscous dampers [16].

CHAPTER 3

3. NUMERICAL AND STRUCTURAL MODELING ANALYSIS

3.0 General

Steel structures are widely used for buildings due to their high strength, good flexibility, and fast fabrication. However, the modeling of steel structures, in this case, emphasizes comparing three different steel structure models of fixed base, (LRB), and (FVD) in the event of resistances from earthquake excitation forces with stiffness and ductility behaviors. The model has been analyzed using SAP2000 v22. And the time history analysis of the earthquake location was taken from Kocaeli, Turkey, on August 17, 1999. Nonlinear analyses are designed in response to the structural dynamic behavior, which may vary according to time and loading design parameters.

Firstly, the structure model has material properties, steel details, and load combinations. Secondly, structural modeling has been defined with non-linear time history analysis and confirmed that the building would behave stable against vibration and seismic forces due to the insertion of rubber bearing and fluid viscous dampers in the structure. Finally, the ground motion data has been downloaded to query earthquake and station information, earthquake waveforms, and response spectra for events with magnitude horizontal components.

3.1 Building description

To reach the study's goal, three models of three-dimension steel buildings with twelve storey are selected the fixed base, (LRB), and (FVD) of the steel structures. They have an area of 45m x 45m. Each spacing of the gridline is 7.5m on both sides. The height of the first storey is 4.5m, and the other structure storeys are 3.5m.

The structure's entire height is 43m. The steel structural system featured the lateral system comprised of Special Moment Frames (SMF) in the x-axis, and Special Concentrically Braced Frames (SCBF) in the y-axis, and the same structural systems were used for both steel buildings designed and analyzed for this study using SAP2000 v22 software.

3.1.1 Building framing and elevations 3D plan

The plan and elevation views of the frames of three different structures project model:

- The square shape of the floor plan provides a fully symmetrical plan layout where the frame can be identically designed in both directions.
- The steel braced frames are developed with two varieties of steel braced frames in the y-axis Special Concentrically Braced Frame (SCBF) with chevron, inverted-v type, and Special Moment Frame (SMF) in the x-axis.
- The brace position regularizes the design and aligns the center of stiffness with mass.
- Typical floor plans a layout and the roof plan layout have been put in service.

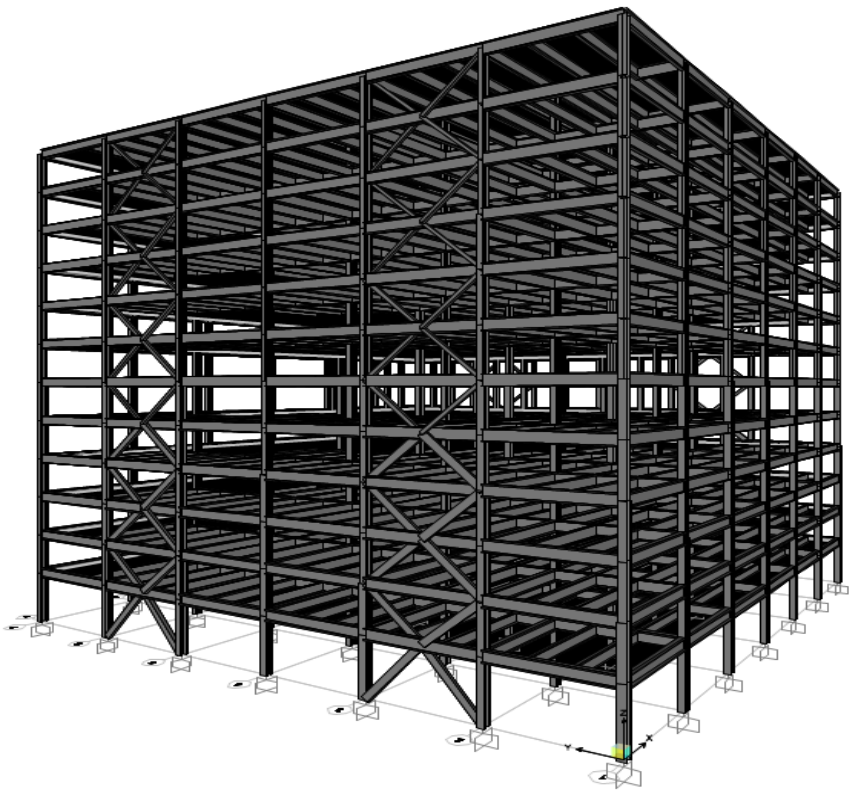

Figure 3. 1 Three-dimensional structural rendering of the steel-frame building view.

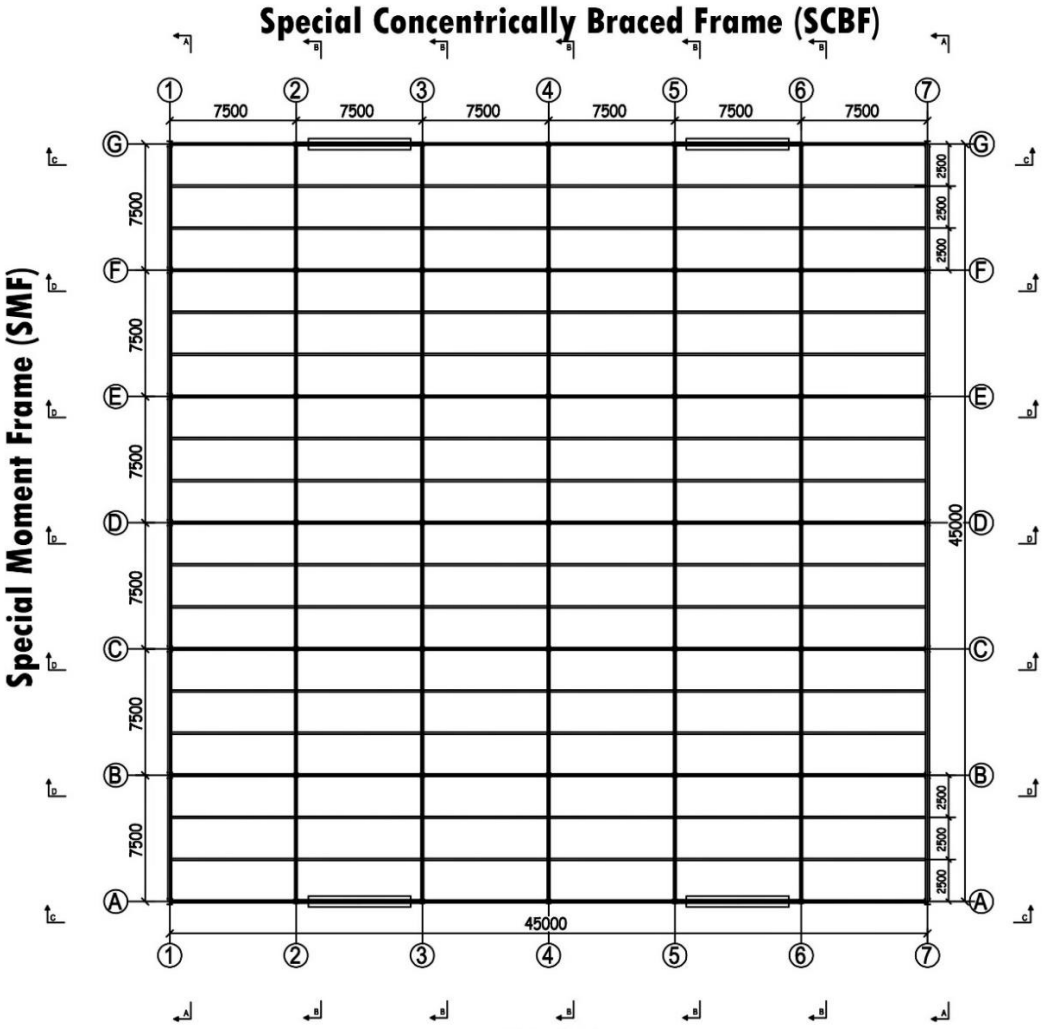

Figure 3. 2 Plan view.

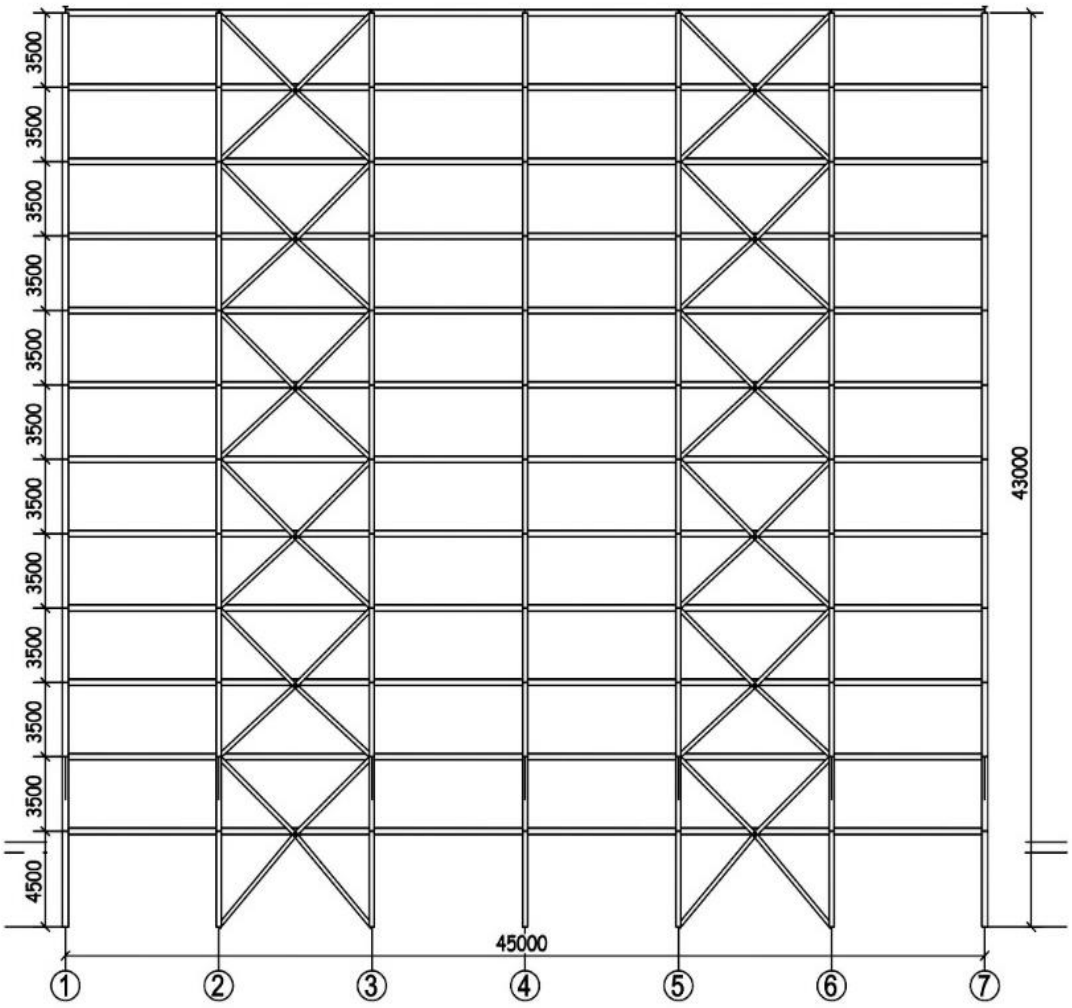

Figure 3. 3 Special concentrically braced elevation view (SCBF).

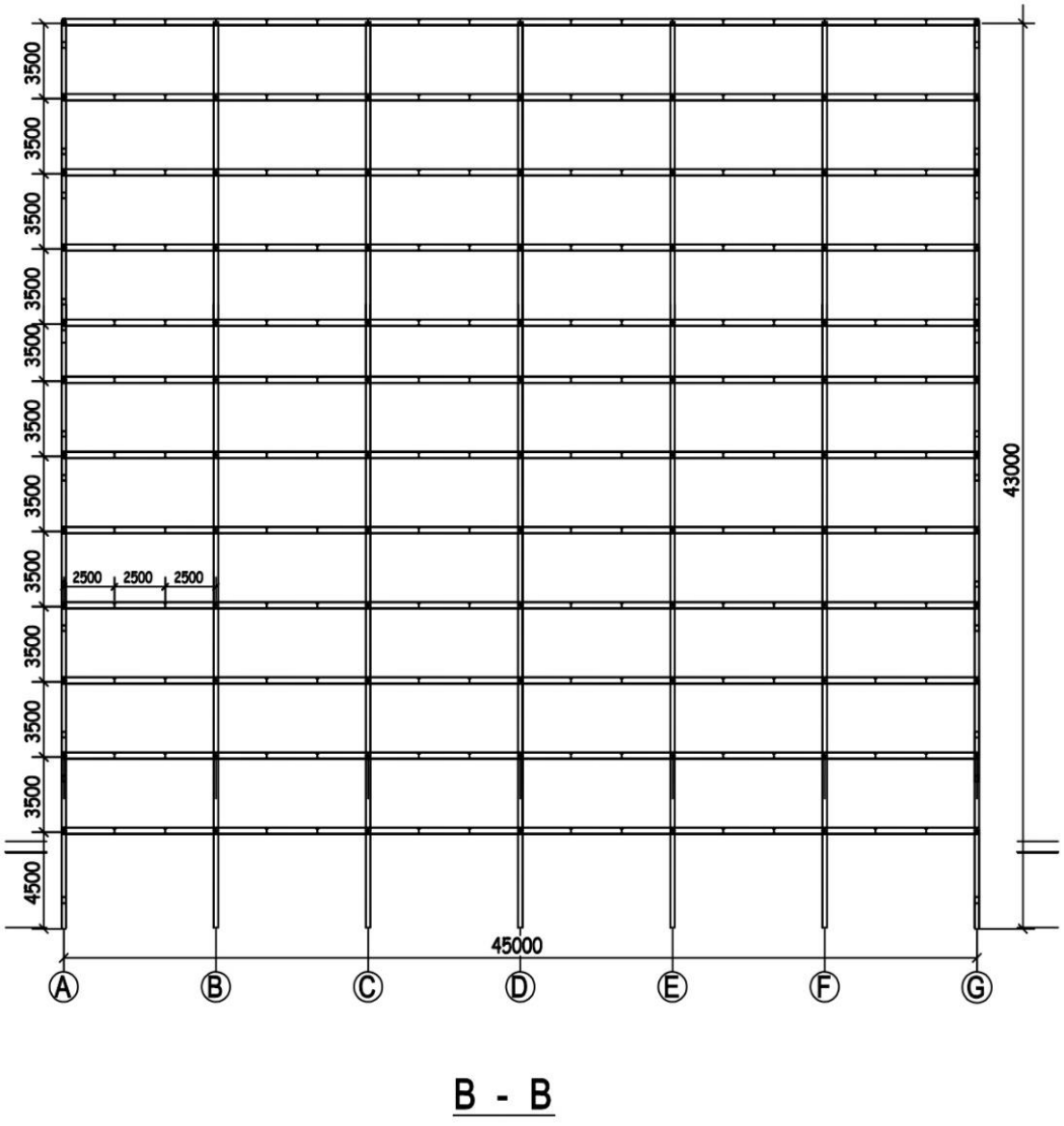

Figure 3. 4 Special moment frame elevation view (SMF).

3.1.2 Steel building detailing frames and sections

Structural steel comes in a variety of forms, including “W-shapes, L-beams, Z-shapes, HSS-shapes, and L-shapes (angles),” etc. The building model has been implemented with frame wide flange type with W-shape frames (columns and beams) and hollow type with HSS-shape (brace frames). The steel structures contain beams, columns, and bracings. The cross-section frames are modeled using force-based non-

linear section frame elements to represent the possible inelastic material response beside the element's diameter. Force-based elements were chosen because they have been proven to be more accurate than displacement-based elements under the same amount of calculation, especially in the non-linear range. The reason is that in the force-based unit (i.e., compliance method), the force interpolation function is used to reproduce the change of the internal unit force along the length of the member.

A column, beam, and brace are modeled with different elements per every three-storey level to represent the stress waist at both ends and the middle part of the frame. However, according to the given data, I-profiles, and Tube-profile, to define the cross-sectional properties of structural elements, are selected frame section property types is (AISCLRFD3.pro).

Table 3. 1 Steel frame sections used for the structural design.

Storey	Interior column	Exterior column	Beam	Brace
1	W14x550	W14x808	W30x326	HSS20x8x.625
2	W14x550	W14x808	W30x326	HSS20x8x.625
3	W14x550	W14x550	W30x326	HSS20x8x.625
4	W14x426	W14x550	W30x191	HSS20x8x.625
5	W14x426	W14x426	W30x191	HSS20x8x.625
6	W14x426	W14x426	W30x191	HSS10x10x.625
7	W14x398	W14x398	W30x173	HSS10x10x.625
8	W14x398	W14x398	W30x173	HSS10x10x.625
9	W14x398	W14x398	W30x173	HSS8x8x.625
10	W14x311	W14x311	W30x148	HSS8x8x.625
11	W14x311	W14x311	W30x148	HSS7x7x.500
12	W14x311	W14x311	W30x148	HSS7x7x.500

3.1.3 Material property

Material properties used for the structural model are based on AISC 360-16 (Specification for structural steel building). The regular steel models are considered special moment frames and concentrically brace frames based on data I-profile and Tube-profile of steel material named A992 grade 50 respectively, the other properties for steel material nominal values of the yield strength (fy) and the ultimate strength (Fu) for structural steel. The details of material properties in all models are presented in Table 4.3.

Table 3. 2 Material properties of steel frame.

Steel Grade at 50	Fy(N/mm^2) (MPa)	Fu(N/mm^2) (MPa)
A992	345	448

- E = 200,000 MPa is the modulus of elasticity (Young's modulus).
- Shear modulus [G = E / [2 · (1 + ν)] ≈ 76923 MPa
- Poisson's Ratio ν = [0.30]
- Thermal Coefficient α = 1.170E-05 /^{o}C
- Weight Density = 76.98 kN/m^3

3.1.4 Load combination

The load combination allows to be increased the allowable stress for seismic loads and wind loads. It is usually related to checking for uplift in the structure. Combination of various loads according to the conditions while in corresponding specifications. Therefore as basic rule, the following load combinations are implemented, no matter which combination has the far more negative impact on the relevant structural, base, or building frame. It should also be a predictable load combination. That is, the highest wind, earthquake, imposed, and snow loads cannot occur instantaneously to integrate to form a rise for strength and stress allowed design. The following is a list of design load combinations:

- ✓ 1.4DL
- ✓ 1.2DL+1.6LL
- ✓ 1.2DL+LL+WL
- ✓ 1.2DL+LL-WL
- ✓ 1.5664DL+LL+EX
- ✓ 1.5664DL+LL-EX
- ✓ 1.5664DL+LL+EY
- ✓ 1.5664DL+LL-EY
- ✓ 1.5664DL+LL+LX
- ✓ 1.5664DL+LL-LX

Where DL is the dead load, LL is live load, WL is wind load, and EX is earthquake load in the x-direction.

3.2 Specification, codes, and standards used

The following are the design parameters and software utilized in this study:

- Calculations data of isolation system (lead rubber bearing) were adopted using UBC-97, [17].
- Spectral analysis and seismic loading were assessed according to ASCE7-16 [18]
- Wind load the all buildings by using code ASCE7-05 [19]
- The building were designed according to AISC 360-16
- SAP2000 v22 software (https://www.csiamerica.com/) was used for the analysis and design of structural elements.

3.3 Analysis option

When it comes to the analysis options, the inter-storey drifts and storey accelerations of three models, the conventional structure, base-isolated, and fluid viscous damper steel structures, Non-linear (THA) are used to provide information at the (DBE), and (MCE) levels. In addition, the building performance levels were investigated by recording plastic hinge rotations in building frames in accordance with ASCE 41-06 criteria [20].

3.3.1 Analysis option procedure

The following is an overview of the analysis option procedure:

1. Model damping with lead rubber bearing and fluid viscous damper.
2. Steps for defining building models by using SAP2000 program [21].
3. Analysis of earthquake structural methods.
4. Response spectrum analysis.
5. Select ground motions record data level (via PEER website ngawest2.berkeley.edu) [22].
6. Time history analysis (non-linear dynamic analysis).
7. Structures, loads, and analysis criteria were modeled using ASCE 41-06 specifications.

3.4 Structure and effectiveness of lead rubber bearing in seismic isolation.

A laminated rubber isolator is a lead rubber bearing (LRB). It is composed of multiple layers (such as top loading and sealing steel plates, rubber cover, lead core, elastomeric pad, bottom sealing steel plate, bottom loading plate) featuring a central lead core, made of elastomeric material and vulcanized reinforced steel plates, which produces large deformations and consume to avoid injury, the majority of the energy is expended. Because of its diameter and height, LRB provides certain unique design characteristics that directly affect its function to absorb and dissipate energy. Furthermore, the flexure rigidity and yield stiffness of the support, as well as their ratio, are the major elements that determine the earthquake design of the building to the technical definitions, uniform building code (UBC 97) shown in appendix (D) calculations. The design procedures the isolator parameters that comply with the rule were calculated using UBC-97 and the study are as follows:-

Target period and material properties

The vibration period of the isolation system should have a period between 2 and 3 seconds. The elasticity module E, shear modulus G, and maximum shear deformation max vary based on the type of isolator chosen.

Design and calculation of maximum displacement

Using the following formula, the isolation system must be designed and built to resist minimal lateral seismic displacements operating in the direction of each of the building's principal horizontal direction:

$$D_D = (g \times CvD \times T_D) / (B_D \times 4\pi^2) \qquad (3\text{-}1)$$

Here, g is gravitational acceleration, CvD seismic coefficient, T_D design period, B_D damping coefficient. The value of B_D is calculated using Table 3.3. When calculating the horizontal displacement of the isolation device at its greatest, CvM instead of, CvD, TM instead of T_D and B_M instead of B_D.

$$D_m = (g \times C_{VM} \times T_M)/(B_M \times 4\pi^2) \qquad (3\text{-}2)$$

The damping coefficient shall be computed using the efficient damping of the isolation system built in accordance with Section 1665. 5. 2-The applied load shall be calculated using linear interpolation for effective damping values other than those stated.

Table 3. 3 Damping coefficients, BD and Bm (Table A 16-C)

Effective damping β_D or β_m (Percentage of critical)[1,2]	**B_D or B_m factor**
≤ 2	0,8
5	1,0
10	1,2
20	1,5
30	1,7
40	1,9
≥ 50	2,0

Effective horizontal stiffness calculation

In the direction discussed, the horizontal stiffness of a single isolator in the isolation system is computed as follows.

$$K_H = K_eff = W/ g \times [(2\pi / T_D)]^2 \quad (3\text{-}3)$$

(W), would be the ordinary force exerted on a single isolator and is computed by reducing the structure's total weight by the number of isolators.

Energy dissipated per cycle at the specified displacement (Wd)

The energy absorbed by the seismic isolator for each cycle can be calculated with the formula below. This value is used to calculate the characteristic strength Q_d.

$$W_D = 2\pi \times K_eff \times (d_D)^2 \times \beta_eff \quad (3\text{-}4)$$

Force at zero displacement under cyclic loading

The characteristic strength of a single isolator is calculated as follows, as *d*y is the displacement in the flow state, since this value is too small compared to the d_D design displacement.

$$Q_D = W_D / (4 \times d_D) \quad (3\text{-}5)$$

Calculation of yield displacements

The displacement in the case of shear yielding where the change in the horizontal stiffness of the seismic isolator occurs is calculated as follows. The pre-yield stiffness is represented by Ku, while the post-yield stiffness is indicated by Kd.

Post yield stiffness of the isolator

$$K_d = Keff - (Qd / d_d) \quad (3\text{-}6)$$

Yield displacement

$$D_y = Q_d / (9 \times K_d) \quad (3\text{-}7)$$

Yield Force

$$F_y = (K_U \times K_d) \quad (3\text{-}8)$$
$$K_U = 10 \times K_d$$

Maximum force

$$Fm = QD + Kd\ d_D \quad (3\text{-}9)$$
$$Ku = Fy / Dy$$

Check for Keff

$$Keff = Fm / d_D \quad (3\text{-}10)$$

The rigidity of the main core of the (LRB)

The horizontal stiffness provided by the lead core can be calculated with the formula below.

$$K_{pb} = Q_d / d_D \quad (3\text{-}11)$$

Stiffness of rubber in (LRB)

The rigidity provided by the rubber part is found by removing the stiffness provided by the lead core from the total lateral stiffness of the isolator.

$$K_{rub} = K_d = K_H - K_{pb} \quad (3\text{-}12)$$

Total thickness of lead rubber bearing

$tr = d_D / \Upsilon = 0.3313 / 0.5$ (3-13)

Where Υ is the design shear strain which is 0.5 (as per T.K. Dutta).

Diameter of lead rubber bearing

$$D_{bearing} = \sqrt{\frac{Krtr}{400\pi}} \quad (3\text{-}14)$$

Where,

$D_{bearing}$ = Diameter of (LRB)
tr= Total (LRB) thickness.

D_{pb}= Diameter of main core of (LRB)

$$Dpb = \sqrt{\frac{4Qd}{\pi\sigma pb}} = \sqrt{\frac{4x83.32}{\pi x11000}} = 0.09821\ m \quad (3\text{-}15)$$

Where,

σpb = Total yield stress in lead, it is assumed to be 11 pa

Lead core area in (LRB)

$$Apb = \frac{\pi}{4} x\ (Dpb)^2 \quad (3\text{-}16)$$

Diameter of force free section

$D_{ff} = D_{bearing} - 2t$ (3-17)

Where t is the single layer thickness which is 0.01 m

Force free area

$$A_{ff} = \frac{\pi}{4} x\ (Dff)^2 \quad (3\text{-}18)$$

Totally loaded surface area

AL = Force free area – Area of lead core (3-19)

Total height of lead rubber bearing

Height = (N x t) + (N-1)ts + 2tap (3-20)

Number of rubber layer $= \frac{0.2}{t} = \frac{0.2}{0.01} = 20$

t is the single layer thickness which is 0.01 m

ts is the thickness of steel lamination which is 0.003m

tap is the laminated anchor plate thickness which is 0.04 m

Horizontal strength of the bearing

$K_b = \frac{G\ Ar}{H}$

Where,

G indicates the shear modulus (varying from 0.4 to 1.1 Mpa) Using 1 Mpa,

Ar = rubber surface area = 0.3100 m2

(LRB) height = 0.337 m

Totally vertical bearing

$Kv = \frac{6GSi^2 Ar\ K}{(6GSi^2+K)H}$ Vertical rigidity is calculated. (3-21)

The main isolator parameters used in the building are specified in the table

Table 3. 4 Rubber isolator parameters to be used in the subject structure.

Inertia due to rotation	1 KN/m
U1 – Effective stiffness (kN/m)	1067391.17
U2 – Effective stiffness (kN/m)	1067.39
U2 – Stiffness (kN/m)	1050.64
U2 – Yield Strength (kN)	5.088
U2 – Distance from End-J	4.8436E-4
U2 – Post Yield Stiffness Ratio (Kd/Ku)	0.1
U3 – Effective stiffness (kN/m)	1067.39
U3 – Stiffness (kN/m)	1050.64
U3 – Yield Strength (kN)	5.088
U3– Distance from End-J	4.8436E-4
U3 – Post Yield Stiffness Ratio (Kd/Ku)	0.1

3.5 Fluid viscous damper structure and efficacy

A fluid viscous damper is made from a piston head has orifices in the chamber that are filled with visco-elastic material (silicone or oil). When the damper is compressed, the incompressible fluid volume decreases due to piston area movement, which provides restoring force. An accumulator prevents this force via absorbing and holding a quantity of liquid released by the hydraulic cylinder in the preparation zone. Fluids escape due to the vacuum formed as the rod retracts. Previous research indicates that it is the optimum energy dissipating device due to its efficient energy dissipation, high dependability, and low cost. Visco-elastic dampers are typically utilized as horizontal dampers above the basement level. Modern dampers are classified as metallic yielding dampers, viscoelastic dampers, and friction dampers.

Damping Force (F) = Damping Constant (C) x Velocity (V) $^{\alpha}$ (3-22)

Where:

- F: damper force
- C: damping coefficient
- V: velocity
- α: Damping exponent that can range from 0.01 to 1.00. (Linear behavior equal to 1.00). Many optimized structures use **α = .3** (Nonlinear damper). However, in this work due to the seismic code that is being considered it was taken as minimum value 0.3.

In this equation, there is no spring force; the damper energy varies only with velocity. At a specific speed, the force will be the same at any point in the stroke. Due to the lack of restoring force provided by dampers, the building must endure overall static lateral stresses.

For velocities less than 0.1mm/s, standard value setups of (FVD), usually have very modest response forces. When the stimulation or vibration motion speed exceeds 1mm/s, the (FVD) begins to counteract with an increasing response force, as shown in Figure 3.5. A higher the alpha value in the graph the more elliptical it will look. For this reason, to achieve being in the nonlinear range a small alpha (less than 1.00) value should be taken.

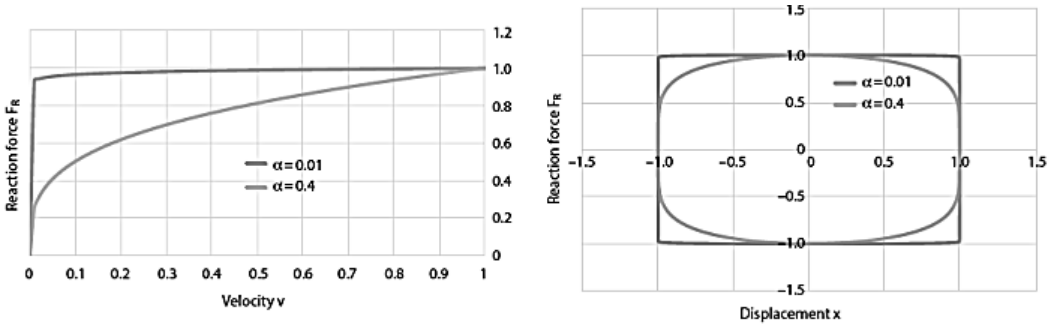

Figure 3. 5 A typical viscous fluid damper's action. The right side shows a typical force/velocity diagram, while the left side shows a typical force/displacement diagram.

Energy considerations clearly demonstrate the influence of introducing a supplemental viscous damper to a structure in seismic-resistant design [23]. The following energy equilibrium equation describes the occurrence of a building reacting to ground movement caused by an earthquake:

$$EI = Ek + Es + Eh + Ed \quad (3\text{-}23)$$

In this case, EI represents seismic energy required, Ek represents mechanical energy, Es represents recovered flexible strain energy, Eh represents irreparable energy absorption effort, and Ed represents the vibrations generated by the supplemental viscous dampers. The right side is essentially the resource capability, while a left side is the energy consumption caused by the earthquake shaking on the building. The energy grid has to be greater than energy consumption for a designed to resist a seismic. The power generation in conventional earthquake resistance is mostly dependent on the term stress - strain energy, Eh, which originates from the building's deformations. The addition of energy will boost the system's energy absorption capability for a building with dampers (Ed). In general, the design is made should facilitate early connection of the (FVD), by absorbing the energy input prior to the primary building's deformations. In other terms, the building's substructure would be adequately insulated, and the building's efficiency when subjected to ground shaking will be enhanced [24].

Fluid viscous damper installation in buildings

The installation of the dampers in the structure is relatively simple and similar to that required by steel frames. It consists of placing a metal frame in one of the vanes of the portal frames in concrete (columns- beam) previously the dampers are described

in the building system and are located at the edges of the corners, are installed as shown in Figure 3.6

Chevron:

The device is placed horizontally parallel to the roof in such a way that the devices absorb the horizontal forces directly using all their capacity before the action of this type of load. Its main disadvantage is that they occur on stresses in the middle part of the beam near the damper, as shown in Figure 3.6

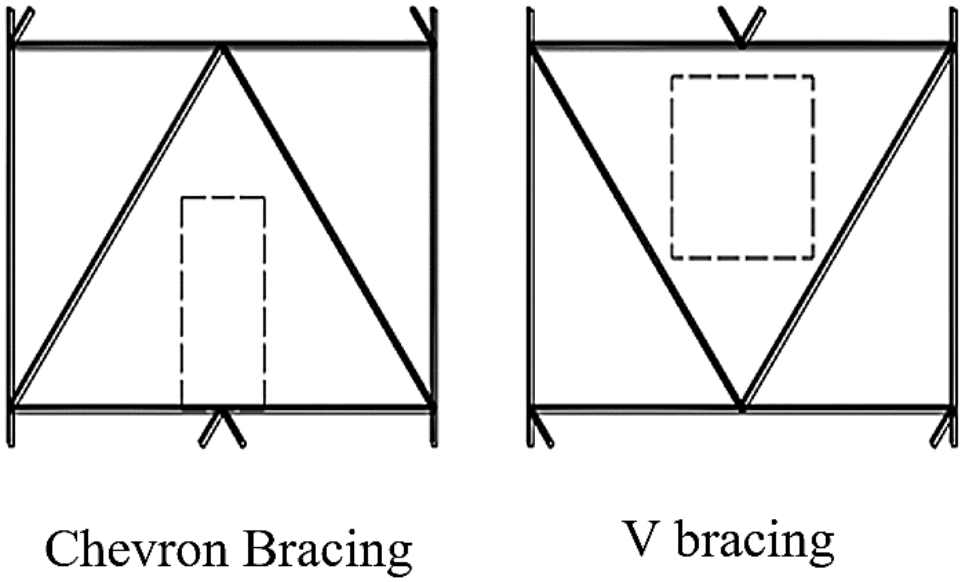

Figure 3. 6 Typical chevron designs

Firstly, the damping coefficient C for non-linear devices from equation (3-22) should be calculated the equation is provided for obtaining the aforementioned value, (3-23).

$$\xi d = (\sum \lambda Cj\phi rj^{1+\alpha}) (\cos^{1+\alpha} j\ \theta j) / (2\pi A^{1-\alpha)} (\omega^{2-\alpha} \sum mi\phi i^{2}) \quad (3\text{-}24)$$

Where:

- ξd = The system's corresponding damping rate as a function of non-linear dampers,
- λ = Lambda value,
- Cj = Absorber damping efficiency.
- mi = Mass of level.
- θj = Damper sloping angle.

- ϕi = Movement mode at the level.
- ϕrj = Damper top and bottom walls motion.
- A = Amplitude.
- ω = Angler frequency.

It is vital to remember that in a multidimensional degree - of - freedom (MDOF) system, the mean cumulative dissipation rate is specified by equation (3-24)

$$\xi eff = \xi 0 + \xi_{\mathrm{d}} \qquad (3\text{-}24)$$

Where $\xi 0$ signifies the natural dynamic response of the device without dampers while ξd indicates the viscous dissipation rate caused by the dampers. For steel buildings, the intrinsic damping is typically set at 5%, whereas the (FVD) is determined by the desired damping to be obtained. Inverting equation (3-24), the viscous damping ratio is defined by:

$$\xi d = \xi eff - \xi 0 \qquad (3\text{-}25)$$

Once the viscous damping coefficient has been defined, the stiffness K of the device can be computed. Even though the device depends only upon the velocity, the software requires a stiffness value. Therefore, the K value to be taken for the modelling is the bracing/metallic arm which links the device to the structure. This parameter can be computed as:

$$\mathrm{K} = \mathrm{EA} / l \qquad (3\text{-}26)$$

Where:

- E: steel elastic modulus,
- A: area of the steel section,
- l: length of the brace.

It is important to have a significant area (A), in order to minimize the elastic deflections and maximize the damper deflections, achieving in this way a complete activation of the device under a seismic excitation.

The result properties of a fluid viscous damper

Finally, results values shown in table below. In Sap2000 input the viscous damper values are assigned to the structure in the form of V or V inverse like chevron bracing throughout the height of the structure at two sides Central of the structure.

Table 3. 5 Fluid viscous damper parameters to be used in the subject structure.

Stiffness	5158.699 E3 KN/m
Damping coefficient	2282.17 (KN. s)/m
Velocity exponent	0.3

3.6 Steps for defining building models by using SAP2000 program

A three dimension digital model of each building was developed in SAP2000 to models and designs buildings utilizing modal (RSA) and (THA), by inside SAP2000 software analysis tool. The study provide, the modelling and analytical decisions (input) used to create structural models, such as material specifications, structural system part types, connection details, loads, weight, and design standards.

3.6.1 Model structural input

The typical material characteristics in SAP2000, such as A992 steel, grade 50 steel, and concrete, were utilized to generate the structural models for this study. SI KN/m-in units were used. All-steel structural members were designated A992 steel, whereas HSS braces were assigned grade 50 steel. The materials' masses and weights were calculated, the masses were included into the supplied loads and recorded as equivalent point masses connected to the diaphragms.

For all steel frames with wide-flanges, SAP2000 v22's the section's default property values were applied. SAP2000 supported default section characteristics for Hollow/Tube structural sections (HSS) and I profile sections. There were no property modifiers assigned to any structural sections (for area, rotational inertia, mass, or weights).

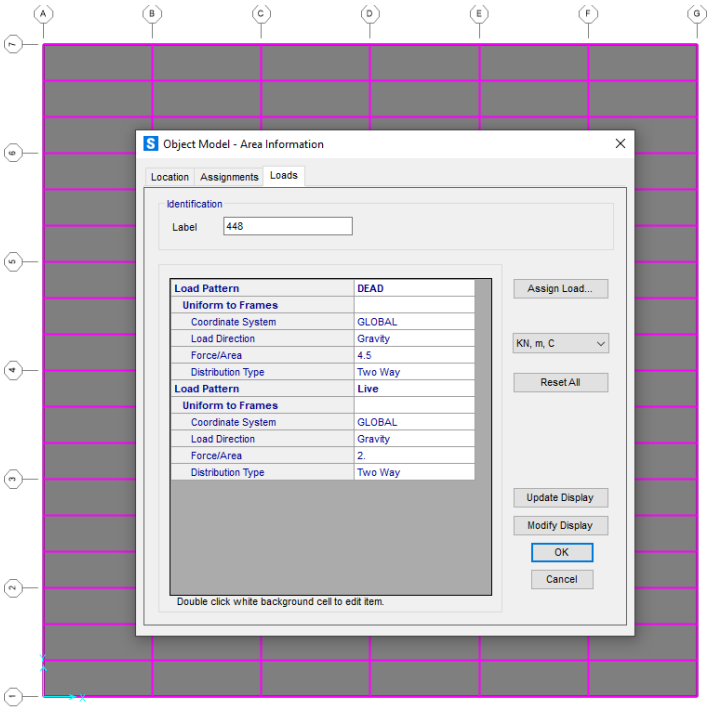

Figure 3. 7 Floor typical membrane and bending thickness of the slab.

All typical flooring were given the section attribute "slab." The part was designated as shell-thin, and the slab's membrane and bending thickness were inputted as 0.025cm to effectively equalize the membrane and bending characteristics. This modest stiffness assignment was created to mimic simply the lateral rigidity of the slab, this has already been taken into consideration by the rigid diaphragm assignments. As seen in Figure 3.7, every point on each level was designed as a rigid diaphragm.

The design load combinations were constructed once the loads were input into SAP2000. The modal analysis was performed using 12 modes, which were sufficient to output the 90% mass modal participation criterion of the x and y-transnationals, and z-torsional axis. The assessment involves a few more categories.

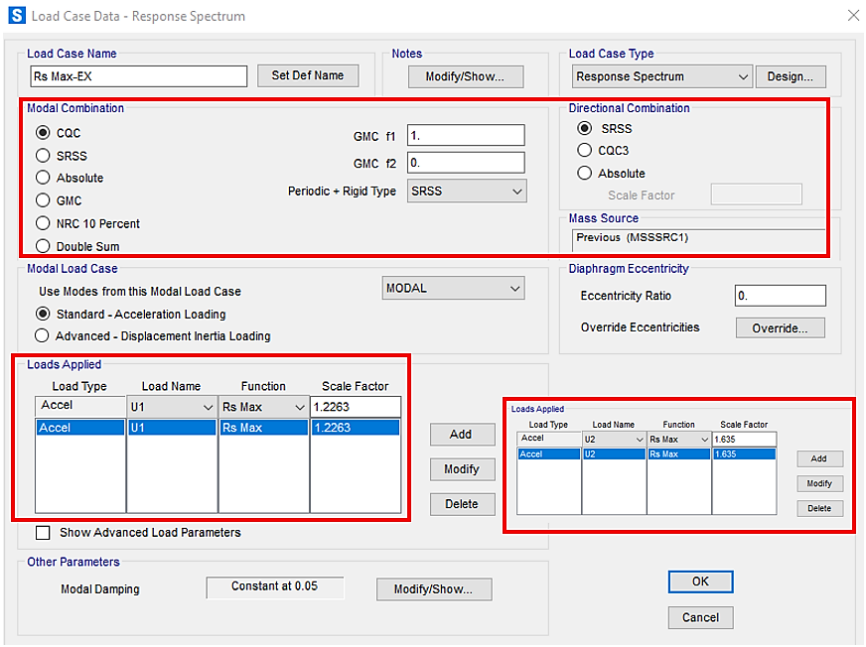

Figure 3. 8 Response spectrum analysis function.

The baseline design seismic and maximum considered seismic response spectra were imported into SAP2000 with a damping factor of 5% (0.05). Directional combinations of perfect quadratic combination (CQC), mode combination methodology, and root sum of squares (SRSS) methods were used to generate response spectral functions for each direction. The acceleration units of the response spectrum function were converted from g to inches/s2 using a scaling factor of 1.2263 in the x-axis and 1.635 in the y-axis, as seen in Figure 3. 3.8 Below.

3.6.2 Model rubber isolation system input

The proper way to implement a lead rubber bearing is through elements with link properties, according to the SAP2000 manual, as shown in Figure 3.9. After entering the link properties menu, select the "Rubber isolator" link type. It is well known that the adjuster operates in the system's axial axis, and a non-linear lead rubber bearing device is being used. Therefore, the direction must be U1, U2, U3 and nonlinear characteristics must be selected.

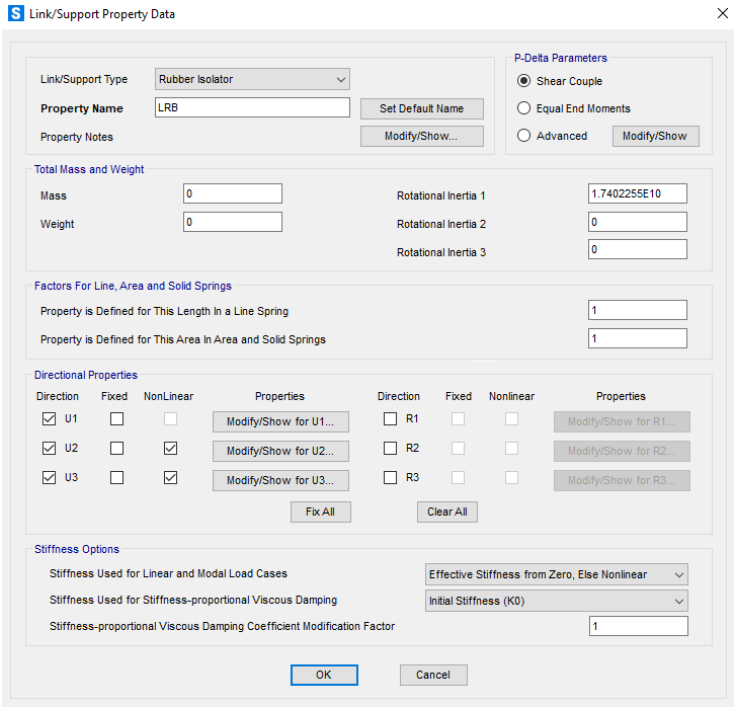

Figure 3. 9 Model lead rubber bearing isolation system property data.

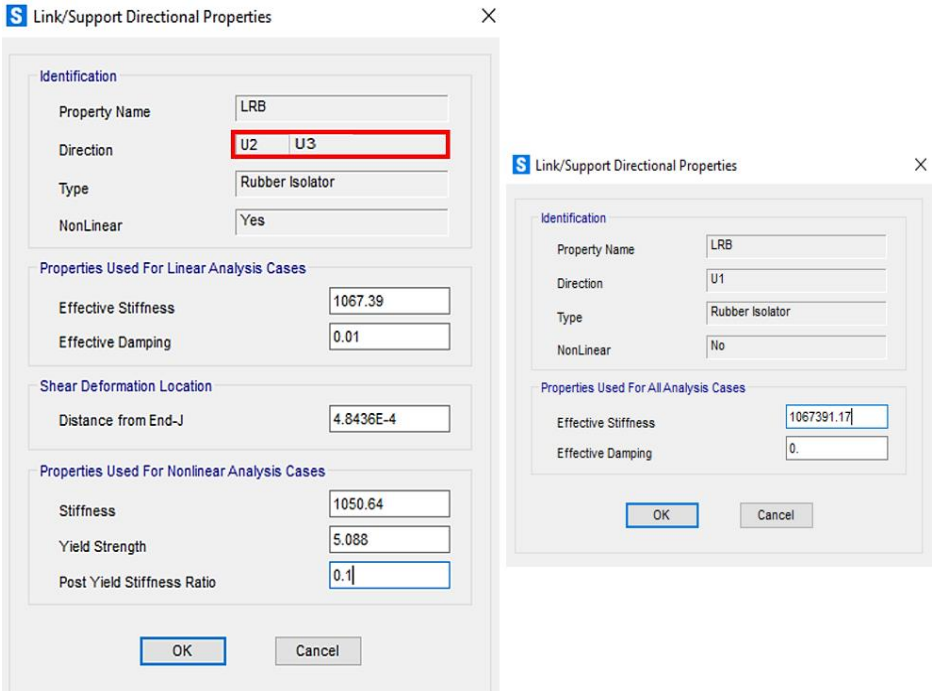

Figure 3. 10 Directional properties lead rubber bearing isolation system property data.

After knowing the values of the input parameters of the rubber isolator, it is possible to add the parameters required by the program, shows in figure 3.10 effective rigidity, yield force rigidity, absorption, and post yield rigidity proportion are all factors to consider.

To allocate the damper device in the building, the process to be performed is the same as drawing the frame element, but in this case, the link element is selected. The starting point of the drawing process does not matter. However, it is important to be consistent and keep the same direction for everyone.

Once the model analysis is complete, you can observe the behavior of each damper assigned in the model through the hysteresis diagram generated in each damper after activation.

3.6.3 Model fluid viscous damper system input

According to the SAP2000 documentation, the components with link attribute are the best technique to build a viscous damper (see Figure 3-31). The "Damper – Exponential" link type is selected once in the link property menu. A damper, as is widely known, functions in the device's on-axis, and non-linear (FVD) are employed. As a result, U1 must be chosen as the direction, and the nonlinear attribute must be chosen.

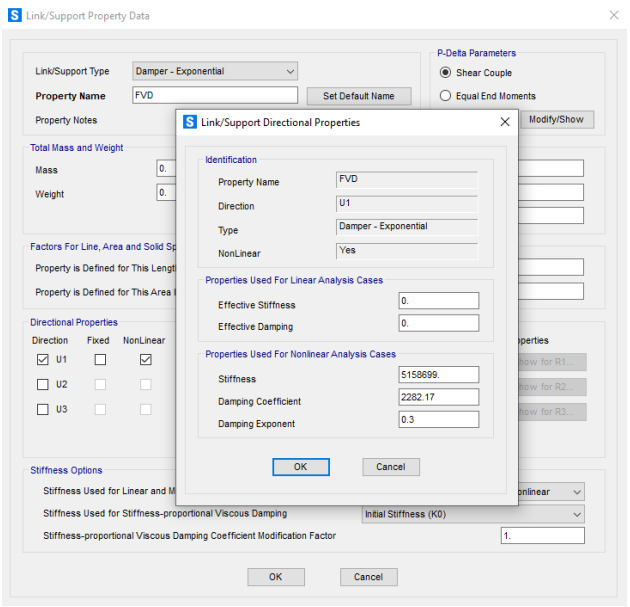

Figure 3. 11 Property data model fluid viscous damper system.

It is feasible to add the parameters required by the software after knowing the values of the damper's input parameters, as shown in figure 3.11. Rigidity, damping, exponential.

To assign the damper devices in the building, the process to be carried out is the same as drawing a frame element, but in this case, it is the link element the selected one. It does not matter the starting point for the drawing process. However, it is important to be consistent in keeping the same direction for each of them.

Once the model analysis is finished, it is possible to observe the behavior of each damper assigned in the model through the hysteresis graph that is generated in each one after its activation.

3.6.4 Steel design check input

Steel design check input in SAP2000 is required to analyze and design structural components in each structure. For strength and deflection needs, load combinations were used to develop the Special-Moment-frame (SMF), and Concentrically-Braced-Frame (SCBF) systems. A special moment frame was given the appropriate load combinations for the U1/x-direction modal response spectrum research, while the (SCBF) was given the suitable loads for the U2/y-direction. The gravity loads with the most significant controlling load and (LRFD) were 1, 2, and 3.

Point bracing was assigned alongside the chevron and inverted-v types, in which gravity beams are framed into moment frame beams, the length points of the (SMF) beams. At the midpoints of the (SCBF) beams, where the lateral braces crossed, point bracing was allocated. Due of stress studs linking the beams to the metal decking uniform bracing was applied to the top of the (SCBF) beams. The studs were expected to be positioned near enough together to provide appropriate constant bracing. To offer restriction against lateral torsional buckling, point bracing and uniform bracing were assigned throughout the design of the steel frames.

Following that, specific seismic data was entered by SAP2000. The “Section 4.2 ASCE 7-10 Design Criteria” defined a rho factor of 1 and design category C. In the steel frame design preferences interface, a (LFR) system and over strength factors of 3, 2 for the (SMF) and (SCBF), respectively, were set by default.

The design coefficients, factors, and analysis preferences for each lateral system, were specified using SAP2000, Interfaces for (SMF) and (SCBF) for steel frame

design preferences, as indicated in table 4.1 on page 52. The direct analysis approach was chosen as the design method. The constraint reduction factor (τb) changed with the axial force in each frame in this technique, which employed general second-order analysis. In SAP2000, these were the default analysis parameters. The following are the equations for these settings:

$$EI^* = 0.8\tau_b EI$$

$$EA^* = 0.8EA$$

$$\tau_b = \begin{cases} 1.0 \text{ for } \dfrac{\alpha P_r}{P_y} \le 0.5 \\ 4\left(\dfrac{\alpha P_r}{P_y}\right)\left(1 - \dfrac{\alpha P_r}{P_y}\right) \text{ for } \dfrac{\alpha P_r}{P_y} \ge 0.5 \end{cases}$$

$$B_1 \text{ and } B_2 \text{ not used}$$

$$K_2 = 1 \text{ (used for } P_n\text{)} \qquad \text{(3-33)}$$

Where:

- E = Modulus of Elasticity [KN/mm2]
- I= Moment of Inertia [mm4]
- A= Area [mm2]
- Tb = Stiffness Reduction Factor
- α = Design philosophy factor (1.0 for LRFD)
- Pr = Required second-order axial strength [KN]
- Py = Axial yield strength [KN]
- B1, B2 = Moment magnification factors
- K2 = Effective length factor

In the steel frame design choices interface, for each loading type, the standard lateral resistance frame design factors (ϕ) were also determined. So the double plate was not intended to be filler welder, the accumulated column net and double panel diameter was left out of the panel zone's minimum thickness local buckling check. As for purpose of welding the hollow structural parts (HSS), the submerged arc welding (SAW) procedure was used by default, allowing the HSS members' design wall thickness will not be lowered. The standard deflection ratio limitations were used to

assess the dead load, live load, and all deflections. All of the essential data was entered into SAP2000 when the steel frame design preferences interface was built, and the structures were complete and ready for development.

3.7 Analysis of earthquake

The term earthquake analysis refers to the study of analysis of buildings that involves predicting how a building (or non-building) structure will respond during an earthquake. It is a critical component of the approach of building system, seismic analysis, or structural evaluation and alteration in seismic-prone areas. During a quake or a violent windy storm, the building has the ability to 'wave' back and forth. This is known as the “Fundamental Mode”, because it has the lowest repetition rate of developing response. For the most part of the structures, yet having advanced modes of reaction, they are engaged individually during seismic events. Mainly seismic opposing structures were required for the design of a horizontal force corresponding to a building weight ratio delivered at every storey level. The dynamic qualities of the structure are obviously prejudicial to the loads generated during an earthquake.

Structural analysis methods

- Response spectrum analysis
- Time history analysis (Non-linear dynamic analysis)

3.8 Response spectrum analysis

The peak or steady-state reaction is represented by a response spectrum (displacement, velocity, or acceleration). It is a linear-dynamic statistical analytic approach in order to identify the expected greatest seismic reaction of a fundamentally elastic building by processing the role of each natural mode of vibration. The real-time history record is essential while doing Earthquake design and analysis of a building to be developed in a specific place. Nonetheless, it’s tough to keep all of the records at every place. Furthermore, structural model is not possible taken as merely dependent represents the building's maximal value of ground shaking reaction since it is built upon the occurrence It is independent of ground movement which has its own elastic properties. The seismic (RS) is a widely used tool in seismic design evaluation, with significant computing benefits in employing this approach of seismic response for the determination of deformations and modal analysis in structural systems.

Generally, most of the structures are analyzed using that response spectrum which is specified in the code of practice. And this analysis has become easy of using earthquake engineers for quite hardly small reasons now that is the mainly prominent component of this analysis because it is very appropriate it also allows very clear effects of different vibrational modes. It is a fundamental method for calculating the forces acting for earthquake-resistant structural elements. This approach calculates the maximum reaction of a structure when it is subjected to ground shaking. To determine the modal parameters and rates of the building, a dynamic study of the system must be performed and has to solve an eigen value problem the coda provisions as per ASCE 7-16 method for multi-story building response spectrum method The approach entails calculating just the largest quantities of deformations and modal analysis in each excitation frequency utilizing uniform design frequencies which are the aggregate of seismic motion lateral forces are applied to the building to generate a building reaction that response happens to be equivalent to the maximum dynamic response that the structure would have undergone where vibration is only mode. So, if it is understood that the structure is vibrating in one mode only then this equivalent lateral force can straight away and provide us the maximum response and the structure would undergo in that particular mode of vibration.

3.8.1 Response spectrum analysis – ASCE 7-16

In order to assess earthquake load demands for structural a design basis earthquake intensity response spectrum was created based depending on the project's location, soil composition, and other criteria. A design basis earthquake seismic occurrence is characterized as having a uniform ten percentage chance of occurring in the next fifty years, or a recurrence interval of 475 years (ASCE 7-16). The design basis earthquake response spectrum was developed by reducing a maximum considered earthquake level spectrum to Sa-design basis earthquake = (2/3) Sa-(MCE), where (Sa). (MCE) level earthquake event is one that has a uniform 2 percentage probability of occurring in the next fifty years. The maximum considered earthquake intensity response spectrum was used to estimate the optimum movement of the isolators and, as a result, to design the isolation system's displacement capacity. The seismic performance levels of the structure were also gauged using DBE and MCE

seismic levels, which are detailed in the analytical part of this thesis. Figure 3.12 shows, the DBE and MCE response spectra employed in this work [25].

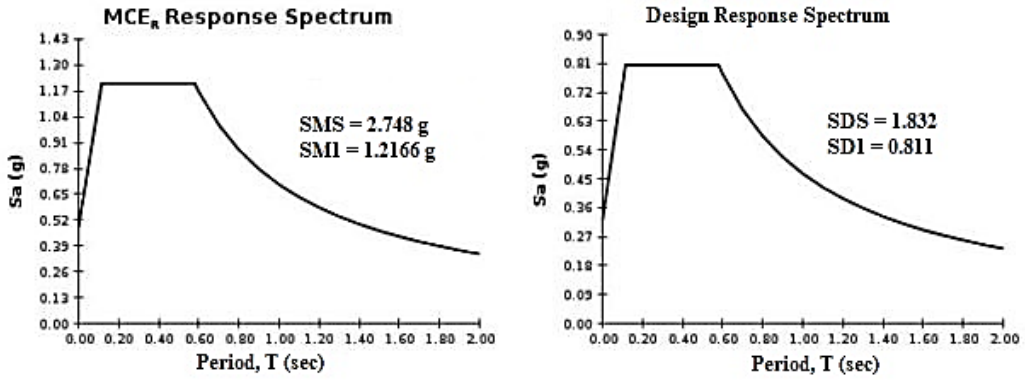

Figure 3. 12 Response spectrum analysis MCE and DBE.

According to ASCE 7-16 Modal (RSA) is detailed in chapter 12.9, requires establishing the structure's natural mode shapes and includes "an optimal inventory of modalities to ensure modal participation of at least 90% of an entire actual mass." of every horizontal orthogonal direction. The reaction of the structure must be calculated for each mode form and then put together, relative to the mass participation value of each mode, to provide the overall response value. A design basis seismic response spectrum with 5 percent critical damping is applied in the analysis for the building of conventional structure. While designing an isolated building, the damping value of the isolated modes must be "nothing except the efficient dissipation of the isolators or 30% essential, however is much less," according to ASCE 7-10 section 17.6.3.3.

3.9 Ground motion data

3.9.1 Selection of ground motion

This study aims to ascertain the behavior of regular steel structures while exposed against to horizontal earthquake excitations. The earthquake records used for this study have been obtained from the peer database. The (PGA) is 0.390 g, as well as the magnitude (M) of the ground motions range is 7.51, the ground acceleration records for component 150, as shown in Table 3.6.

Table 3. 6 Selected ground motion record.

Earthquake Name	Year	Station	NPTS	DT	Mw	PGA (g) H
Koceali-Turkey	1999	Yarimca	7000	0.0050	7.51	0.390

Where Mw is the magnitude of earthquake and PGA is peak ground acceleration, a ground motion record within 10km from the fault is referred to as near-fault earthquakes while ground motion recorded in a site located 4.83km away from is called far-field earthquakes, so the earthquake records selected for this study are all near-fault earthquakes with distance from the fault which is less than 10km. The earthquake records obtained from the peer database contained time histories in horizontal components of an earthquake.

3.10 Time history analysis (Non-linear dynamic analysis)

A time history study was necessary to account for the variation in the steel building's reaction during of the seismic ground shaking, includes modeling seismic ground motion acceleration that varies over time and recording the building reaction to the ground movement. This analysis took into account the following seismic response parameters:

- Displacements and velocity
- Accelerations
- Plastic hinge rotations

As well as the non-linear conduct of the isolation rubber bearings and the plastic hinge rotations of the building components, the time history studies performed in this study were non-linear. Hysteresis loops were used to track the non-linear behavior of the isolation rubber bearings over time (strength and displacement). The quantity of energy dissipated by the bearings was proportional to the area inside the hysteresis loops.

3.11 Properties of non-linear plastic hinges (ASCE 41-06)

The nonlinear hinge properties used in the study are described in this portion of the thesis.

3.11.1 Structural component plastic hinges deformation

Once building frames or linkages reach their material yield limit, plastic conduct ensues. Plastic conduct is described as a condition between yielding and failure (crushing and rupture, etc.) in which a material deforms when a load is applied to it, but the deformation persists when the stress is withdrawn. A basic steel stress-strain curve under tensile force is depicted in Figure 3.13 below.

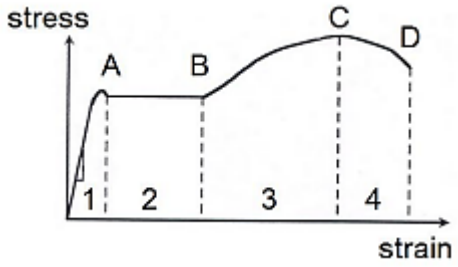

Figure 3. 13 Typical steel stress vs. strain curve.

The material's yield zone is the flat area of the figure area 2 in the middle of points “a” and “b” on the graph, for which no further force is required for the material to deform "Point B" is the point at which the steel achieves its plastic limit after yielding, at which point it regains rigidity and demands more stress to deform further. The strain-hardening zone 3 is shown in this diagram. The material may be deformed with less pressure at its ultimate strength “Point C”, until failure occurs at “Point D” owing to rupture.

The necking zone is the area between these two spots (zone 4). The nominal (lower bound) yield strength is usually employed when constructing a structural element. When analyzing a member's seismic performance (for yielding), on the other hand, the predicted "upper limit" strength of the frame is employed. The anticipated/ surrender strength ratios connect expected and yield stresses. Table 3.7 shows the ratios that were employed in this study.

Table 3. 7 Strength ratios required.

Seismic force-resisting system	Table 1-6-1, (AISC 327-05) Expected/Minimum yield stress ration Ry	Expected/Minimum tensile stress ration Rt
Steel special moment frames (SMF)	1.1	1.1
Steel special concentrically braced frames (SCBF)	1.4	1.3

That once steel has yielded, the stress-strain line of the material becomes curved. Non-linear analysis “in contrast to approximation linear-elastic techniques” is required to accurately capture this curvilinear behavior, As a result, non-linear time history analyses were used in this study. In non-linear building analysis, one method of measuring stress in a relinquished link or segment of a structural steel portion of the assumption is that a plastic hinge has developed. It was the approach utilized in this analysis. For plastic hinges, all yielding is believed to act regionally at a single location throughout the length of the each yielding zone of the structural element.

Ductility is the amount of plastic distortion that a structural element can endure before failing. Based on the projected ductility of the members, for defined degrees of strain/rotation of structural elements, structural actual performance are produced. A next section discuss through the exact standard also used assess the overall structural behavior for steel structures of this study.

3.11.2 Plastic deformation analysis guidelines

The (ASCE 41-06) code, titled “Seismic Rehabilitation of Existing Buildings”, divides building performance levels into three categories based on the degree of plastic deformation. In order to increase deformation/damage, the following categories were evaluated for this thesis:

- Immediate availability “S-1”: Minor damage and no long-term drifting.
- Protection of life “S-3”: Some permanent inter-drifts, significant damage.
- Preventing collapse “S-5”: The steel "back-bone curve" (force and deformation plot) in figure 3.14 below shows extensive damage and larger permanent drifts depicts these performance levels.

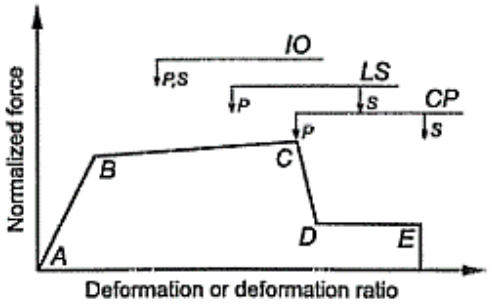

Figure 3. 14 Acceptance criteria for deformation.

The criteria for assessing chapter five contains steel factors of ASCE 41. The "backbone curve" of the material is formed by these structural strength criteria values, as shown in Figure 3.15 below. The requirements were resolute by the kind of element, the type of loading operation, and the size of the member “to account for slenderness”. As shown in Tables 3.8 and 3.9.

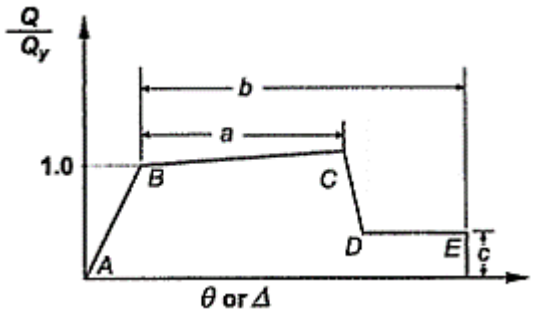

Figure 3. 15 Steel element or component force deformation relationship.

Table 3. 8 Parameters for non-linear modeling and acceptability criteria-Steel building

	Modeling Parameters			Acceptance Criteria[a]				
	Plastic Rotation Angle, Radians		Residual Strength Ratio	Plastic Rotation Angle, Radians				
					Primary		Secondary	
Component/Action	a	b	c	IO	LS	CP	LS	CP
Beams—Flexure								
a. $\frac{b_f}{2t_f} \le \frac{52}{\sqrt{F_{ye}}}$ and $\frac{h}{t_w} \le \frac{418}{\sqrt{F_{ye}}}$	$9q_y$	$11q_y$	0.6	$1q_y$	$6q_y$	$8q_y$	$9q_y$	$11q_y$
b. $\frac{b_f}{2t_f} \ge \frac{65}{\sqrt{F_{ye}}}$ or $\frac{h}{t_w} \ge \frac{640}{\sqrt{F_{ye}}}$	$4q_y$	$6q_y$	0.2	$0.25q_y$	$2q_y$	$3q_y$	$3q_y$	$4q_y$
c. Other	Linear interpolation between the values on lines a and b for both flange slenderness (first term) and web slenderness (second term) shall be performed, and the lower resulting value shall be used							
Columns—Flexure[a,f]								
For $P/P_{CL} < 0.2$								
a. $\frac{b_f}{2t_f} \le \frac{52}{\sqrt{F_{ye}}}$ and $\frac{h}{t_w} \le \frac{300}{\sqrt{F_{ye}}}$	$9q_y$	$11q_y$	0.6	$1q_y$	$6q_y$	$8q_y$	$9q_y$	$11q_y$
b. $\frac{b_f}{2t_f} \ge \frac{65}{\sqrt{F_{ye}}}$ or $\frac{h}{t_w} \ge \frac{460}{\sqrt{F_{ye}}}$	$4q_y$	$6q_y$	0.2	$0.25q_y$	$2q_y$	$3q_y$	$3q_y$	$4q_y$
c. Other	Linear interpolation between the values on lines a and b for both flange slenderness (first term) and web slenderness (second term) shall be performed, and the lower resulting value shall be used							

Table 3. 9 Steel brace frames- non-linear modeling parameters and acceptability criterion

	Modeling Parameters			Acceptance Criteria[6]				
				Plastic Deformation				
	Plastic Deformation		Residual Strength Ratio	Primary			Secondary	
Component/Action	*a*	*b*	*c*	IO	LS	CP	LS	CP
Braces in Compression (except EBF braces)[1,2]								
a. Slender								
$\frac{Kl}{r} \geq 4.2\sqrt{E/F_y}$								
1. W, I, 2L In-Plane[3], 2C In-Plane[3]	$0.5\Delta_c$	$10\Delta_c$	0.3	$0.25\Delta_c$	$6\Delta_c$	$8\Delta_c$	$8\Delta_c$	$10\Delta_c$
2. 2L Out-of-Plane[3], 2C Out-of-Plane[3]	$0.5\Delta_c$	$9\Delta_c$	0.3	$0.25\Delta_c$	$5\Delta_c$	$7\Delta_c$	$7\Delta_c$	$9\Delta_c$
3. HSS, Pipes, Tubes	$0.5\Delta_c$	$9\Delta_c$	0.3	$0.25\Delta_c$	$5\Delta_c$	$7\Delta_c$	$7\Delta_c$	$9\Delta_c$
b. Stocky[4]								
$\frac{Kl}{r} \leq 2.1\sqrt{E/F_y}$								
1. W, I, 2L In-Plane[3], 2C In-Plane[3]	$1\Delta_c$	$8\Delta_c$	0.5	$0.25\Delta_c$	$5\Delta_c$	$7\Delta_c$	$7\Delta_c$	$8\Delta_c$
2. 2L Out-of-Plane[3], 2C Out-of-Plane[3]	$1\Delta_c$	$7\Delta_c$	0.5	$0.25\Delta_c$	$4\Delta_c$	$6\Delta_c$	$6\Delta_c$	$7\Delta_c$
3. HSS, Pipes, Tubes	$1\Delta_c$	$7\Delta_c$	0.5	$0.25\Delta_c$	$4\Delta_c$	$6\Delta_c$	$6\Delta_c$	$7\Delta_c$
c. Intermediate	Linear interpolation between the values for slender and stocky braces (after application of all applicable modifiers) shall be used.							
Braces in Tension (except EBF braces)[5]	$11\Delta_T$	$14\Delta_T$	0.8	$0.25\Delta_T$	$7\Delta_T$	$9\Delta_T$	$11\Delta_T$	$13\Delta_T$
Beams, Columns in Tension (except EBF beams, columns)[5]	$5\Delta_T$	$7\Delta_T$	1.0	$0.25\Delta_T$	$3\Delta_T$	$5\Delta_T$	$6\Delta_T$	$7\Delta_T$

Especially at higher of rotations in yield were used to create building overall performance for flexural frames such as moment frames, whereas scale factors of yield movements are used to define structural performance levels for axial members such as braces as shown in tables 3.8 and 3.9 above and figure 3.16. Condition "a" characterized the majority of structural members in this study (i.e., non-slender).

The anticipated yield stress, Fye is used in the calculations that determine the yield revolve and forces of the beams-columns, as shown in figure 3.16. As previously mentioned, the anticipated yield tension is an upper-bound, more realistic strength for what the structural components would accomplish prior to actually yielding. It better realistic performance is crucial for appropriately analyzing building components for flexibility when due to earthquake loads, which is what this study did.

Beams: $\theta_y = \frac{ZF_{ye}l_b}{6EI_b}$ (Eq. 5-1)

Columns: $\theta_y = \frac{ZF_{ye}l_c}{6EI_c}\left(1 - \frac{P}{P_{ye}}\right)$ (Eq. 5-2)

Q_{CE} is the component expected strength. For flexural actions of beams and columns, Q_{CE} refers to the plastic moment capacity, which shall be calculated using Eqs. 5-3 and 5-4: k

Beams: $Q_{CE} = M_{CE} = ZF_{ye}$ (Eq. 5-3)

Columns: $Q_{CE} = M_{CE} = 1.18ZF_{ye}\left(1 - \frac{P}{P_{ye}}\right) \leq ZF_{ye}$ (Eq. 5-4)

Figure 3. 16 Force-deformation equations.

CHAPTER 4

4. DESIGN STRUCTURES PHASE

4.0 General

The lateral system of the conventional structure, the lead rubber bearing, the fluid viscous damper structure, and the steel system of the three structures are all developed for gravity and seismic loads during the design process. Each building is designed in compliance with ASCE 7-10 specification utilizing modal (RSA). SAP2000 is used to model and assess three structures for design.

4.1 Design specifications (ASCE 7-16)

(ASCE 7-16) “Minimum design loads”, for buildings and other structures is the specification for the design of structures and accept isolation systems. The basic design approach for any project includes the use of load and (LRFD), load combinations to test the structures ability to handle static, live, and seismic loads.

- Consider diaphragms to be rigid diaphragms.
- There aren't any horizontal or vertical regularities, = 1.0
- Soil categorization site type = C “Very dense soil and soft rock”
- Earthquake design type = C
- Site risk category = I “Low risk human life”
- Factor seismic significance = (Ie = 1.25)
- Design storey drift limit: Δ = (0.025)(Storey H)

ASCE 7-16 Chapters 12, 17 specify a design storey inter-drift limit of 0.025 for three models: conventional structure, base-isolated, and fluid viscous damper structures. The model structure in this study, on the other hand, was created with a tougher design storey inter-drift limit range of 0.003 - 0.160. Earthquake prevention systems (EPS) advised this storey drift limit range to enhance the lateral stiffness and seismic performance of base-isolated and fluid viscous damper structures. As previously stated, base isolation and fluid viscous damper work best for short, rigid structures with short durations. The severe designed inter-drift limit requirement was originally intended to keep the superstructure (building above the isolation platform) generally elastic, with very little to no yielding.

The design factors and coefficients in table 4.1 below were obtained from Chapters 12 – 17 of ASCE 7-10 and were utilized to design the structures in this study:

Table 4. 1 Coefficients and elements for designing a seismic force-resisting system.

Seismic force-resisting system	Table 1-6-1, (AISC 327-05)			Table 17.5.4.2 (ASCE 7-10)
	Response modification coefficient R	Over strength factor Ω_0	Deflection amplification factor Cd	Isolated response modification coefficient R_1
Steel special moment frames (SMF)	8	3	5.5	2
Steel special concentrically braced frames (SCBF)	6	2	5	2

Table 4.1 shows that the seismic isolated reaction made specific RI = 2, is less than the usual structural reaction made specific R = 8 and 6, (ASCE 7-16) limits the highest limit of RI to 2, in order to modify the base-isolated superstructure's comparatively low elastic seismic demand should be almost equal to or greater than the value obtained of a conventional building. The comparatively low RI value is intended to retain the superstructure's fundamental elasticity during design basis earthquake occurrences, “such that, the superstructure must have little or no persistent deformation owing to design basis earthquake events."

4.2 Design of the conventional steel building.

The conventional steel structure was created with SAP2000's seismic dynamic analysis and the “steel design and verification of structural” function. The analysis produced a completed horizontal structure with frame system sections figures 4.1 and 4.2 show an instance of this.

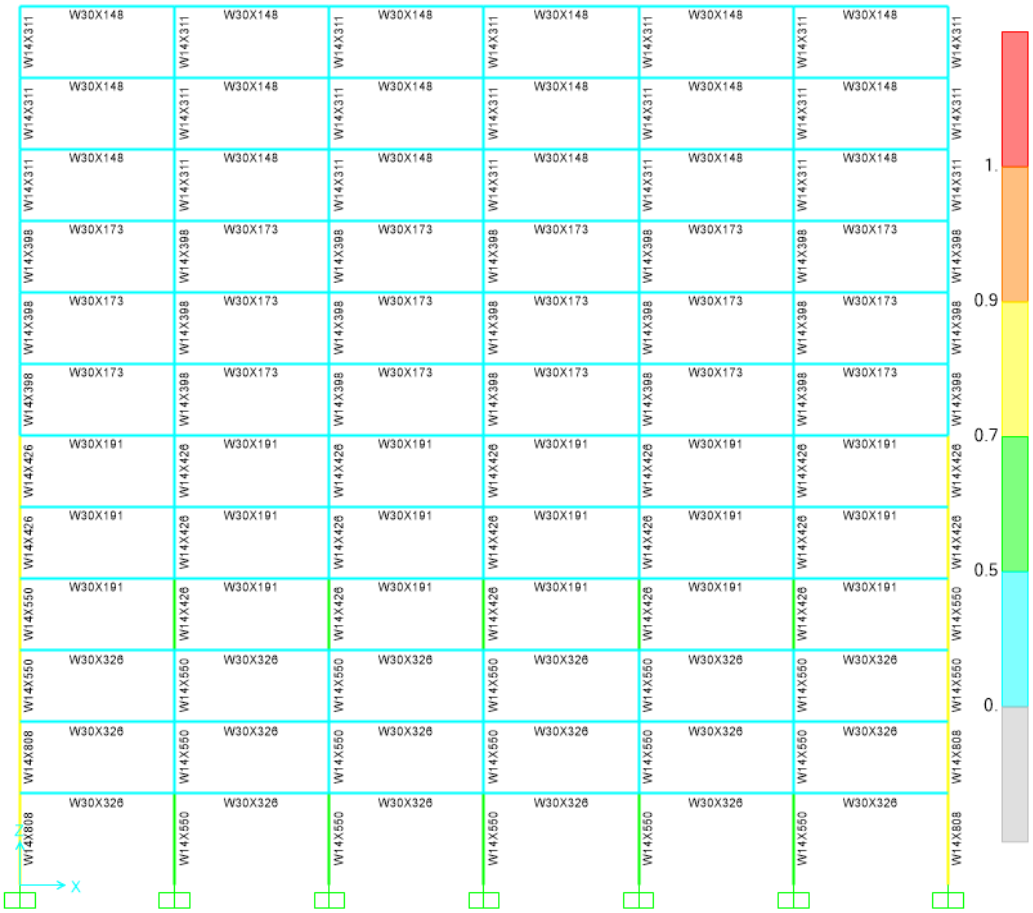

Figure 4. 1 Conventionally designed building (SMF).

The special moment framework (SMF) produced W14x columns and W30x beams. To facilitate construction, column joints are placed on each floor, and the same cross-section is used for the SMF columns of every three floors. The above figures 4.1 and 4.2 also illustrate the color-coded demand capacity ratio of structural members in the "Steel Structure Design/Structural Inspection" tool in SAP2000 (the severity ranges from green less than 0.50 to red greater than 0.95). The drift limit and relative stiffness limit govern the design of a special moment frame. The outside columns readily meet the comparative rigidity requirements, while the interior W14x columns

are regulated by W30x beams on either side. Categorically, as seen by the color coding in figure 4.2, the demand capacity ratio of the inner column remains above 0.70, and in some cases, 0.90.

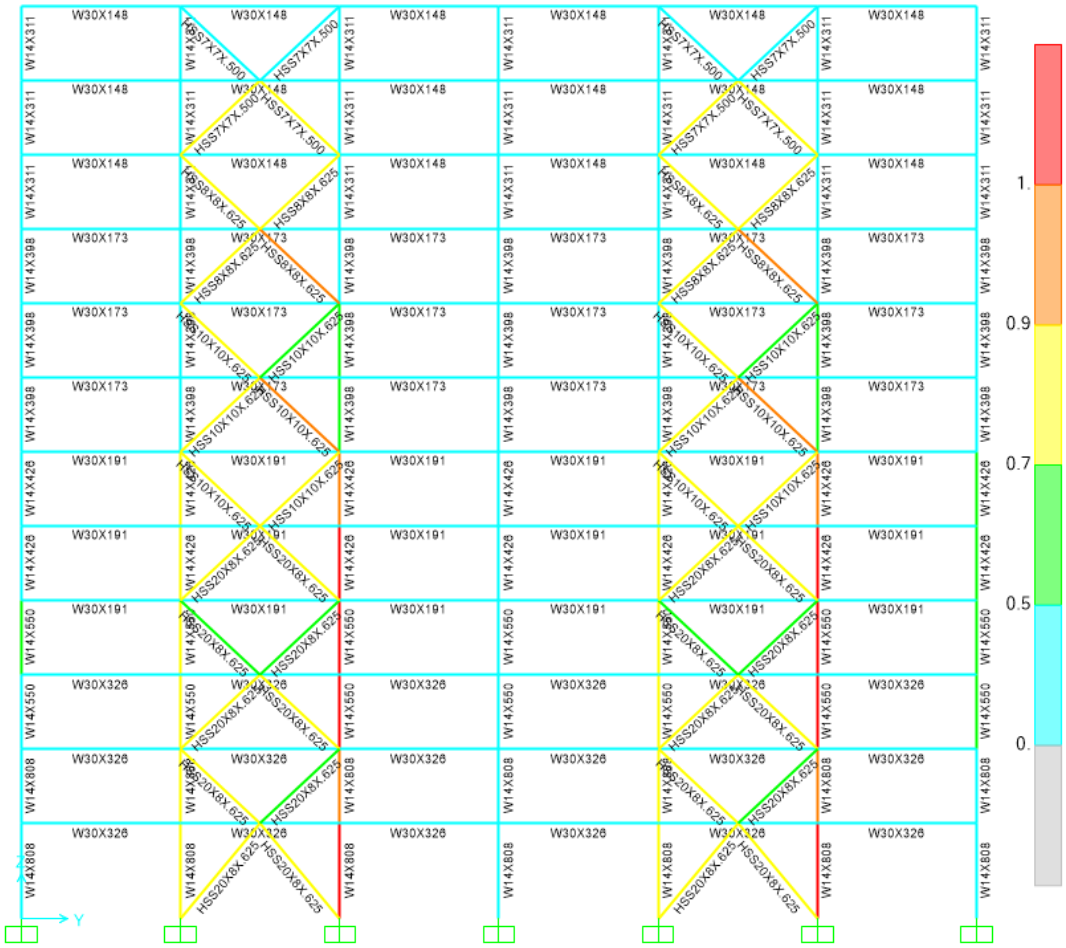

Figure 4. 2 Conventionally designed building (SCBF)

W14x columns, W30x beams, and HSS braces were produced via the special concentrically braced frame (SCBF). The force limitations of the braces and the respective stiffness limits of the frame elements were utilized to determine the design of the SCBF. The braces were built in such a way that they may give earlier than the frame participants such as the braces sustained greater demand-capacity ratios than the corresponding frame frames on every level. The most of the braces had demand-capacity factors more than 0.70, and many of the body members also had ratios greater than 0.70. As a result, the structural components that were carefully picked matched their plan criteria, and the conventional structure was effectively developed.

4.2.1 Design of the conventional steel building model

This part contains the final modal facts that were utilized to design the conventional building using dynamic response spectrum. Table 4.2 shows the structural with methods and overall mass participation rates of the designed conventional building.

X= U1 (SMF); Y= U2 (SCBF); RZ= Torsional

Table 4. 2 Conventional building modes (SAP2000 Modal analysis).

Mode	Period [Sec]	Governing Direction	Cumulative Mass Participation [%]		
			X	Y	RZ
1	2.5969	X	73.04		
2	2.202656	Y		66.60	
3	1.421308	RZ			69.66
4	0.904358	X_2	86.55		
5	0.679532	RZ_2			69.66
6	0.522668	Y_2		89.24	
7	0.476506	X_3	92.61		
8	0.365704	RZ_3			89.42
9	0.342932	Y_3		94.85	
10	0.26716	X_4	95.46		
11	0.248281	RZ_4			95.00
12	0.238677	Y_4		97.00	

In the 12 modes shown above the table 4.2, the minimum criteria of 90% mass participation was met in all modal directions (x, y-transnationals, and z-torsional). The conventional structure mode types. The 1st of two modes were translational in the x and y axes, as predicted, while the third mode-shape was once torsional around the z-axis.

4.2.2 Design of the conventional steel building drifts and strengths

The drift of the conventional infrastructure generated by the dynamic response spectrum analysis is shown in Table 4.3 below. It is important to noting that the design inter-drift in the x-axis (U1 – SMF) is 0.076, which is quite near to the 0.025 design drift limit. A similarity of these values is due to the fact that the design of SMF is restricted by inter-drift rather than frame strength, which is typical when constructing moment frames due to their higher flexibility than supporting members. In the y-

direction, the design inter-drift (U2-SCBF) is 0.0064. Since the strength of the SCBF is adjusted rather than the drift limit, drift can quickly exceed the specified drift limit.

Table 4. 3 Conventional steel building drifts modal

Storey	Special Moment Frame (SMF)	Special Concentrically Brace frame (SCBR)
	X-U1	Y-U2
12	0.072765	0.00475
11	0.100595	0.0058
10	0.127105	0.00635
9	0.14091	0.0064
8	0.15598	0.00655
7	0.166155	0.0064
6	0.16874	0.00625
5	0.166155	0.00525
4	0.147565	0.00485
3	0.121165	0.00385
2	0.10296	0.0036275
1	0.076725	0.0031725

4.3 Design of the lead rubber bearing isolation building.

The base-isolated structure was also developed by SAP2000 utilizing dynamic response spectrum analysis and the “steel design and verification of structural” function. The study yielded the final lateral system shown in figures 4.3 and 4.4 below.

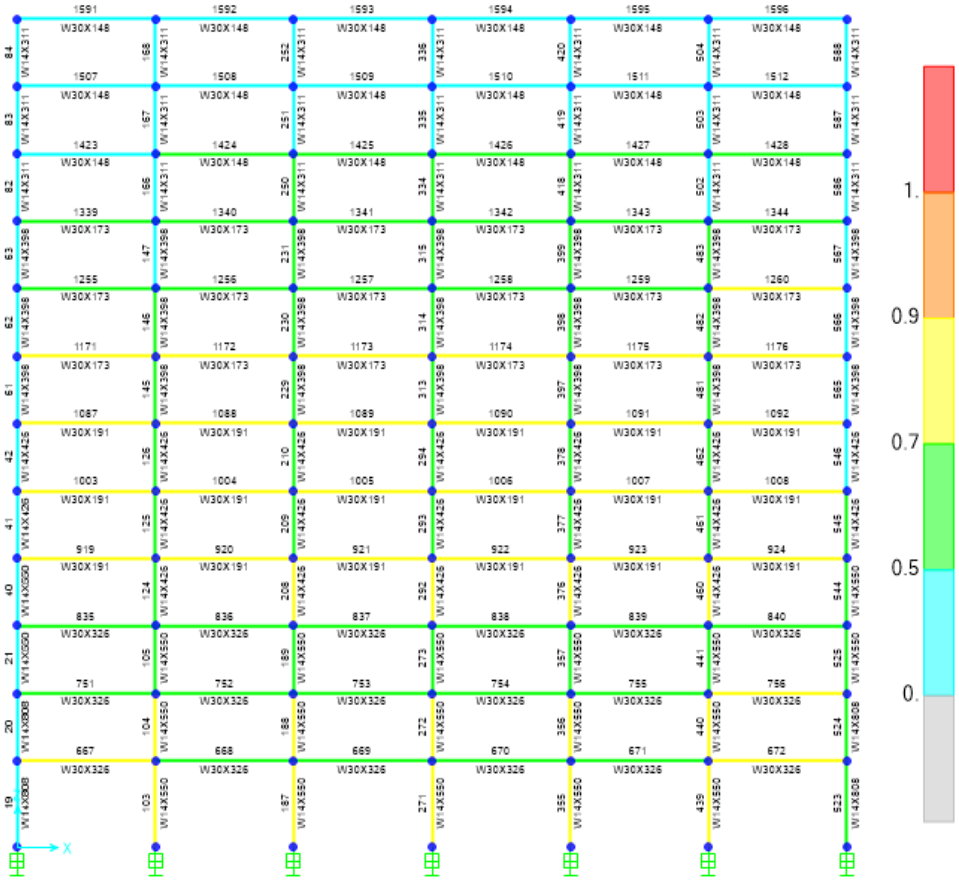

Figure 4. 3 Lead rubber bearing designed building (SMF).

The special moment frame (SMF) provides the same structural participants as the lead rubber bearing structure, with (W14x columns and W30x beams). Third, in terms of constructability, a column splicing has been locally on each floor, and different pieces have been utilized for the SMF columns on each of the three floors. The identical color-coded demand capacity ratio of structural components (severity ranging from less than 0.50 for blue to higher than 0.95 for red) has attained the same level as in the conventional structure and fluid viscous damper. The three structural (SMFs) utilize the same structural participants, in part because the design of the (SMFs) is governed by the inter-drift limit and relative stiffness limit in each situation. The main variations between the three buildings used to be a stricter design inter-drift limit used to be used for the lead rubber bearing structure (instead of the standard structural design drift limit of 0.0025, a range of 0.003-0.160 is used), and the lead rubber bearing structure incurred smaller storey inter-drifts than the conventional structure at the design basis earthquake design basis earthquake strength level.

When the same structural members are used, the smaller inter-layer drift and stricter drift limits of the basic isolation structure result in a demand capacity ratio similar to that of a standard framework. The outside columns of the lead rubber bearing structure, such as the conventional structure, readily exceed the relative rigidity requirements, whereas the interior W14x columns are regulated by W30x beams linked on either side. Additionally, as seen by the color-coding in figure 4.4, the internal column of the sustained demand capacity ratio reaches 0.50, and in certain cases 0.90.

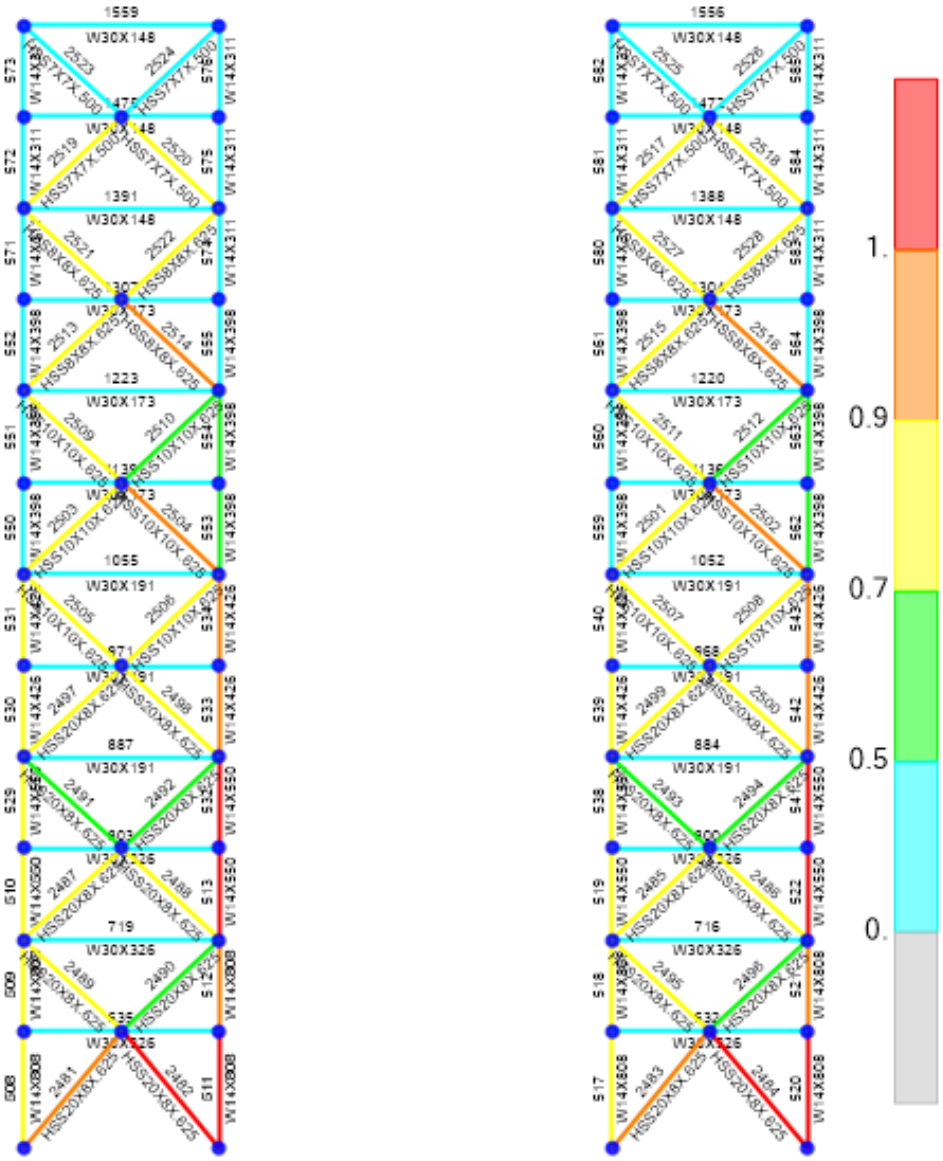

Figure 4. 4 Lead rubber bearing designed building (SCBF).

A same structural elements are produced by the special concentrically braced frames (SCBF) as the conventional structure and fluid viscous damper, with (W14x columns, W30x beams, and HSS brace). The design of (SCBF) is governed once again by the limit of the support's durability and the limit of the relative stiffness of the frame parts. Due to the use of similarly designed basic shears, these structures achieve a similar demand-to-capacity ratio. Compared with the fixed base and fluid viscous damper structures, the nominal base shear force generated by the base isolation and fluid viscous damper superstructures at the DBE is smaller, but the design base shear force is scaled down to a comparable value. Since the isolated response correction factor (RI=2), is less than the conventional structural response correction factor (R=6), the SCBF direction achieves a similar design base shear.

Similar to conventional structure, base isolation, and fluid viscous dampers, most braces are designed so they are more prone to yield than structural frame (i.e., braces have a larger demand-to-capacity ratio compared to each layer's associated frame members). The required capacity ratio of most braces has also reached 0.70 or more, and many frame members have also exceeded 0.70 ratios. Therefore, the closely selected structural section meets its design standards, and the base isolation structure is effectively designed. Since the fixed base, base isolation, and fluid viscous damper structures all use the same structural components, this thesis also covers the enhancement of seismic performance of a 12-storey steel structure with a fixed foundation utilizing the same base-isolation as before and fluid viscous dampers. The viscous damper in this study.

4.3.1 Design of lead rubber bearing isolation building model

The section contains the comprehensive seismic information needed to develop the lead rubber bearing building utilizing dynamic response spectrum analysis. Table 4.7 shows the modes and ultimate mass participation rates of the suggested base isolated building.

X= U1 (SMF); Y= U2 (SCBF); RZ= Torsional

Table 4. 4 Lead rubber bearing building modes (SAP2000 Modal analysis)

Mode	Period [Sec]	Governing Direction	Cumulative Mass Participation [%]		
			X	Y	RZ
1	5.079233	X	0.98231		
2	5.045302	Y		0.96562	
3	4.123765	RZ			0.99342
4	1.48983	X_2	0.98231		
5	1.39216	RZ_2			0.99342
6	0.921471	Y_2		0.99958	
7	0.675647	X_3	0.9994		
8	0.475889	RZ_3			0.99984
9	0.415867	Y_3		0.99992	
10	0.341583	X_4	0.99974		
11	0.291616	RZ_4			0.99996
12	0.286973	Y_4		0.99997	

The minimal condition of 90% mass participation was achieved in either modal axis x, y-transnationals, and z-torsional in the 12 modes shown above, exactly as it was in the (LRB) structure. The mode forms of the (LRB), structure are shown in table 4.4. The 1st of two mode-shapes were translational in the x, y axes, as expected, while the third mode was torsional about the z-axis.

4.3.2 Design of lead rubber bearing isolation building drifts and strengths

The drifts of the lead rubber bearing structure as a result of modal response spectrum analysis are shown in Table 4.5 below. It is important to noting that the design waft in the x-axis (U1 – SMF) used to be 0.14, which was within the rubber bearing design drift limit range of 0.0065-0.170. The similarity of the figures used to be due to the SMF's design being governed by the inter-drift limit rather than element force restrictions, which is common when building moment frameworks because to their greater flexibility when compared to brace frames. Once upon a time, the design inter-drift as in y-axis (U2 – SCBF) were 0.0065. The SCBF's design was formerly governed by way of strength rather than drift constraints, hence the design drift easily reached the design drift limit.

Table 4. 5 Lead rubber bearing building drifts model.

Storey	Special Moment Frame (SMF)	Special Concentrically Brace frame (SCBR)
	X-U1	Y-U2
12	0.07876	0.00665
11	0.106865	0.0078
10	0.133595	0.0084
9	0.147675	0.00855
8	0.162855	0.00875
7	0.173525	0.0088
6	0.176715	0.0087
5	0.176165	0.00795
4	0.162525	0.00755
3	0.149875	0.0066
2	0.17193	0.0065
1	19.83009	2.2728

4.4 Design of the fluid viscous damper building

The (FVD), structure was likewise created in SAP2000 utilizing dynamic response spectrum analysis and the "steel design and verification of structural" function. The study yielded the ultimate lateral system shown in figures 4.5 and 4.6 below.

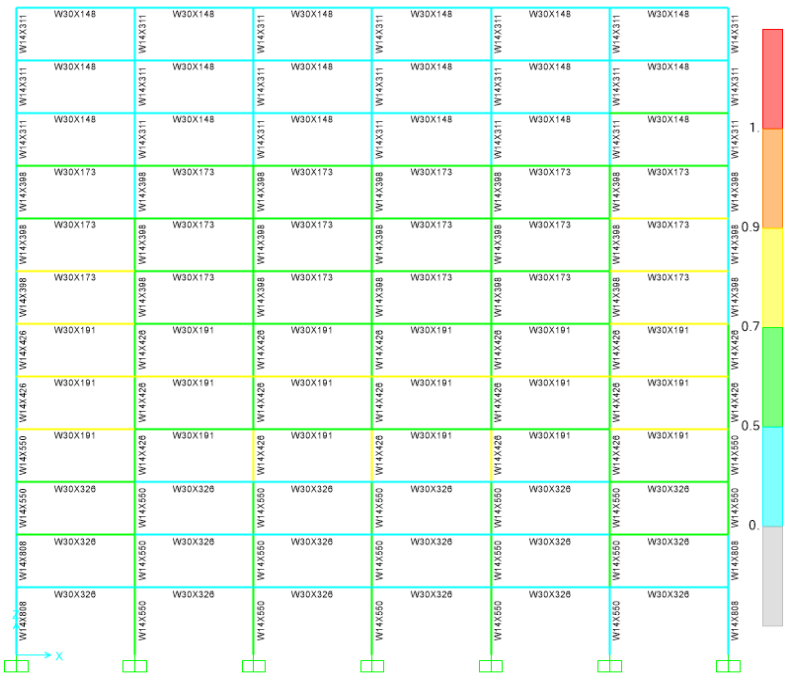

Figure 4. 5 Fluid viscous damper designed building (SMF).

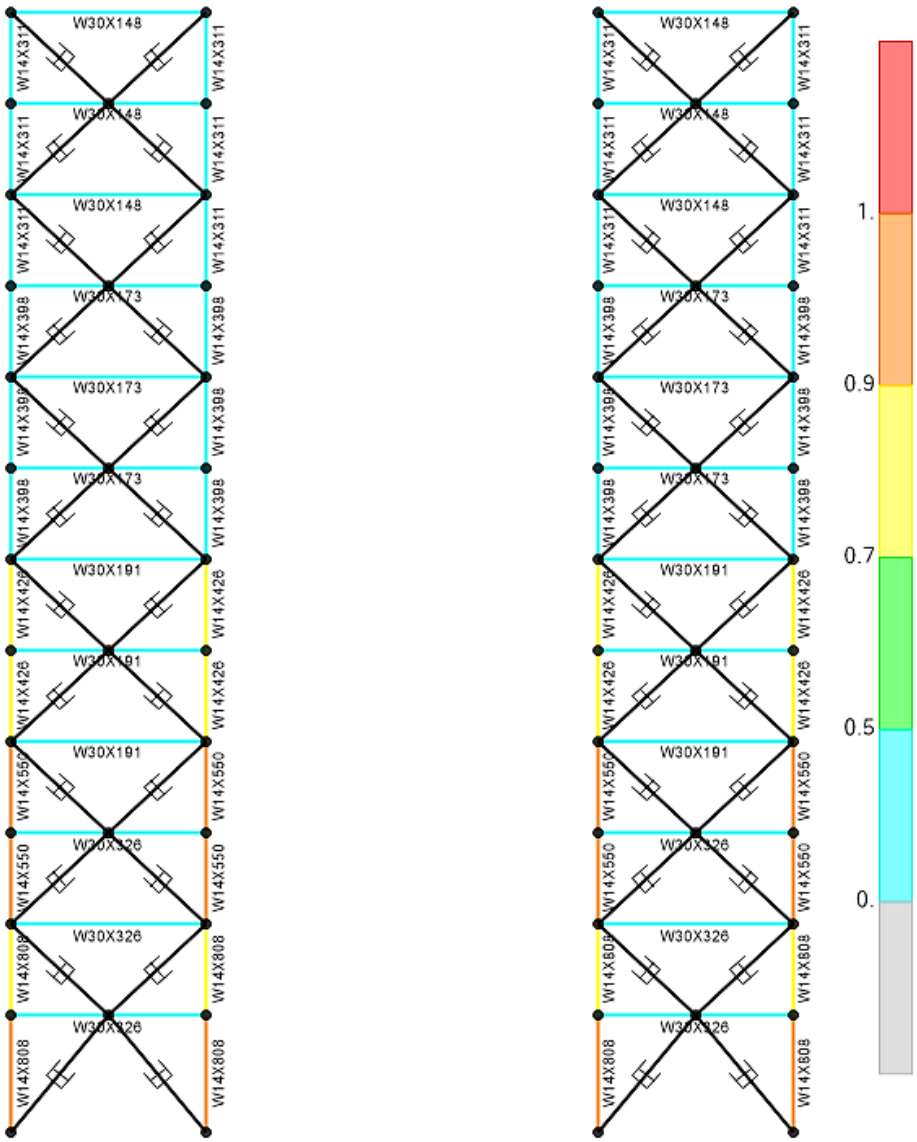

Figure 4. 6 Fluid viscous damper designed building (SCBF).

4.4.1 Design of fluid viscous damper structure model

The whole mode shapes information needed to construct the fluid viscous damper structure utilizing dynamic response spectrum method is shown in this section. Table 4.6 shows the modes and resultant mass participation ratios of the specified fluid viscous damper structure.

X= U1 (SMF); Y= U2 (SCBF); RZ= Torsional

Table 4. 6 Fluid viscous damper building modes (SAP2000 Modal Analysis)

Mode	Period [Sec]	Governing Direction	Cumulative Mass Participation [%]		
			X	Y	RZ
1	2.592414	X	0.73057		
2	2.498997	Y		0.72155	
3	1.546688	RZ			0.73536
4	0.902395	X_2	0.86558		
5	0.803428	RZ_2			0.73536
6	0.52921	Y_2		0.90707	
7	0.521505	X_3	0.92615		
8	0.41827	RZ_3			0.90417
9	0.342194	Y_3		0.95292	
10	0.293446	X_4	0.95466		
11	0.284131	RZ_4			0.95362
12	0.238143	Y_4		0.97163	

It should be noted that the minimal condition of 90% mass participation was achieved in every of the 12 modes shown above x, y-translational, and z-torsional. The fluid viscous damper structure's mode forms. The 1st of 2 mode-shapes were translational in the x, y axis, as predicted, while the third mode was torsional about the z-axis.

4.4.2 Design of fluid viscous damper building drifts and strengths

The drifts of the fluid viscous damper structure as a result of modal response spectrum analysis are shown in Table 4.7 below. The x-direction design drift (U1 – SMF) is 0.076, which is within the viscous damper design inter-drift limit range of 0.003-0.160. The closeness of the values was owing to the SMF's design being guided by the drift limit rather than member force restrictions, which is usual when constructing moment frames because of their greater flexibility than brace frames. The y-direction design inter-drift (U2 – SCBF) is 0.00905. Because the SCBF's design was guided by strength rather than drift constraints, the design drift rapidly exceeded the design drift limit.

Table 4. 7 Fluid viscous damper building drifts model.

Storey	Special Moment Frame (SMF)	Special Concentrically Brace frame (SCBR)
	X-U1	Y-U2
12	0.072545	0.006
11	0.10021	0.00905
10	0.126665	0.01165
9	0.14036	0.01275
8	0.155375	0.0143
7	0.16544	0.01525
6	0.16797	0.0155
5	0.16544	0.0154
4	0.14685	0.01355
3	0.12056	0.01055
2	0.102355	0.0075
1	0.076065	0.0054

CHAPTER 5

5. RESULTS AND DISCUSS

5.0 General

This study included a comparative analysis and the design of a 12-storey structure with a steel structure has a conventional building, a lead rubber isolator, and a fluid viscous damper used to be carried out for the analysis. The results obtained by using the SAP2000 program are mentioned in this chapter. Parameters related to data, which includes storey displacement, inter-storey drifts, shear force, acceleration of all models, and evaluates its performance using various techniques including (LRB) and (FVD).

The earthquake location time history analysis peer NGA strong motion database record in Kocaeli Turkey, 8/17/1999, yarimca, that providing non-linear assessment of dynamic structural behavior under stress that varies with function of time. Therefore, dynamic modeling and development of steel frame buildings are extremely significant in explaining the behavior of the steel framed building during dynamic stress.

5.1 Displacement and inter-drift analysis earthquake in the x-direction for fixed-base structure.

Displacement and inter-drift of the dissimilar storeys are determined by the use of earthquakes in the x-axis for conventional building table-5.1 below show information with graphs.

Table 5. 1 Fixed base displacement and drift analysis earthquake in the x-direction.

Fixed base in x-direction due to earthquake analysis						
	Cd	5.5	T	2.59	Δa = 0.025	
Storey	H (m)	Elastic Displacement (mm)	Amplified Displacement	Story Drift	Allowable	Check
		δ	Δm	Δi	Δa	
12	3.5	285.45	606.167954	28.7529	87.5	Safe
11	3.5	271.91	577.415058	39.64672	87.5	Safe
10	3.5	253.24	537.76834	49.98842	87.5	Safe
9	3.5	229.7	487.779923	55.31853	87.5	Safe
8	3.5	203.65	432.46139	61.13707	87.5	Safe
7	3.5	174.86	371.324324	65.06564	87.5	Safe
6	3.5	144.22	306.258687	66.02124	87.5	Safe
5	3.5	113.13	240.237452	64.91699	87.5	Safe
4	3.5	82.56	175.320463	57.65444	87.5	Safe
3	3.5	55.41	117.666023	47.31274	87.5	Safe
2	3.5	33.13	70.3532819	40.28378	87.5	Safe
1	4.5	14.16	30.0694981			

5.1.1 Fixed base for the displacement analysis earthquake in the x-direction.

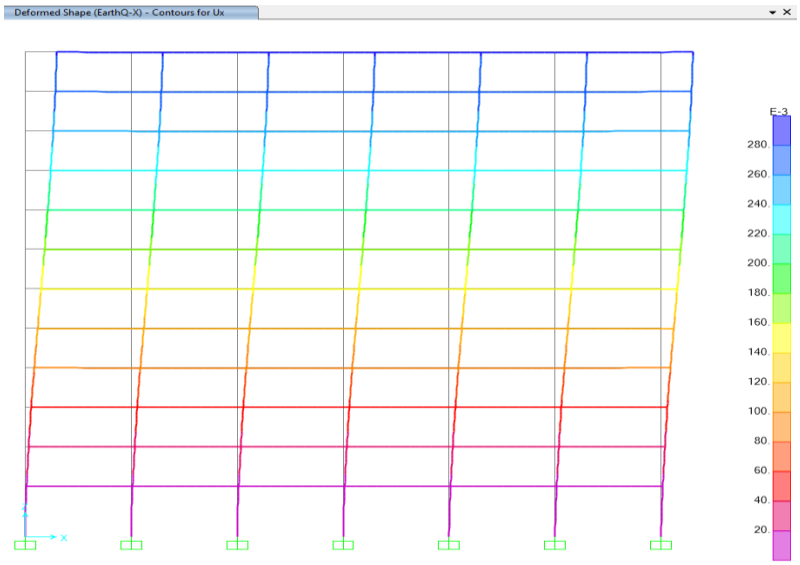

Figure 5. 1 Fixed base displacement analysis earthquake in the x-direction.

Each level increases of displacement moved from the original point to the upper end concerning the ground floor of the x-direction (SMF), from the bottom floor to the top floor, the displacement values shown in figure 5.1 above.

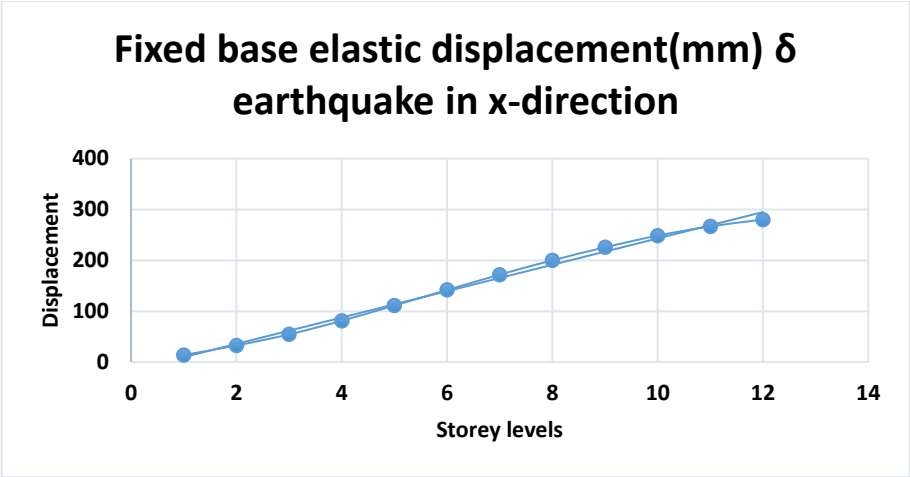

Figure 5. 2 Fixed base displacement analysis earthquake in the x-direction.

Figure 5.2 above also shows how this line rises from the first floor to the top floor. Because when the structure goes into the top floor, there will be a time period difference between the floors, and that is why the displacement increases on every level on the floors.

5.1.2 Fixed base for the inter-drift analysis earthquake in the x-direction.

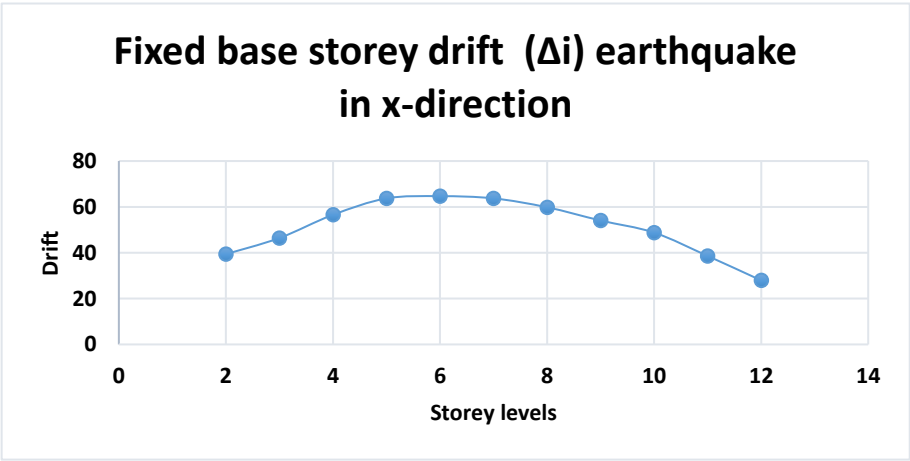

Figure 5. 3 Fixed base storey drift analysis earthquake in the x-direction

Figure 5.3 above shows the graph-line increases from the bottom to the upper level. Therefore when the growth goes into the middle part then reduces until the top floor, the floors will be divided by a time difference. The drift, on the other side, increases for each floor level.

5.2 Fixed base for the shear-force analysis in the x-direction earthquake.

Shear force in the 2-2 diagram in the x-direction is the one that shows the variation along the length of the beam and the column. The word Shear force is described as a force operating in a direction parallel to a surface or plane of a body's cross-section. The large shear-force occurs in ground floor columns because the lateral load and distributed load are acting at the level floors of a building frame. Table 5.2 below; however, the result shows the fixed base structure that greatest the shear-force for the corner column on the first-storey increase value 20%.

Table 5. 2 Fixed base shear force 2-2 diagram earthquake in the x-direction

Storey	Diagrams for Frame object	Diagrams for Frame object	Fixed base Shear Force 2-2 diagram earthquake in x-direction (KN)	
	Corner Column	Center Column	Corner Column	Center Column
12	588-W14x311	240 - (W14x311)	40.343	40.343
11	575-W14x311	239 - (W14x311)	6.109	6.108
10	574-W14x311	238 - (W14x311)	19.8	19.804
9	555-W14x398	219 - (W14x398)	14.699	14.722
8	554-W14x398	218 - (W14x398)	10.99	11.098
7	553-W14x398	217 - (W14x398)	16.23	15.732
6	534-W14x426	198 - (W14x426)	1.348	1.049
5	533-W14x426	197 - (W14x426)	48.174	36.971
4	532-W14x550	196 - (W14x426)	33.164	28.812
3	513-W14x550	177 - (W14x550)	27.316	20.861
2	512-W14x808	176 - (W14x550)	44.948	10.325
1	511-W14x808	175 - (W14x550)	356.908	212.745

5.3 Fixed base for the displacement and drift phase analysis earthquake in the y-direction.

The earthquake in the y-axis (SCBF) for conventional building determines the displacement and drift of different storeys, as shown in table 5.3 below.

Table 5. 3 Fixed base displacement and drift phase analysis earthquake for y-direction.

Fixed base in y-direction due to earthquake analysis						
	Cd	5	T	2.59	Δa = 0.025	
Storey	H (m)	Elastic displacement (mm)	Amplified displacement	Storey drift	Allowable	Check
		δ	Δm	Δi	Δa	
12	3.5	12.65	24.4208494	1.833977	87.5	Safe
11	3.5	11.7	22.5868726	2.239382	87.5	Safe
10	3.5	10.54	20.3474903	2.451737	87.5	Safe
9	3.5	9.27	17.8957529	2.471042	87.5	Safe
8	3.5	7.99	15.4247104	2.528958	87.5	Safe
7	3.5	6.68	12.8957529	2.471042	87.5	Safe
6	3.5	5.4	10.4247104	2.413127	87.5	Safe
5	3.5	4.15	8.01158301	2.027027	87.5	Safe
4	3.5	3.1	5.98455598	1.872587	87.5	Safe
3	3.5	2.13	4.11196911	1.486486	87.5	Safe
2	3.5	1.36	2.62548263	1.400579	87.5	Safe
1	4.5	0.6345	1.22490347			

5.3.1 Fixed base for the displacement analysis earthquake in the y-direction.

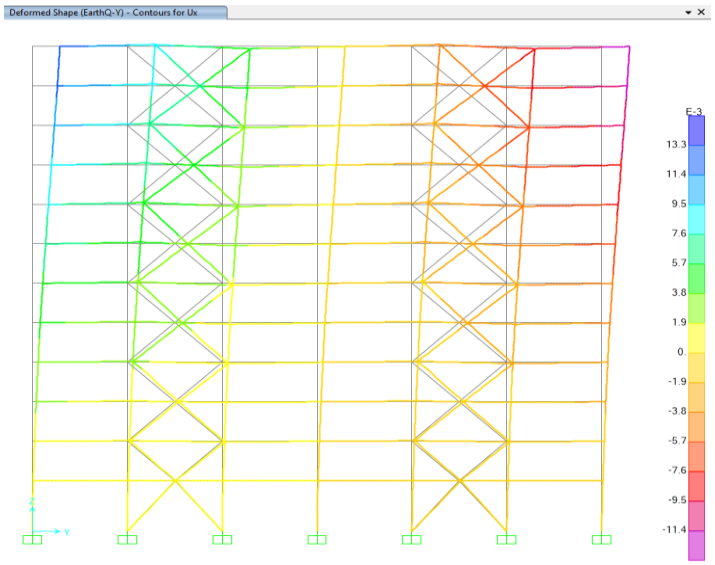

Figure 5. 4 Fixed base displacement analysis earthquake in the y-direction.

The increase of each level of displacement moved from the bottom to upper storey with relation to the bottom storey in the y-axis (SCBF) is compared with x-direction is much greater than y-direction showing in figure 5.4 above.

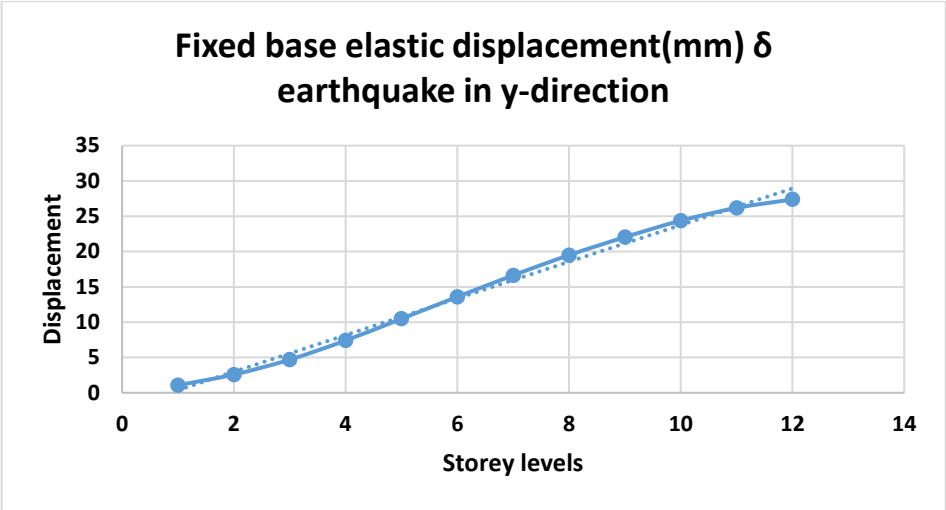

Figure 5. 5 Fixed base displacement analysis earthquake in the y-direction.

Figure 5.5 above also shows how the line increases from the first floor to the top floor. Because when it goes on in your structure onto the top floor, it increases displacement on every level floor. But when compared to y-direction, the displacement value is bigger than the x-direction.

5.3.2 Fixed base for the inter-drift analysis earthquake in the y-direction.

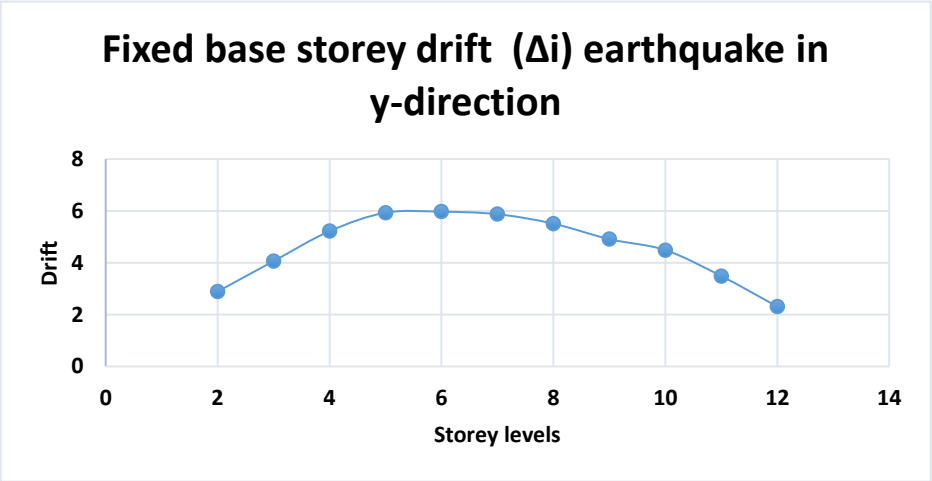

Figure 5. 6 Fixed base inter-drift analysis earthquake in the y-direction.

Figure 5.6 above shows the storey drift in the y-axis. The drift is smaller in the lower floors to higher in middle storeys and then reduced, which is the last floor that is the 12th storey, until reaching the value 1.8339mm.

5.4 Fixed base shear-force for the analysis in the y-direction earthquake.

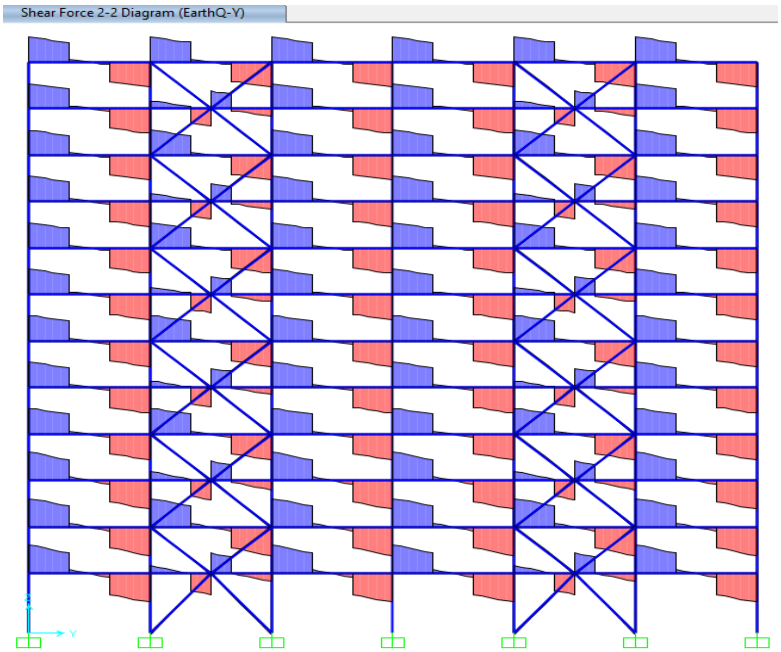

Figure 5. 7 Fixed base shear force 2-2 diagram earthquake in the y-direction.

The effect variant of alternate in storey shear used to be shown for the shear force in 2-2 diagram for y-direction is the one that indicates the variant alongside the length of the beam and column the figure 5.7 above shows.

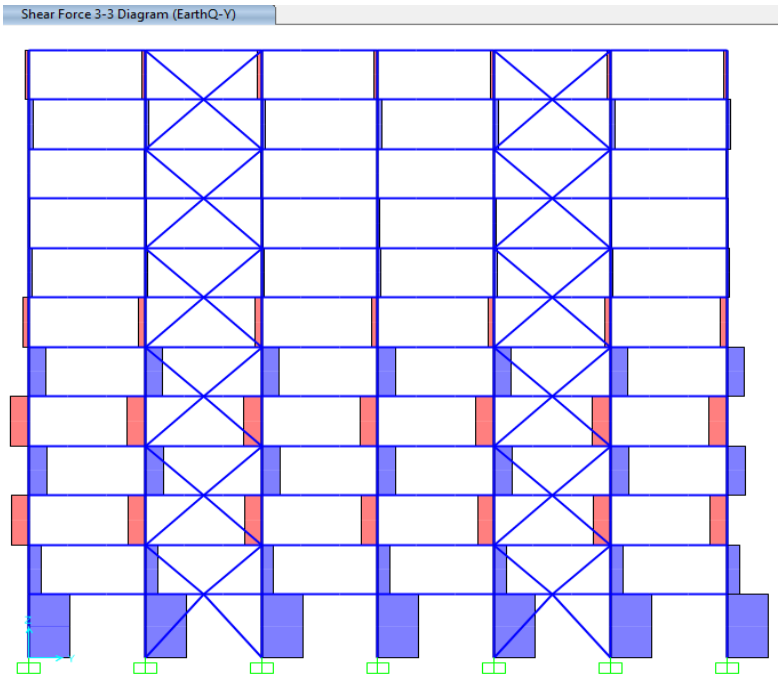

Figure 5. 8 Fixed base shear force 3-3 diagram earthquake y-direction.

Figure 5.8 above is the shear force in the 3-3 diagram in y-direction; as you can see, the large shear force occurs in the ground floor column to the 7th story. Because the external load is acting at the level floors of a building frame, so there is compression and tension on both sides.

5.5 Time period for the fixed base model.

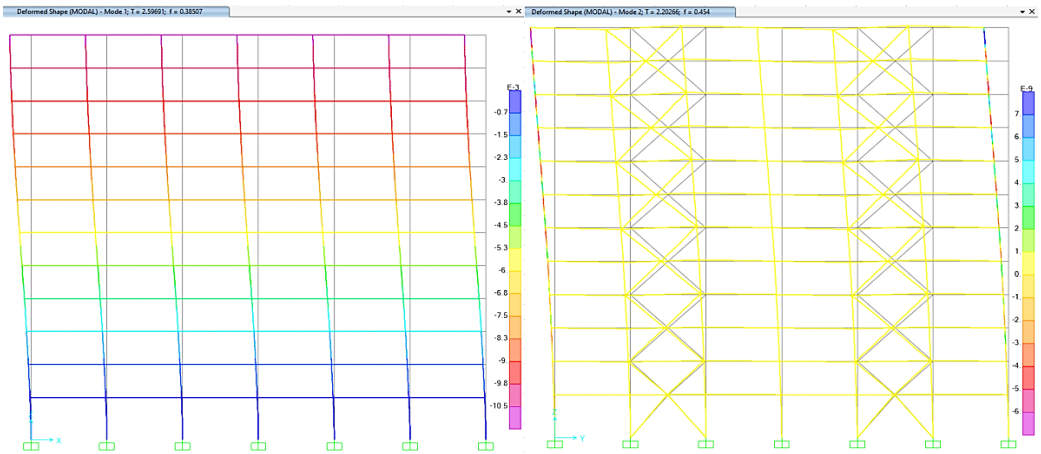

Figure 5. 9 First and second mode shape for fixed base model.

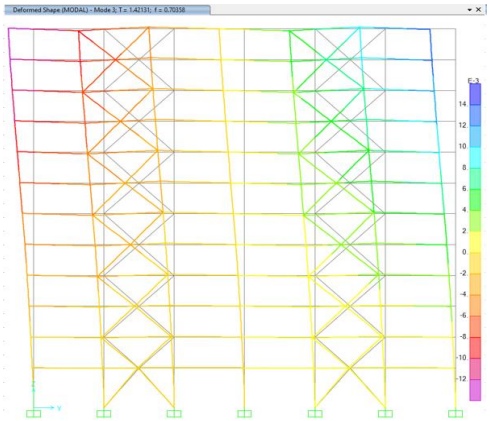

Figure 5. 10 Mode shape three for fixed base model.

The fundamental period in a structure with a fixed base structure first mode shape is 2.59691seconds, the second mode shape is 2.20 seconds, and the third mode shape is 1.42. It is shown in the figures above.

5.6 Time history analysis for the conventional structure model.

The reaction of the building in terms of (Displacement, velocity, and acceleration) the non-linear (THA), study of the steel frame subjected to a specified earthquake shaking was performed using SAP 2000 v21 program. The chosen seismic ground movement is the yarimca seismic dataset. (Kocaeli Turkey, 8/17/1999, Yarimca, 150).

5.6.1 Displacement and velocity for (THA) in the x-direction for the conventional structure model.

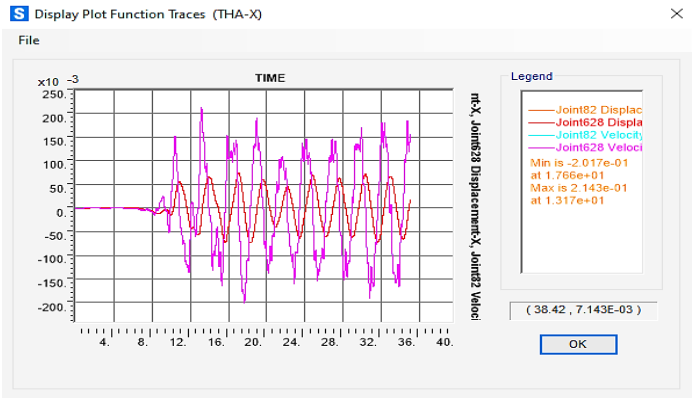

Figure 5. 11 Displacement and velocity (THA) in x-direction for conventional structure model.

Displacement and velocity of the steel member subject to (THA) are documented in the corners-node at roof x-axis. The displacement -velocity values at various levels of the fixed base building are more significant than the velocity because of typically continue the accelerations along with the elevation of the case study structure (shown in figure 5.11 above).

5.6.2 Displacement and velocity for (THA) in the y-direction for the conventional structure model.

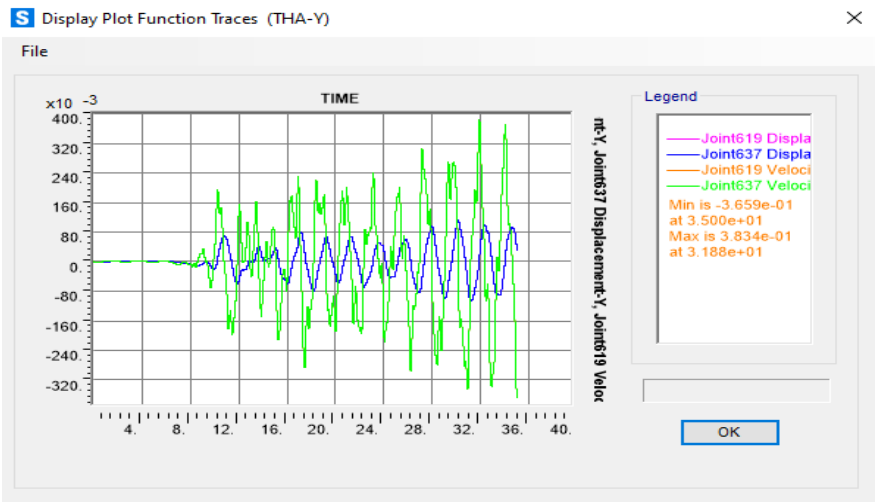

Figure 5. 12 Displacement and velocity (THA) in y-direction for conventional model.

The displacement and velocity values at various levels for the y-direction earthquake of the fixed base building the displacement is greater than the velocity, and also both value increases the acceleration because of contrary to start point and upper at the endpoint the accelerations along with the height of the case study building shown in the figure 5.12 above.

5.6.3 Acceleration for (THA) in the x-direction for the conventional structure model.

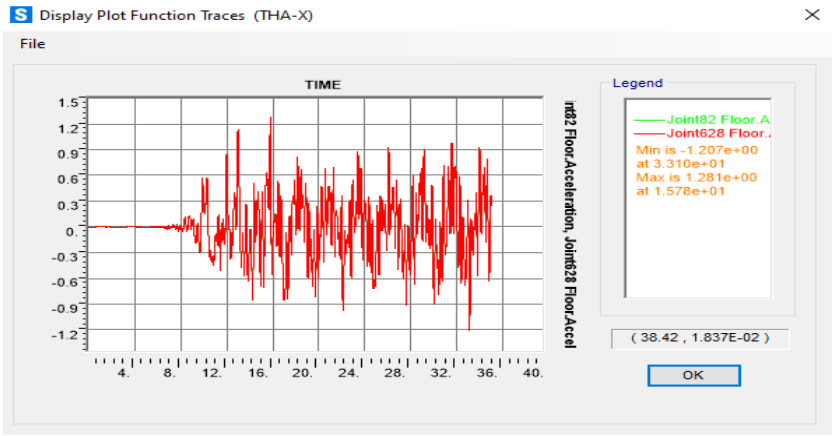

Figure 5. 13 Acceleration (THA) in x-direction for conventional model.

Acceleration of the steel member subject to (THA) is documented in the corners-node for the top floor in the x-direction. The acceleration is plotted with respect to the time period, showing the variation of the ground acceleration with time. The maximum positive value is 1.281e+00 at 1.578e+01, and the negative side minimum value is -1.207e+00 at 3.310e+01. The figure 5.13 above shows.

5.6.4 Acceleration for (THA) in the y-direction for the conventional structure model.

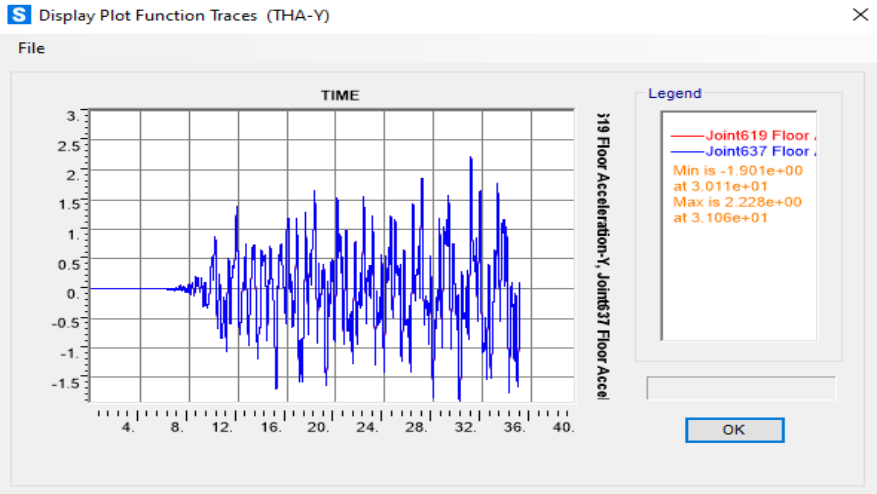

Figure 5. 14 Acceleration (THA) in y-direction for conventional model.

The acceleration from time history analysis for the case study building at roof y-direction of corners node. The values minimum is -1.901e+00 at 3.011e+01 and maximum is 2.228e+00 at 3.106e+01. As seen in figure 5.14 above.

5.7 Lead rubber bearing isolation system for the displacement and drift phase analysis earthquake in the x-direction.

An earthquake in the x-axis (SMF) to calculate storey displacement and storey drift for the base Isolator building, as shown in table 5.4 below.

Table 5. 4 Lead rubber bearing displacement and drift phase analysis earthquake in the x-direction.

Lead rubber bearing in x-direction due to earthquake analysis						
Storey	Cd	5.5	T	5.079	Δa = 0.025	
	H(m)	Elastic displacement (mm)	Amplified displacement	Storey drift	Allowable	Check
		δ	Δm	Δi	Δa	
12	3.5	4377.049	4739.86405	16.9494	87.5	Safe
11	3.5	4361.397	4722.91465	22.72337	87.5	Safe
10	3.5	4340.413	4700.19128	28.13457	87.5	Safe
9	3.5	4314.432	4672.0567	30.92085	87.5	Safe
8	3.5	4285.878	4641.13585	33.96702	87.5	Safe
7	3.5	4254.511	4607.16883	36.05808	87.5	Safe
6	3.5	4221.213	4571.11075	36.68399	87.5	Safe
5	3.5	4187.337	4534.42676	36.40461	87.5	Safe
4	3.5	4153.719	4498.02215	33.64107	87.5	Safe
3	3.5	4122.653	4464.38108	30.93168	87.5	Safe
2	3.5	4094.089	4433.4494	35.25566	87.5	Safe
1	4.5	4061.532	4398.19374			

5.7.1 Lead rubber bearing displacement analysis earthquake in the x-direction.

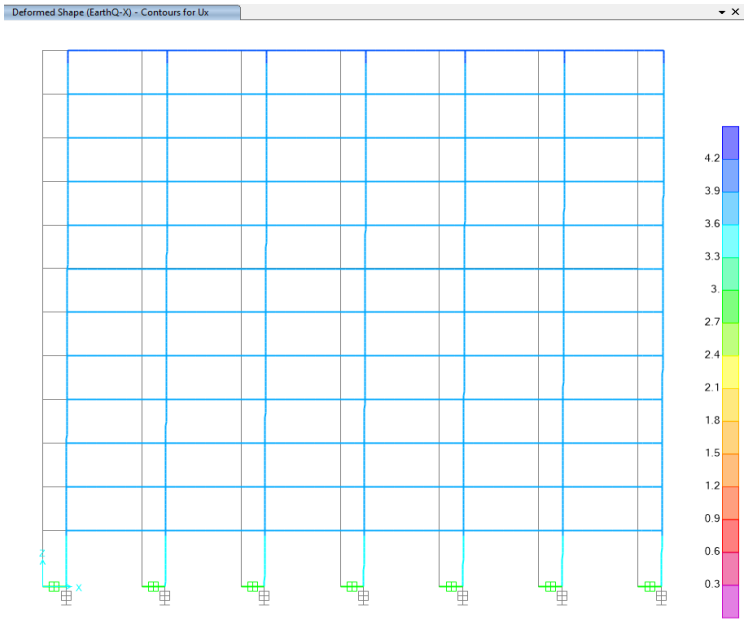

Figure 5. 15 Displacement analysis earthquake in the x-axis for the (LRB).

The storey displacement values at small for various storeys level are determined using earthquake in the x-direction of the base-isolated building. The isolated structural model at the base has a significant degree of lateral movement. It has also been shown that when the floor height rises. Because it is installed at the base ground of the lead rubber bearing isolation system, consequently reducing the displacement of time, figure 5.15 above shows.

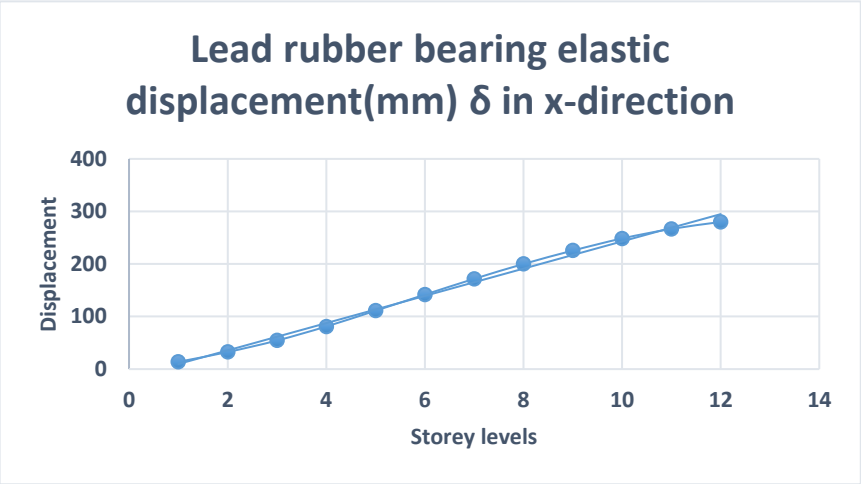

Figure 5. 16 Displacement analysis earthquake in the x-direction for the (LRB).

The figure 5.16 above shows the various displacement the line grew from the first floor to the end floor. It increases displacement on every level floor. Therefore, the period shifting The duration of the building is lengthened owing towards the added flexibility, and the necessity to stretch the stiffness of the structure will result in substantial relative motion throughout the flexible mount.

5.7.2 Lead rubber bearing storey drift analysis earthquake in the x-direction.

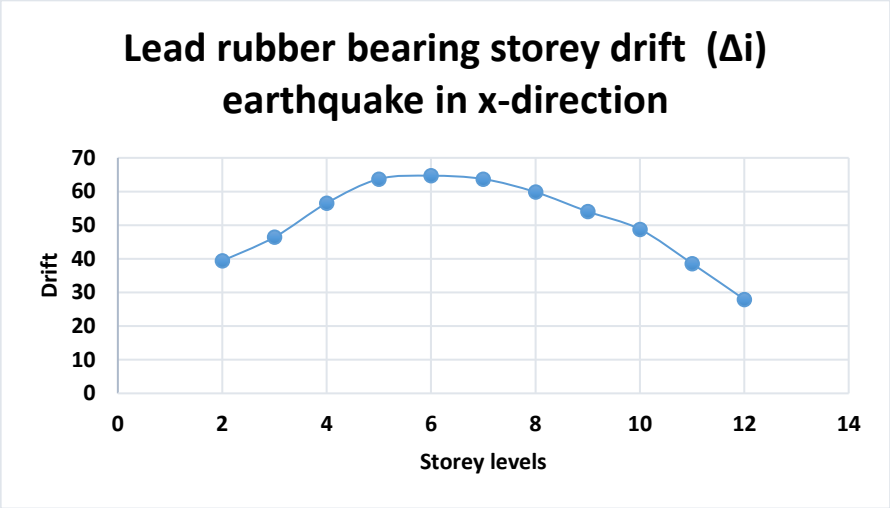

Figure 5. 17 Inter-drift analysis earthquake in the x-direction for the lead rubber bearing.

The figure 5.17 above shows the inter-storey drift ratios are very low at the upper levels of the lead rubber-bearing building when these values are analyzed. As a result, the lead rubber bearing, earthquake damage to the building's structural parts is expected to be minimal.

5.8 Shear force the analysis in the x-direction earthquake for the (LRB).

The figure 5.18 below, the large shear force occurs in the ground floor, the first storey, and second storey columns because lateral load and distributed load are acting at the level floors of a building frame.

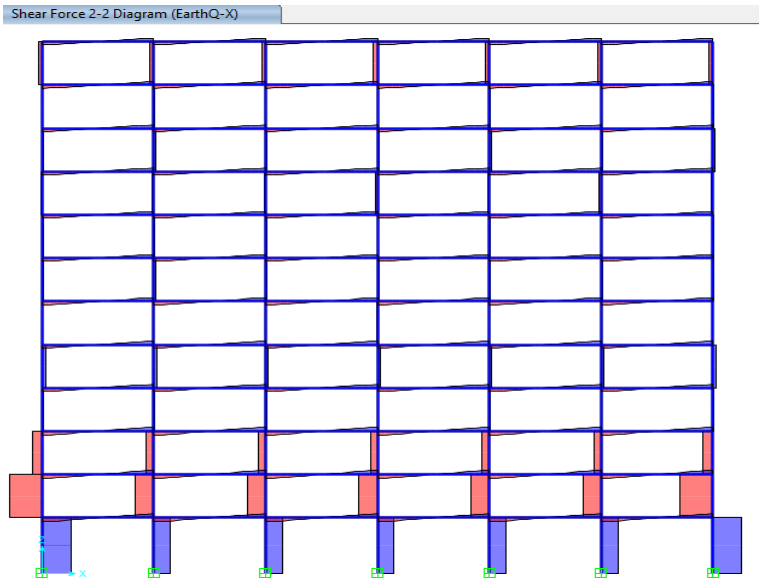

Figure 5. 18 Shear force 2-2 diagram for the analysis in the x-direction earthquake

5.9 Lead rubber bearing isolation system for the displacement and drift phase analysis earthquake in the y-direction.

An earthquake in the y-axis is used to evaluate the displacement and drift of different floors for the base isolator structure shown in table 5.5 below.

Table 5. 5 Lead rubber bearing isolation system displacement and drift phase analysis earthquake in the y-direction.

Lead rubber bearing in the y-direction due to earthquake analysis						
	Cd	5	T	5.079	Δa =0.025	
Storey	H(m)	Elastic displacement (mm)	Amplified displacement	Storey drift	Allowable	Check
		δ	Δm	Δi	Δa	
12	3.5	471.81	464.471353	1.309313	87.5	Safe
11	3.5	470.48	463.16204	1.535735	87.5	Safe
10	3.5	468.92	461.626304	1.653869	87.5	Safe
9	3.5	467.24	459.972436	1.683402	87.5	Safe
8	3.5	465.53	458.289033	1.72278	87.5	Safe
7	3.5	463.78	456.566253	1.732625	87.5	Safe
6	3.5	462.02	454.833629	1.712936	87.5	Safe
5	3.5	460.28	453.120693	1.565269	87.5	Safe
4	3.5	458.69	451.555424	1.486513	87.5	Safe
3	3.5	457.18	450.068911	1.299468	87.5	Safe
2	3.5	455.86	448.769443	1.279779	87.5	Safe
1	4.5	454.56	447.489663			

5.9.1 Lead rubber bearing isolation system displacement analysis earthquake for y-direction.

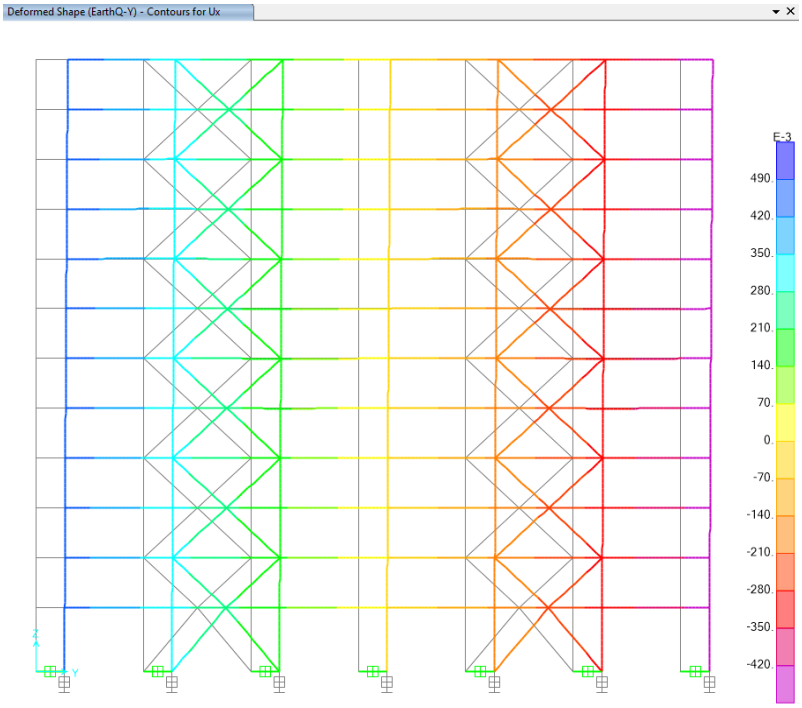

Figure 5. 19 Lead rubber bearing isolation system displacement analysis earthquake in the y-direction.

The storey-displacement is various storey level the determined using earthquake in y-direction obtained less relative displacement when compared than in the x-direction shown in table figure 5.19 above.

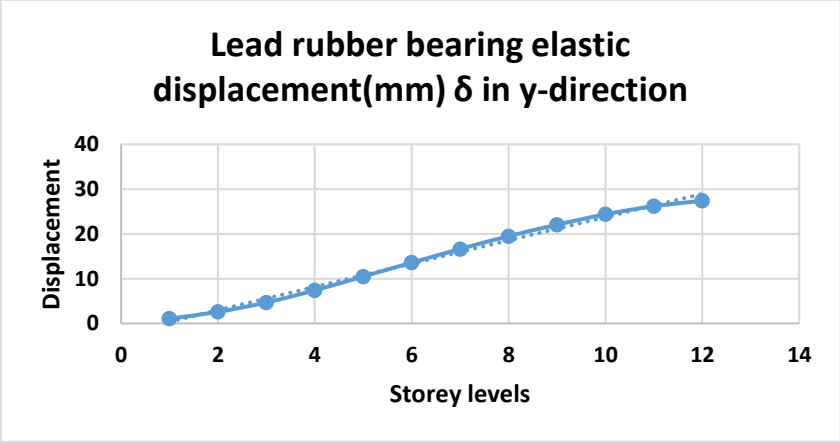

Figure 5. 20 Lead rubber bearing isolation system displacement analysis earthquake in the y-direction.

Figure 5.20 shows above the maximum displacements that occurred at the top (12th-storey level) in the y-axis. However, the top-level displacements in the y-axis were generally higher than in the x-axis.

5.9.2 Lead rubber bearing isolation system inter-drift analysis earthquake in the y-direction.

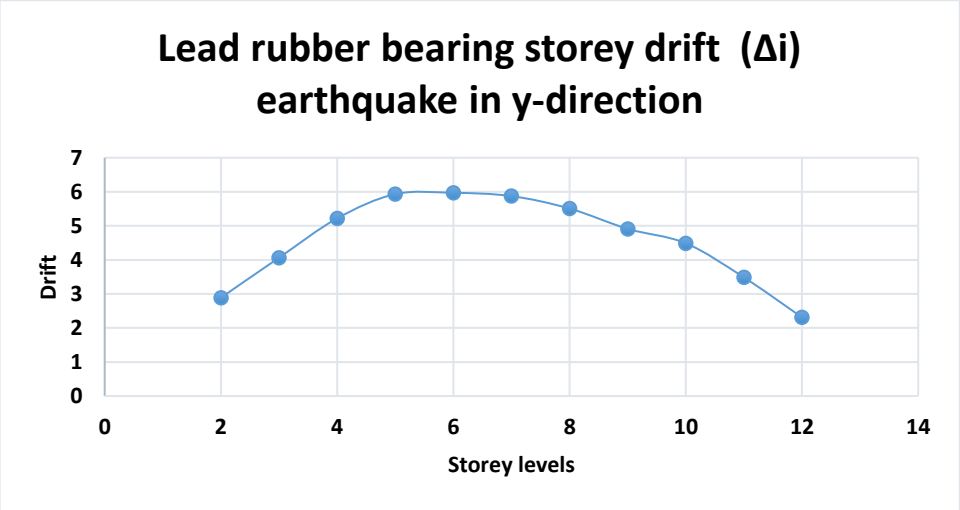

Figure 5. 21 Lead rubber bearing isolation system inter-drift analysis earthquake in the y-direction.

Figure 5.21 above, the line increase when it goes to the middle storeys, then it goes back down to the bottom, which is the last floor that is the 12th storey, until reaching the value of 1.309.

5.10 Shear force the analysis in the y-direction earthquake for the lead rubber bearing.

The shear force in the 2-2 diagram shows variation structure frame along the length of the beam and column in the y-axis shown in figure 5.22 below.

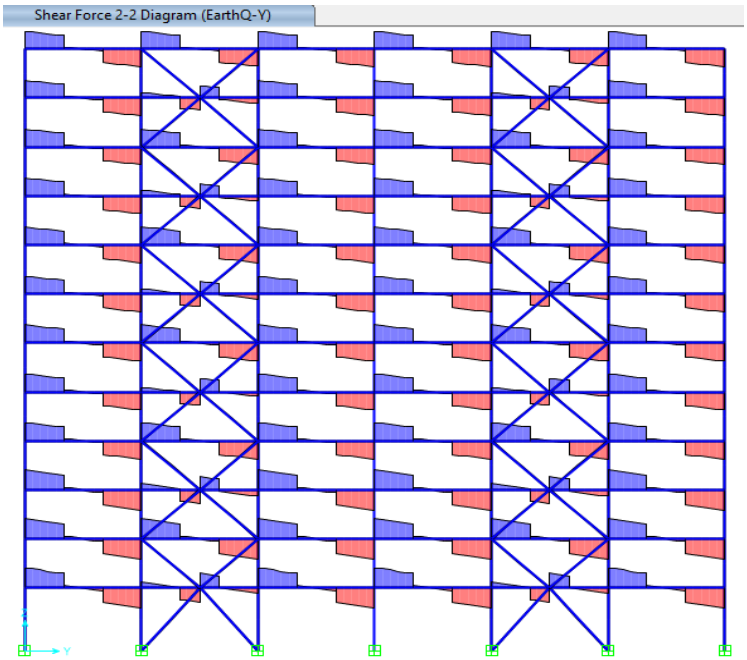

Figure 5. 22 Lead rubber bearing shear force 2-2 diagram analysis in the y-direction earthquake.

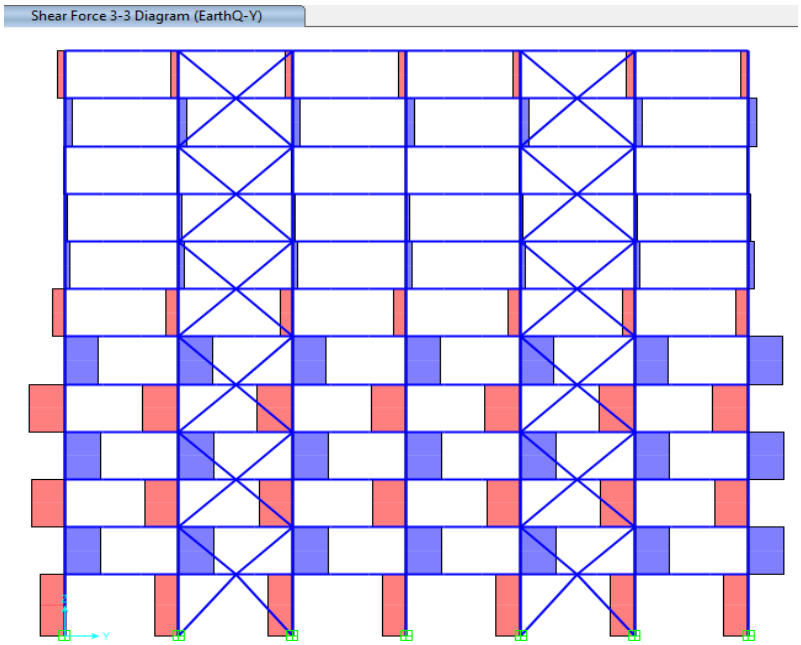

Figure 5. 23 Lead rubber bearing shear force 3-3 diagram analysis in the y-direction earthquake.

Figure 5.23 above, shear force in the 3-3 diagram in the y-direction, the large shear force for the columns occurs in the ground floor up to middle storeys because lateral load and distributed load is acting at the level floors of a building frame.

5.11 Time period for the lead rubber bearing isolation system model.

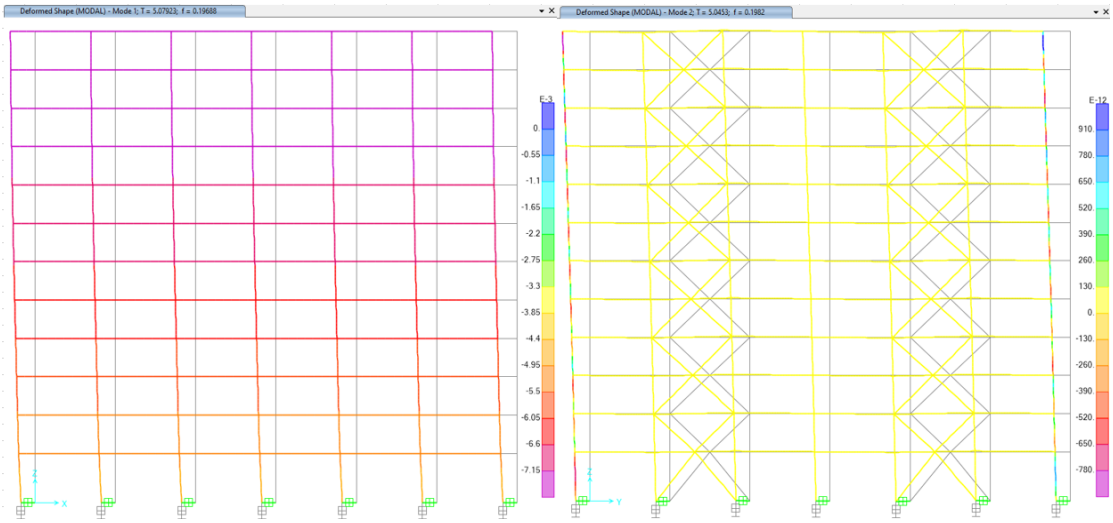

Figure 5. 24 First and second mode shape for the (LRB) model.

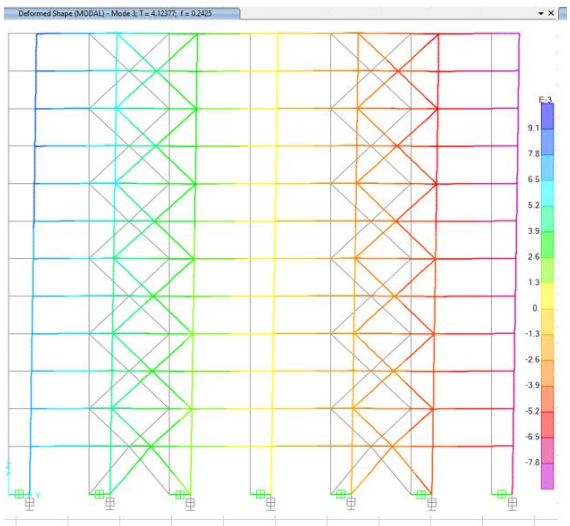

Figure 5. 25 Third mode shape for the (LRB) model.

The fundamental time period in a structure with a fixed base first mode shape is 5.07923 seconds, the second mode shape is 5.0453 seconds, and the third is 4.1237 seconds. However, the lead rubber bearing mode shapes to increase period (flexibility) considerably than other buildings. Therefore as the horizontal stiffness of the multi-

layer rubber bearing is low, strong earthquake vibration is lightened, and the oscillation period of the building is increased, shown figures 5.24 and 5.25 above.

5.12 Time history analysis for the (LRB) model.

The reaction of the building in terms of (Displacement, velocity, and acceleration) the non-linear (THA), study of the steel frame subjected to a specified earthquake shaking was performed by inside SAP 2000 v21 program. The chosen seismic ground movement is the yarimca seismic dataset. (Kocaeli Turkey, 8/17/1999, Yarimca, 150).

5.12.1 Displacement and velocity time history analysis in x-direction for lead rubber bearing isolation system model.

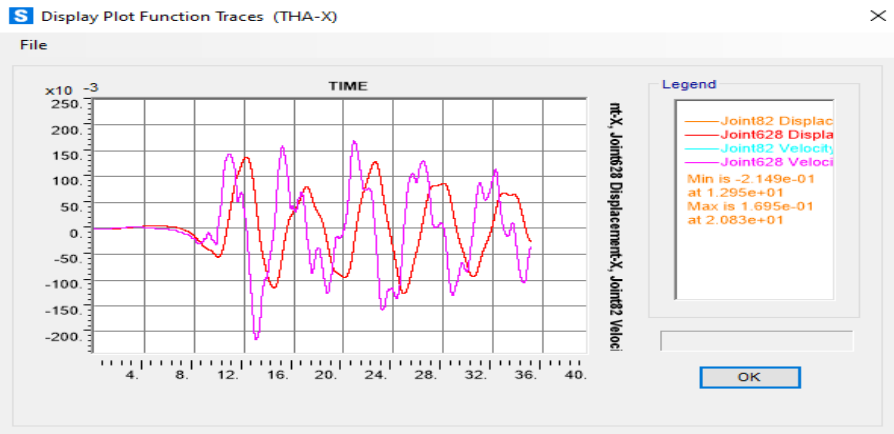

Figure 5. 26 Displacement and velocity time history analysis in x-direction for lead rubber bearing isolation system model.

In the corners node at the roof x-direction, the displacement and velocity of the steel member are subjected to (THA). At 1.295e+01, the displacement joint82 value is -2.149e-01, and at 2.083e+01, it is 1.695e-01. Above figure 5.26 shows the accelerations along with the height of the case study building of the lead rubber bearing building at different levels.

5.12.2 Displacement and velocity time history analysis in y-direction for lead rubber bearing isolation system model.

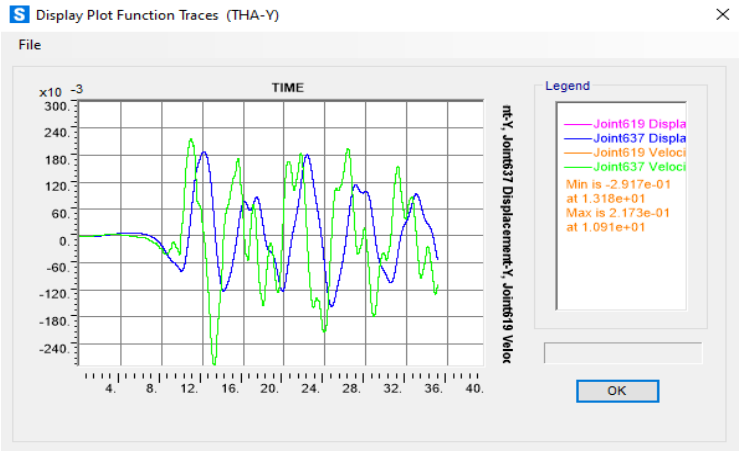

Figure 5. 27 Displacement and velocity time history analysis in y-direction for (LRB) model.

Displacement and velocity for the steel member are subject to (THA) in the corners-node at roof y-direction. The velocity joint619 value minimum is -2.917e-01 at 1.318e+01. The maximum is 2.173e-01 at 1.091e+01; at various levels, the accelerations along with the height of the case study building of the lead rubber bearing building are shown in figure 5.27 above.

5.12.3 Acceleration time history analysis in x-direction for lead rubber bearing isolation system model.

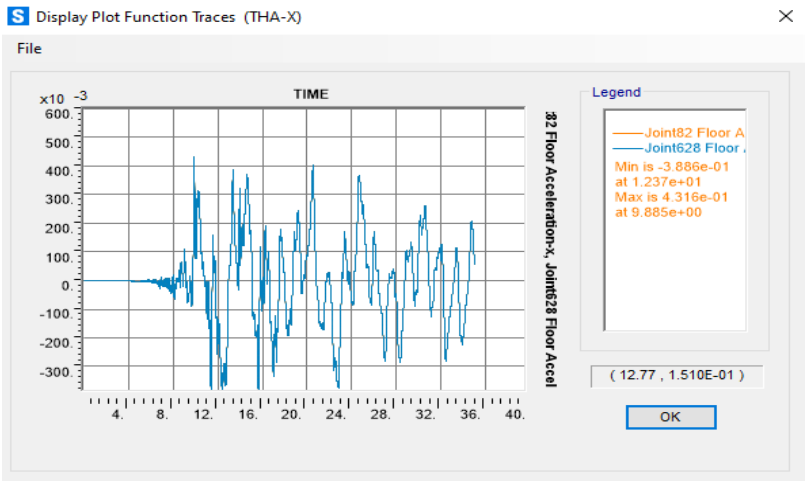

Figure 5. 28 Acceleration time history analysis in x-direction for lead rubber bearing isolation system model.

The storey acceleration from time history analysis for the case study building at roof x-direction of corners node. The acceleration joint82 values minimum is -3886e-01 at 1.237e+01 and maximum is 4.316e-01 at 9.885e+00. As seen in figure 5.28 above.

5.12.4 Acceleration time history analysis in y-direction for lead rubber bearing isolation system model.

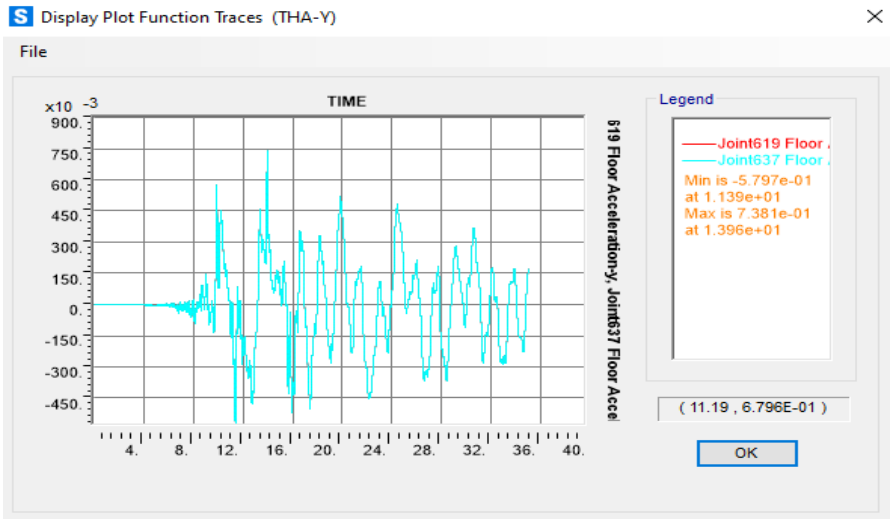

Figure 5. 29 Acceleration time history analysis in y-direction for lead rubber bearing isolation system model.

The acceleration for the steel member is subjected to (THA) at the top floor's corners node in the y-direction. The minimum value is -5.797e-01 at 1.139e+01, while the greatest value is 7.381e-01 at 1.396e+01. As seen in figure 5.29 above.

5.13 Fluid viscous damper for the displacement and drift phase analysis earthquake in the x-direction.

For fluid viscous damper structure, the storey-displacement and storey-drift of various storeys are determined using earthquake in the x-direction table-5.6 is shown below.

Table 5. 6 Fluid viscous damper of displacement and drift phase analysis earthquake in x-direction.

Fluid viscous damper in x-direction due to earthquake analysis						
Storey	Cd	5.5	T	2.5969	Δa = 0.025	
	H(m)	Elastic displacement (mm)	Amplified displacement	Storey drift	Allowable	Check
		δ	Δm	Δi	Δa	
12	3.5	279.97	592.951211	27.93523	87.5	Safe
11	3.5	266.78	565.015981	38.58832	87.5	Safe
10	3.5	248.56	526.427664	48.77546	87.5	Safe
9	3.5	225.53	477.652201	54.04906	87.5	Safe
8	3.5	200.01	423.603142	59.83095	87.5	Safe
7	3.5	171.76	363.77219	63.70673	87.5	Safe
6	3.5	141.68	300.065463	64.68097	87.5	Safe
5	3.5	111.14	235.384497	63.70673	87.5	Safe
4	3.5	81.06	171.67777	56.54819	87.5	Safe
3	3.5	54.36	115.129578	46.42458	87.5	Safe
2	3.5	32.44	68.7049944	39.4143	87.5	Safe
1	4.5	13.83	29.2906927			

5.13.1 Fluid viscous damper of the displacement analysis earthquake in the x-direction.

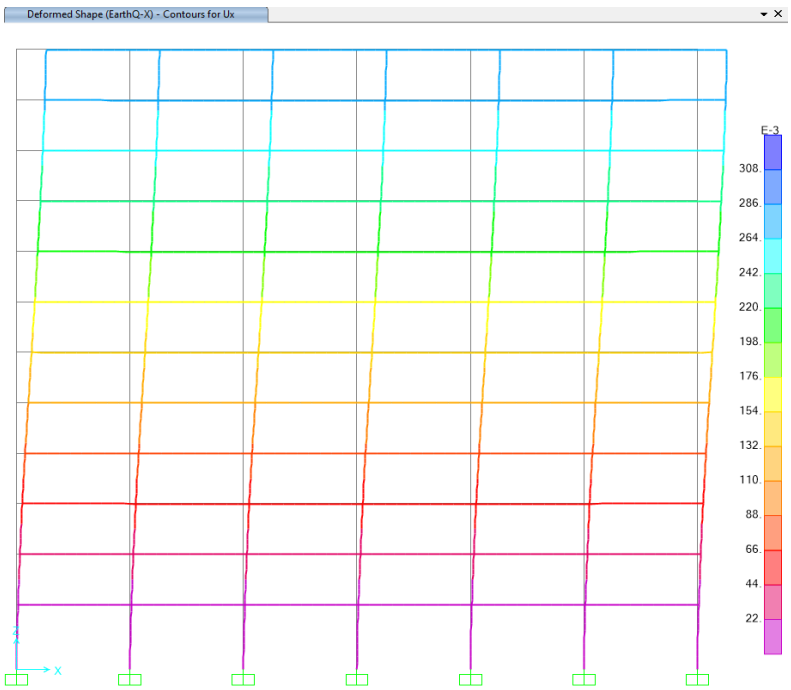

Figure 5. 30 Fluid viscous damper displacement analysis earthquake in x-direction.

The displacement increases each level from the lower storey to the upper storey concerning the ground floor in the x-axis. Therefore, the fluid viscous damper in the x-axis values is close to the fixed base structure shown in figure 5.30 above.

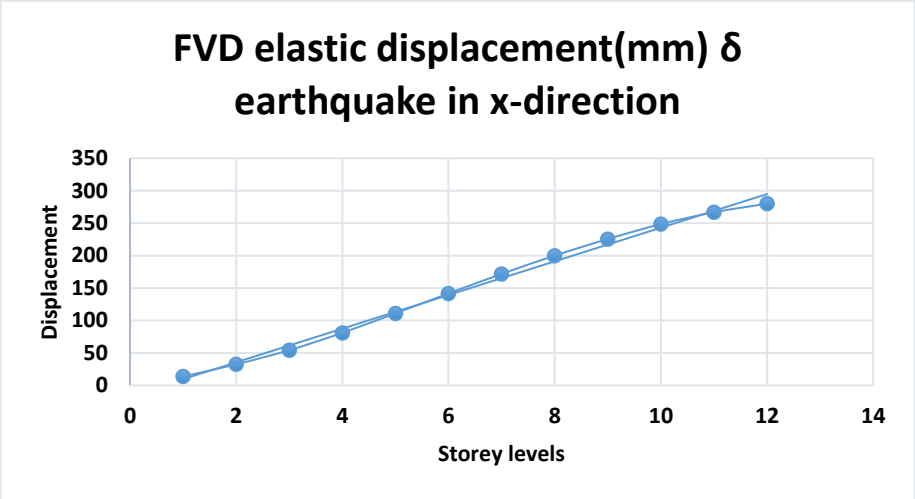

Figure 5. 31 Fluid viscous damper of the displacement analysis earthquake in x-direction.

Figure 5.31 above shows that the blue line from the first floor to the top floor is 13.83mm and 279.97mm. However, the fluid viscous damper for maximum displacement in the x-direction occurs on the top-level floor in the structure.

5.13.2 Fluid viscous damper of the storey drift analysis earthquake in the x-direction.

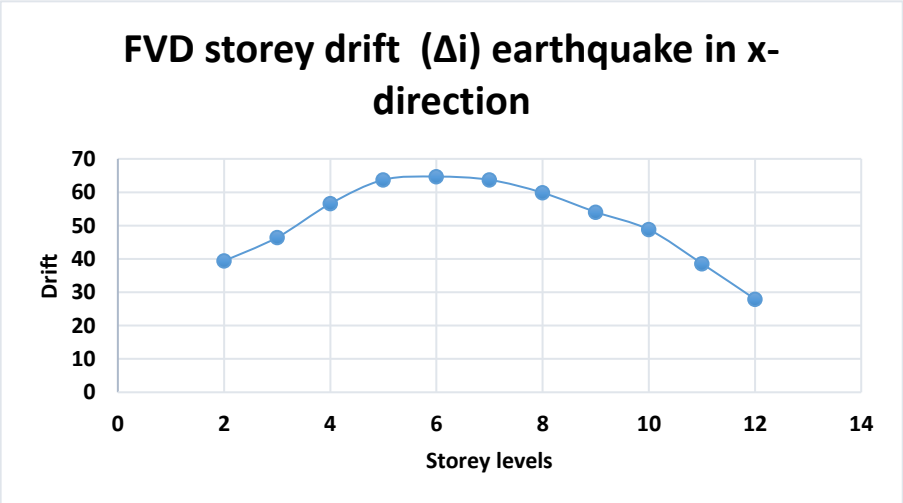

Figure 5. 32 Fluid viscous damper of the drift analysis earthquake in the x-direction.

As you can see in the figure 5.32 above, the line increases when it goes to the middle storeys, and then it goes back down to the bottom, which is the last floor, the 12th storey, until it reaches the value 27.93mm.

5.14 Fluid viscous damper for the shear force analysis in the x-direction earthquake.

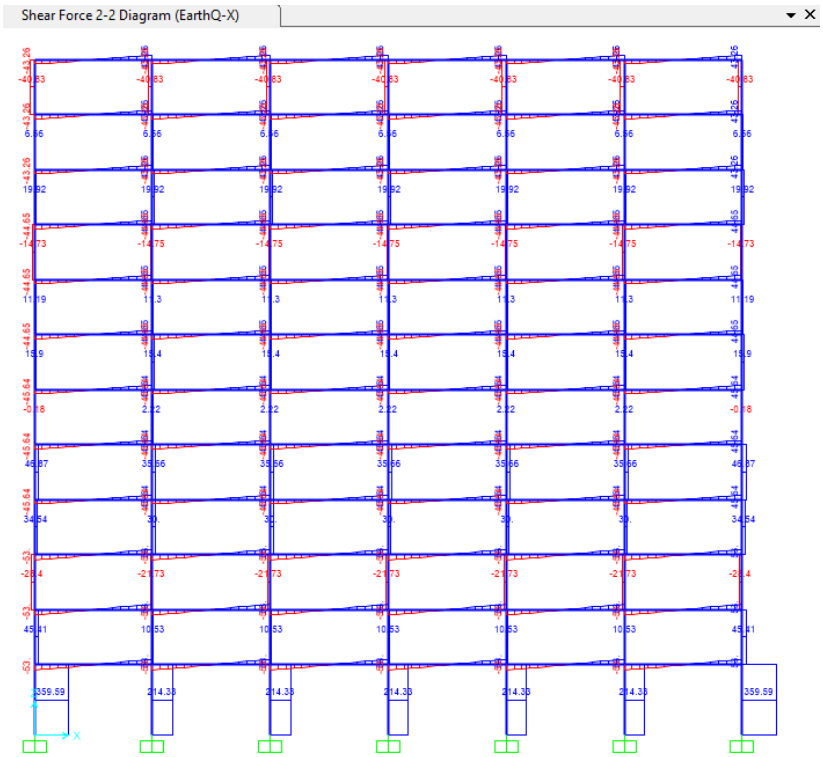

Figure 5. 33 Fluid viscous damper shear force in 2-2 diagram in x-direction.

The shear force in the 2-2 diagram in the x-direction, the most significant shear force occurs at the ground floor columns, and the reason is that lateral loads and distributed loads are happening at the level floors of a building frame as shown in figure 5.33 above.

5.15 Fluid viscous damper for the displacement and drift phase analysis earthquake in the y-direction.

An earthquake in the y-axis obtained storey displacement and storey-drift of various storeys for the base isolator structure. Below are a data table 5.7 with graphics.

Table 5. 7 Fluid viscous damper for the displacement and drift phase analysis earthquake in y-direction.

Fluid viscous damper in the y-direction due to earthquake analysis						
	Cd	5	T	2.5969	Δa =	0.025
Storey	H(m)	Elastic displacement (mm)	Amplified displacement	Storey drift	Allowable	Check
		δ	Δm	Δi	Δa	
12	3.5	27.38	52.7167007	2.310447	87.5	Safe
11	3.5	26.18	50.4062536	3.484924	87.5	Safe
10	3.5	24.37	46.9213293	4.486118	87.5	Safe
9	3.5	22.04	42.4352112	4.9097	87.5	Safe
8	3.5	19.49	37.5255112	5.506566	87.5	Safe
7	3.5	16.63	32.0189457	5.872386	87.5	Safe
6	3.5	13.58	26.1465594	5.968655	87.5	Safe
5	3.5	10.48	20.1779044	5.930147	87.5	Safe
4	3.5	7.4	14.2477569	5.21776	87.5	Safe
3	3.5	4.69	9.0299973	4.062536	87.5	Safe
2	3.5	2.58	4.9674612	2.888059	87.5	Safe
1	4.5	1.08	2.07940236			

5.15.1 Fluid viscous damper of the displacement analysis earthquake in the y-direction.

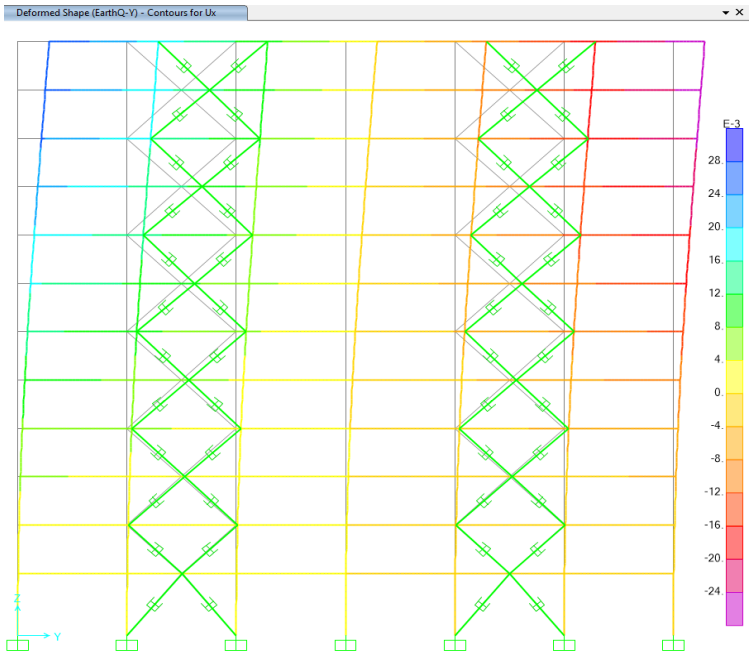

Figure 5. 34 Fluid viscous damper for the displacement analysis earthquake in y-direction.

The displacement of each level relocated the floor joint from the initial position to the upper floor in the y-axis. Compared to the x-axis and determined displacement values, it is higher from the first level to the top floor. Figure 5.34 shows the above.

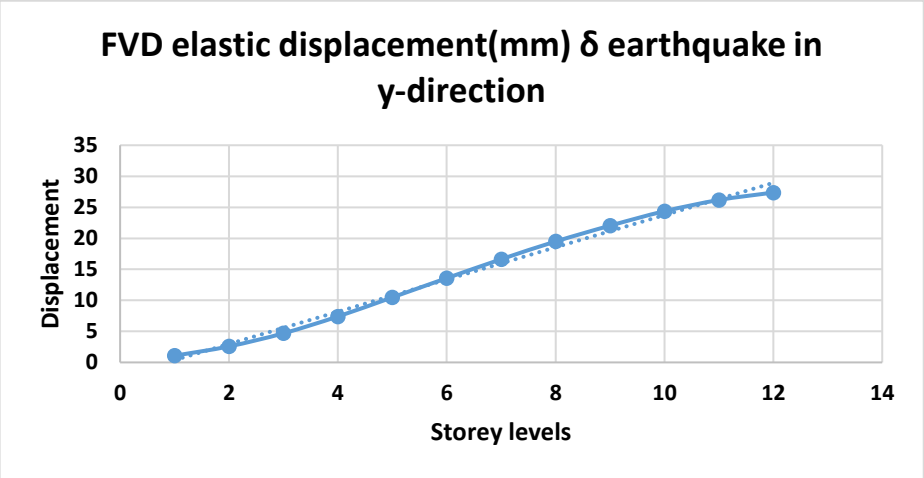

Figure 5. 35 Fluid viscous damper displacement analysis earthquake in the y-direction.

The figure 5.35 above shows the displacement of every storey increase in the y-direction. The blue line rises from the first-floor value 1.08mm to the top floor 27.38mm. Therefore, the displacement in the y-axis is smaller than in the x-axis.

5.15.2 Fluid viscous damper of the inter drift analysis earthquake in the y-direction.

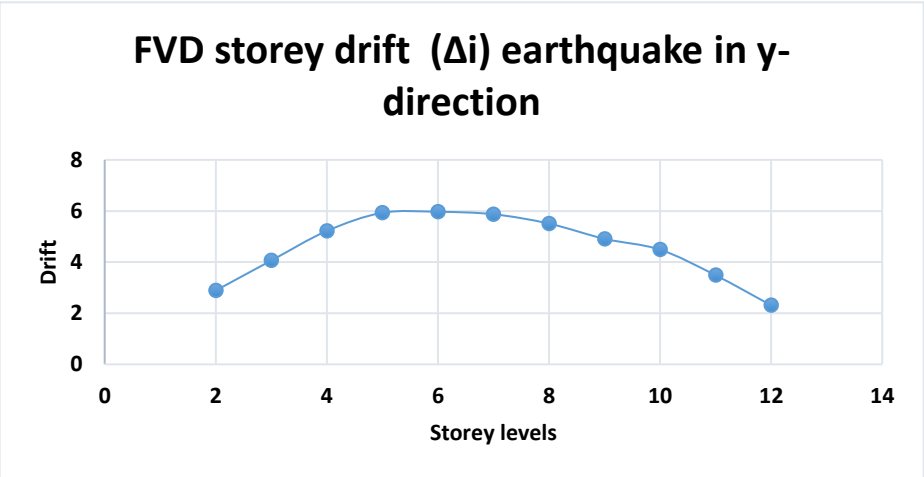

Figure 5. 36 Fluid viscous damper inter-drift analysis earthquake in y-direction.

As you can see in the figure 5.36 above, the line increases and grows every level when it goes to the middle storeys, then it goes back down to the bottom, which is the last floor that is the 12th storey, until reaching the value of 2.31mm.

5.16 Fluid viscous damper for the shear force earthquake in the y-direction.

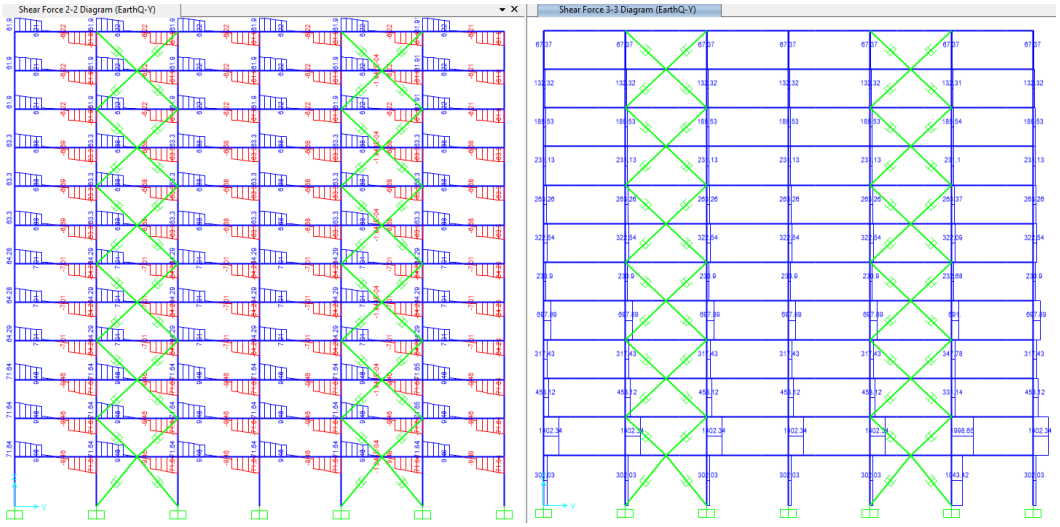

Figure 5. 37 Fluid viscous damper shear force in 2-2 and 3-3 diagrams in y-direction.

The shear strength at various levels of the building are computed by summing the lateral forces (y-component) of components at a section in 2-2 diagram in the y-direction is the one that shows the variation along the length of the frames. Shows in the figure 5.37 above.

5.17 Time period for the fluid viscous damper model.

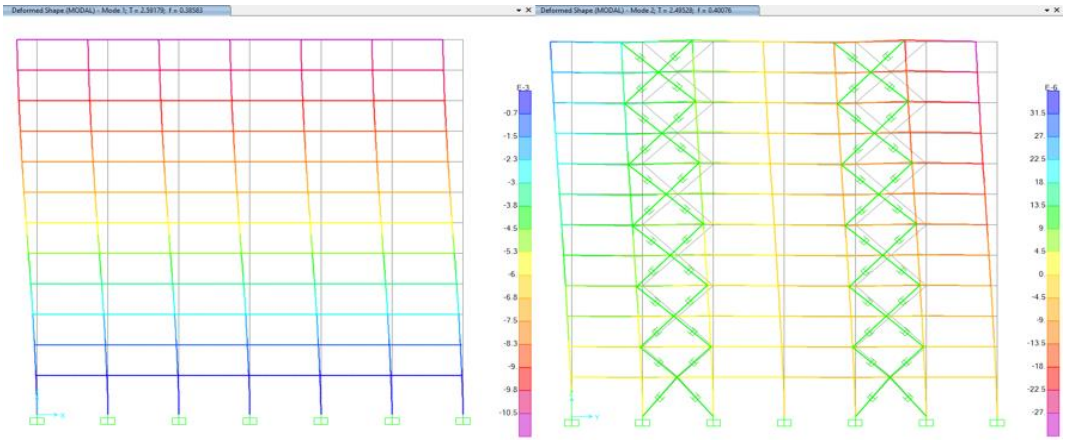

Figure 5. 38 First and second mode shape for fluid viscous damper model

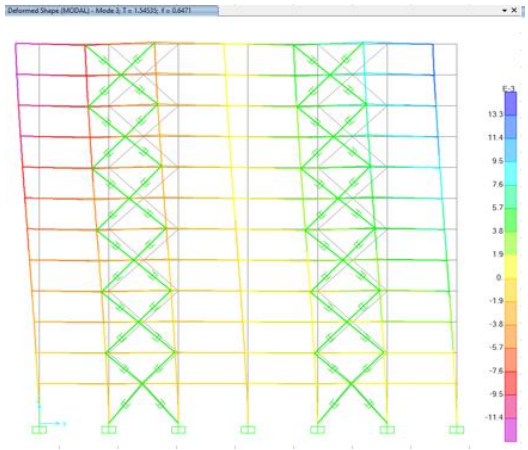

Figure 5. 39 Third mode shape for fluid viscous damper model

The fundamental time period in a structure with fixed base first mode shape is 2.59179 seconds, the second mode shape is 2.49528 seconds, and the third mode shape which is 1.54668 seconds. Shown figures 5.38 and 5.39.

5.18 Time history analysis for the fluid viscous damper model.

The non-linear time history analysis utilizes the SAP 2000 v21 program to determine the structure's response in terms of (Displacement, velocity, and acceleration) the non-linear (THA), study of the steel frame subjected to a specified earthquake shaking.. The earthquake ground motion is the Yarimca Earthquake record (Kocaeli Turkey, 8/17/1999, Yarimca, 150).

5.18.1 Displacement and velocity (THA) in the x-direction for the fluid viscous damper model.

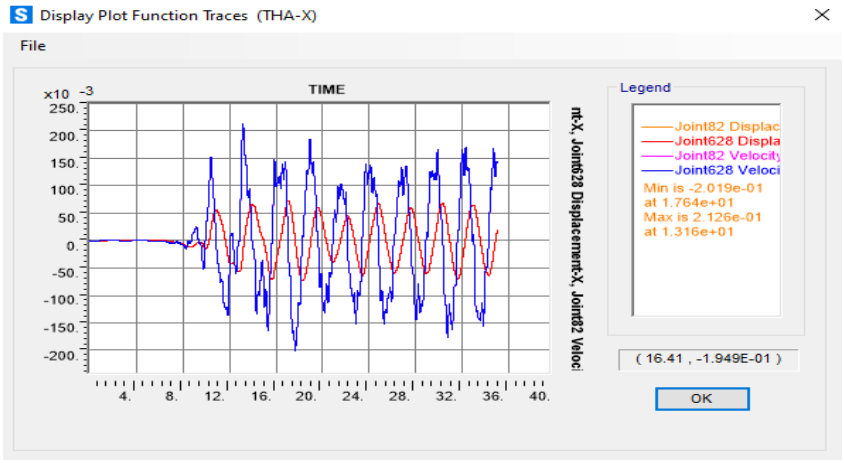

Figure 5. 40 Displacement and velocity (THA) in x-direction for fluid viscous damper model.

Displacement-Velocity for the steel member are subject to (THA) in the corners-node at the roof in the x-direction. The displacement joint82 value minimum is -2.019e-01 at 1.764e+01 and maximum is 1.126e-01 at 1.316e+01; at the various levels, the accelerations and the elevation of the (FVD) structure's case study building are shown in figure 5.40 above.

5.18.2 Displacement and velocity time history analysis in the y-direction for the fluid viscous damper model.

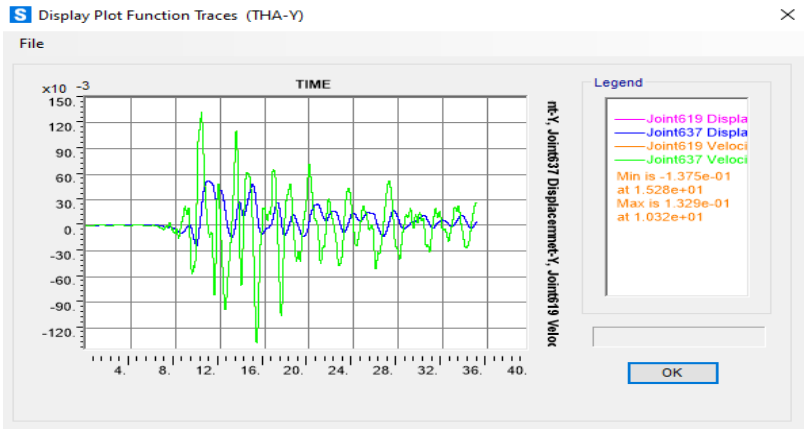

Figure 5. 41 Displacement and velocity (THA) in y-direction for fluid viscous damper model.

Note from plot function (THA-Y) shown above 5.41 the displacements and velocities of the steel member in the y-axis at the corner nodes on the roof. Velocity joint 619 the minimum value is -1.375e-01, located at 1.528e+01. The maximum value is 1.329e-01, located at 1.032e+01; fluid viscous damper building case study the acceleration and the elevation of the structure at different floors.

5.18.3 Acceleration (THA) in the x-direction for the fluid viscous damper model.

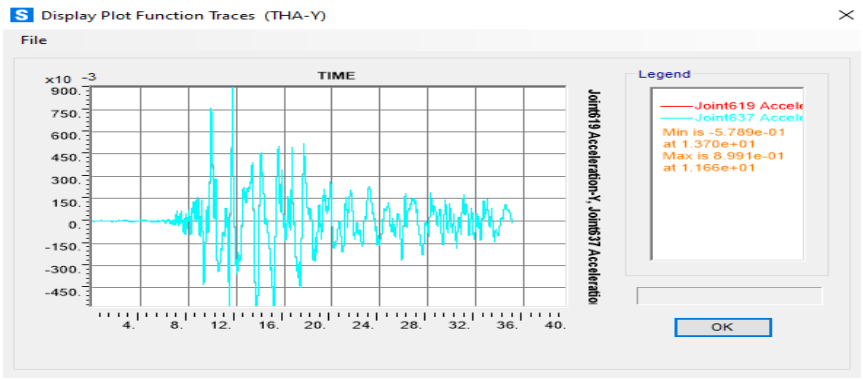

Figure 5. 42 Acceleration (THA) in x-direction for fluid viscous damper model.

The acceleration from time history analysis for the case study building at roof x-direction of corners node. The acceleration joint 82 value minimum is -1.108e+00 at 3.306e+01 and maximum is 1.246e+00 at 1.577e+01. As seen in figure 5.42 above.

5.18.4 Acceleration (THA) in the y-direction for the fluid viscous damper model.

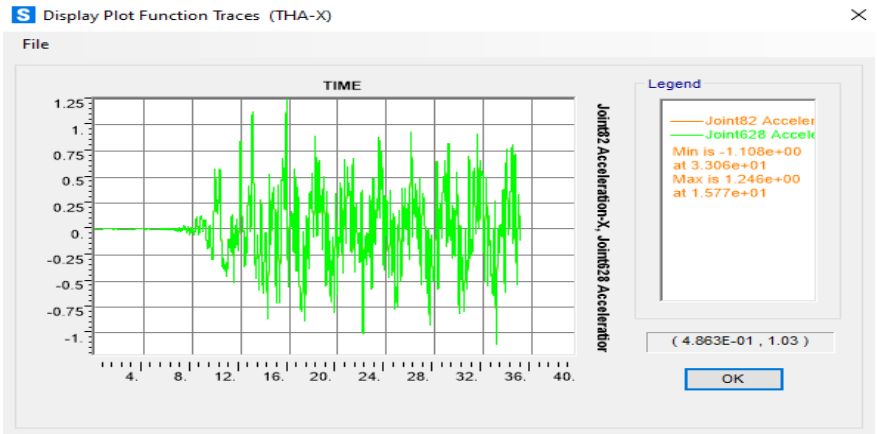

Figure 5. 43 Acceleration (THA) in y-direction for fluid viscous damper model.

The storey acceleration values at various level for y-direction earthquake of the fluid viscous damper building. The value acceleration is reduction, because of contrary to reduction the accelerations from along length of the study structure's elevation as shown in the figure 5.43 above.

5.19 Results for case study building three system comparing model.

Overview

This section discusses the results comparing three system buildings obtained from the analysis phase. Including floor displacement, inter-storey drifts, shear force, base reaction, model participation mas ration analysis, stiffness, and time history analysis are mainly applied to non-linear modeling of building for comparison of conventional structure, (LRB) and (FVD), according to (ASCE 7-16).

5.19 Storey displacement in the x-direction due to earthquake for the conventional structure, (LRB), and fluid viscous damper.

The conventional structure, (LRBs), and fluid viscous damper buildings, the storey displacement is determined using earthquake in the x-direction. Below is a data table-5.8 with graphics.

Table 5. 8 Displacement in the x-direction due to earthquake conventional structure, lead rubber bearing, and fluid viscous damper.

Storey	H(m)	Fixed base displacement(mm)	Lead rubber bearing displacement(mm)	Fluid viscous damper displacement(mm)
		δ	δ	δ
12	3.5	285.45	4377.049	279.97
11	3.5	271.91	4361.397	266.78
10	3.5	253.24	4340.413	248.56
9	3.5	229.7	4314.432	225.53
8	3.5	203.65	4285.878	200.01
7	3.5	174.86	4254.511	171.76
6	3.5	144.22	4221.213	141.68
5	3.5	113.13	4187.337	111.14
4	3.5	82.56	4153.719	81.06
3	3.5	55.41	4122.653	54.36
2	3.5	33.13	4094.089	32.44
1	4.5	14.16	4061.532	13.83

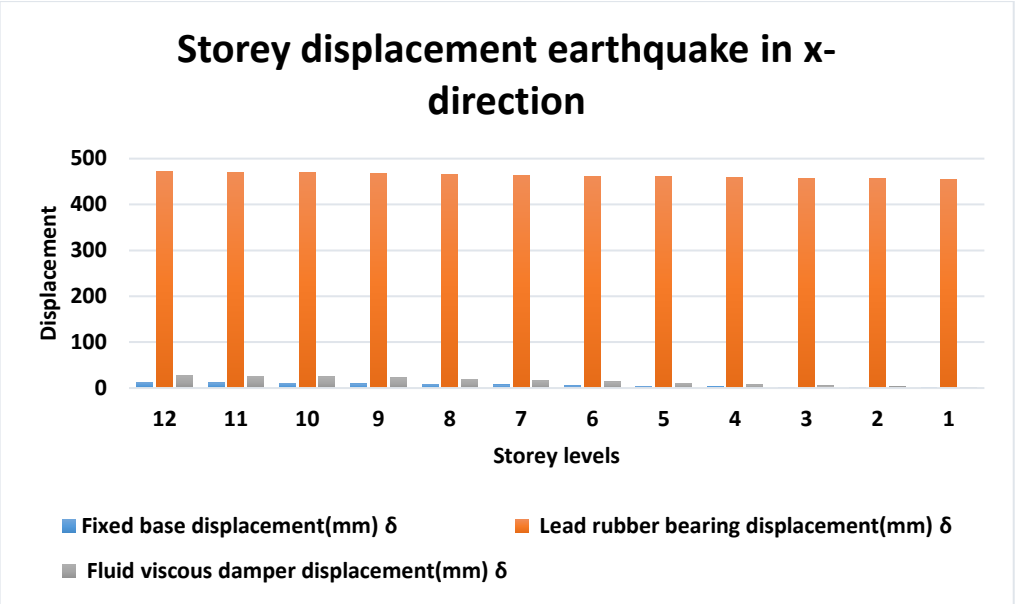

Figure 5. 44 Storey displacement in x-direction due to earthquake conventional structure, (LRBs), and fluid viscous damper.

In the displacement building, it was observed that the building in the x-direction with a fixed base and fluid viscous damper are less relative displacement than the isolated building in general. It is understood that the most significant displacements in the three structures occur on the top floors, and the earthquake effect on these floors is excellent. It was determined that the most considerable displacement was in the lead rubber-bearing building. Therefore, the greater flexibility required to prolong the building's duration will result in significant horizontal motion across the flexible mount. Provides sufficient resistance to the design against service loading. So, lead rubber bearing has a better control effect on displacement shown in figure 5.44 above.

5.20 Storey displacement in y-direction due to earthquake conventional structure, (LRB), and fluid viscous damper.

An earthquake in the y-direction for conventional structure, (LRBs), and fluid viscous damper buildings are used to determine the storey-displacement of different storeys; below is a data table 5.9 with figures.

Table 5. 9 Storey displacement in y-direction due to earthquake fixed base, lead rubber bearing, and fluid viscous damper (FVD).

Storey	H(m)	Fixed base displacement(mm)	Lead rubber bearing displacement(mm)	Fluid viscous damper displacement(mm)
		δ	δ	δ
12	3.5	12.65	471.81	27.38
11	3.5	11.7	470.48	26.18
10	3.5	10.54	468.92	24.37
9	3.5	9.27	467.24	22.04
8	3.5	7.99	465.53	19.49
7	3.5	6.68	463.78	16.63
6	3.5	5.4	462.02	13.58
5	3.5	4.15	460.28	10.48
4	3.5	3.1	458.69	7.4
3	3.5	2.13	457.18	4.69
2	3.5	1.36	455.86	2.58
1	4.5	0.6345	454.56	1.08

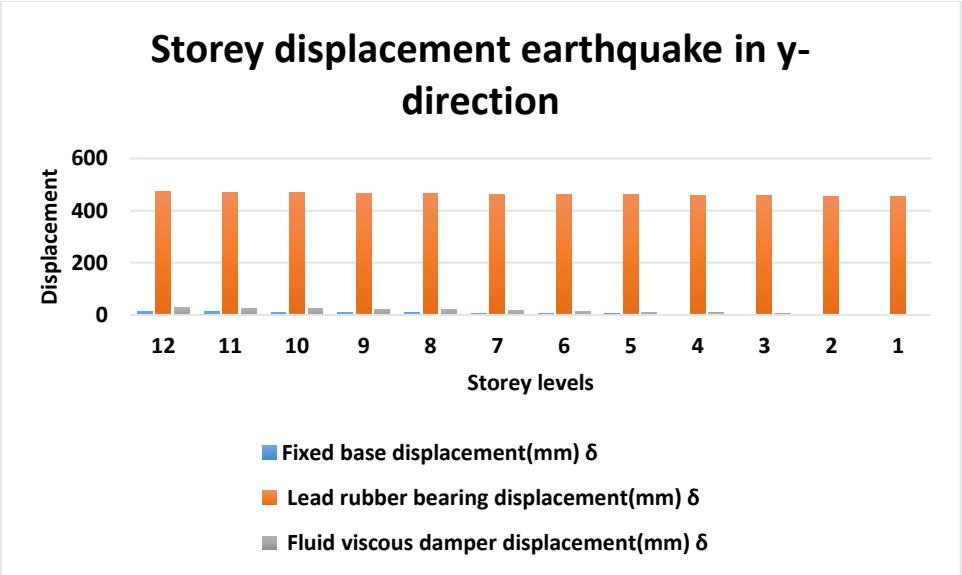

Figure 5. 45 Storey displacement in y-direction due to earthquake fixed base, lead rubber bearing, and fluid viscous damper (FVD).

Storey displacement for the various storeys is determined using the y-direction earthquake. The relative displacement of the fixed base and fluid viscous damper building is smaller than that of the (LRB) building. Therefore, the most significant displacements in the three structures occur in the y-direction of the top floor. In

contrast, the displacements in the y-direction are more effective than the displacements in the x-axis shown in figure 5.45 above.

5.21 Storey drift in the x-direction due to earthquake conventional structure, (LRB), and fluid viscous damper.

The inter-drift of various storeys is analysis for conventional structure, (LRBs), and fluid viscous damper structures utilizing earthquake x-direction; below is a data table 5.10 with figures.

Table 5. 10 Storey-drift in the x-direction due to earthquake conventional structure, lead rubber bearing, and fluid viscous damper.

Storey	H(m)	Fixed base storey drift	Lead rubber bearing storey drift	Fluid viscous damper storey drift
		Δi	Δi	Δi
12	3.5	28.7529	16.9494	27.93523
11	3.5	39.64672	22.72337	38.58832
10	3.5	49.98842	28.13457	48.77546
9	3.5	55.31853	30.92085	54.04906
8	3.5	61.13707	33.96702	59.83095
7	3.5	65.06564	36.05808	63.70673
6	3.5	66.02124	36.68399	64.68097
5	3.5	64.91699	36.40461	63.70673
4	3.5	57.65444	33.64107	56.54819
3	3.5	47.31274	30.93168	46.42458
2	3.5	40.28378	35.25566	39.4143
1	4.5	30.0694981	4398.19374	29.2906927

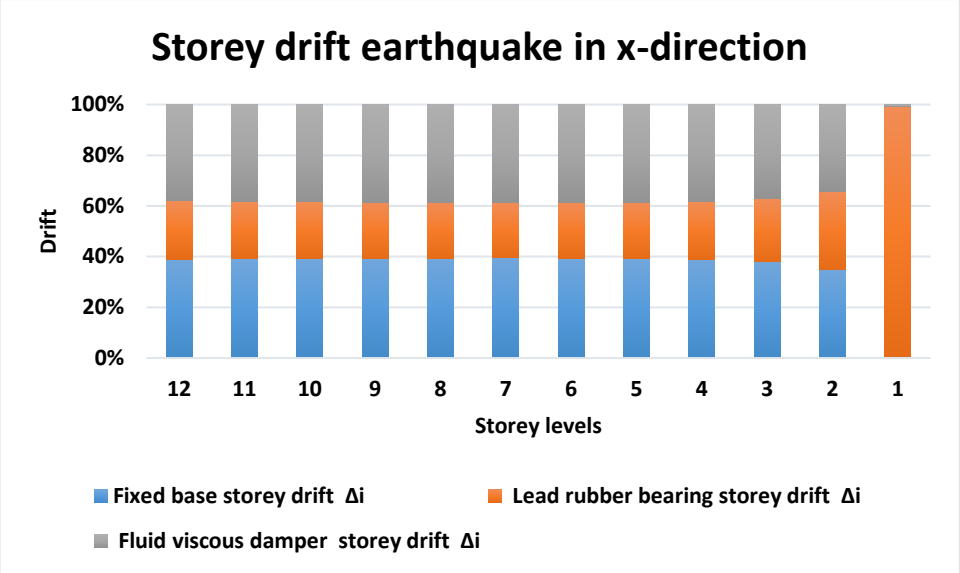

Figure 5. 46 Storey drift in the x-direction due to earthquake conventional structure, (LRB) and (FVD).

The storey drift obtained from the (LRB), fixed base, and (FVD), shows that perhaps the structure integrates lead rubber bearing would raise the inter-drift on the first storey by 93% in the x-axis. Meanwhile, for the fixed-based and fluid viscous damper, there are relative values of both models 5% in the x-axis. Rubber qualities with strong flexibility and damping values produce the comparatively considerable story drift on the (LRB) building on the ground level. The importance between the conventional structure and lead rubber bearing and a fluid viscous damper is shown in the figure 5.46 above.

5.22 Storey drift in the y-direction due to earthquake conventional structure, (LRB), and fluid viscous damper.

The conventional structure, (LRBs), and fluid viscous damper buildings, inter-drift of various storeys is determined using earthquake in the y-direction; figures are given in data table 5.11.

Table 5. 11 Storey drift in the y-direction due to earthquake fixed base, lead rubber bearing, and fluid viscous damper.

Storey	H(m)	Fixed base storey drift	Lead rubber bearing storey drift	Fluid viscous damper storey drift
		Δi	Δi	Δi
12	3.5	1.833977	1.309313	2.310447
11	3.5	2.239382	1.535735	3.484924
10	3.5	2.451737	1.653869	4.486118
9	3.5	2.471042	1.683402	4.9097
8	3.5	2.528958	1.72278	5.506566
7	3.5	2.471042	1.732625	5.872386
6	3.5	2.413127	1.712936	5.968655
5	3.5	2.027027	1.565269	5.930147
4	3.5	1.872587	1.486513	5.21776
3	3.5	1.486486	1.299468	4.062536
2	3.5	1.400579	1.279779	2.888059
1	4.5	1.22490347	447.489663	2.07940236

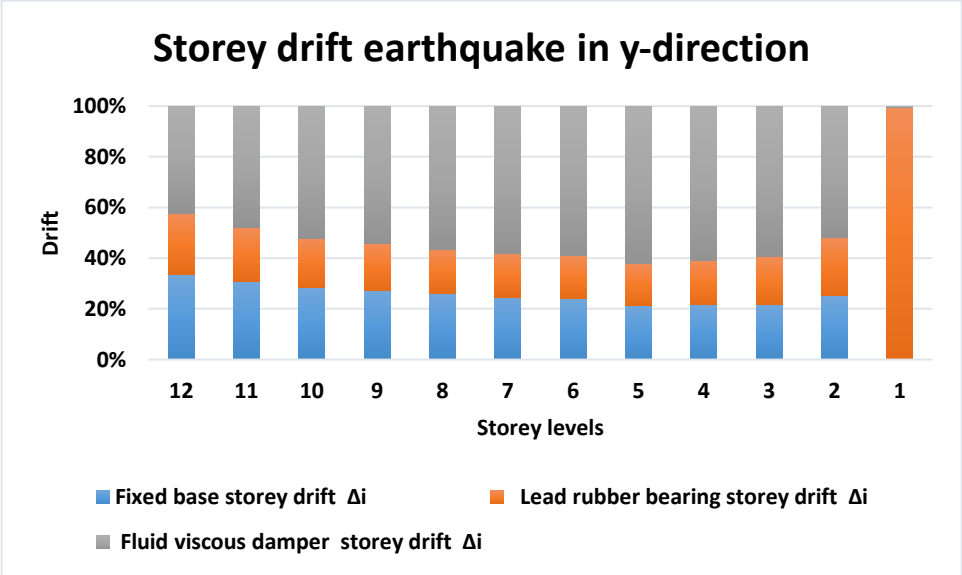

Figure 5. 47 Storey drift in the y-direction due to earthquake conventional strcuture, (LRBs), and (FVD).

The storey drifts determined the (LRB), conventional structure, and (FVD); the system with (LRB), is found to have higher the inter-drift on the first storey by 96% in the y-axis. Meanwhile, for the fixed-based and fluid viscous damper, the values are 5% and 4%. Rubber properties with strong flexibility and absorbing values produce the relatively considerable story-drift on the (LRB) building on the ground level.

Therefore, figure 5.47 shows above, a study of inter-drift between conventional structure, (LRB), and (FVD).

5.23 Time period for the conventional structure, (LRB), and (FVD).

The fundamental time period of different mode shapes is determined using comparing three systems building which are the fixed base, lead rubber bearing, and fluid viscous damper shown in table 5.12 below.

Table 5. 12 Fundamental time period comparing three structures for the conventional structure, (LRB), and (FVD).

Fundamental time period					
OutputCase	StepType	StepNum	Fixed base	Lead rubber bearing	Fluid viscous damper
			Period (Sec)	Period (Sec)	Period (Sec)
MODAL	Mode	1	2.591795	5.079233	2.596913
MODAL	Mode	2	2.495278	5.045302	2.202656
MODAL	Mode	3	1.545349	4.123765	1.421308

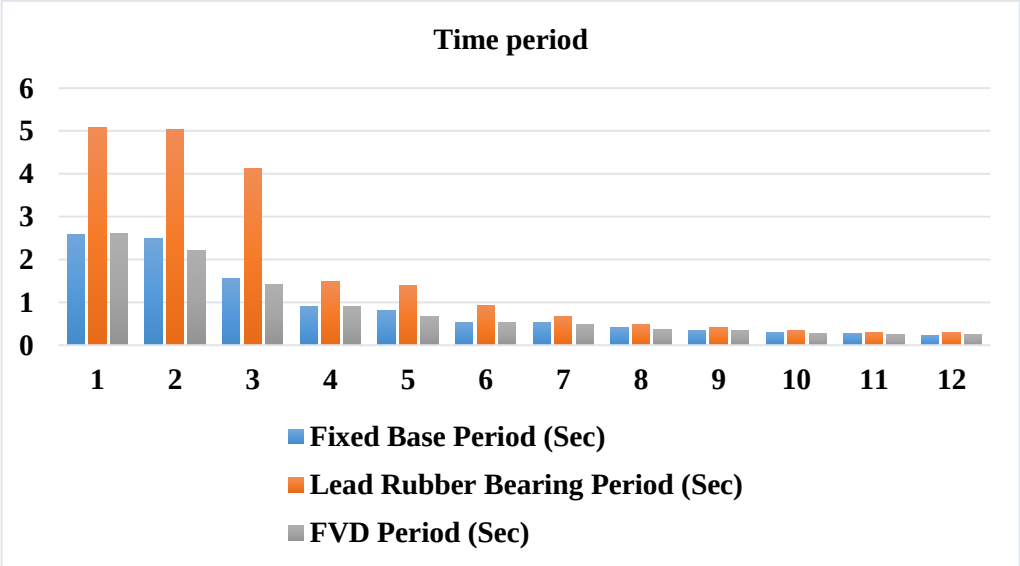

Figure 5. 48 Mode shape for the conventional structure, (LRB), and (FVD).

After the result of the analyses, it was seen that the periods of the lead rubber bearing building are longer than the fixed base and fluid viscous damper building periods. In particular, the first period and second period of the building are determined to be about two times greater than the lead rubber bearing shown in figure 5.48 above.

5.24 Base Shear for the conventional structure, (LRB), and (FVD).

The table-5.13 below shows the variation of the base shear building is determined using earthquake. The base shear value for lead rubber bearing from earthquake analysis is more than the fixed base and fluid viscous damper.

Table 5. 13 Base shear comparing three systems for the earthquake in both directions.

Direction	Fixed base	Lead rubber bearing	Fluid viscous damper
	KN	KN	KN
Earthquake x-direction	18001.833	18254.019	18086.431
Earthquake y-direction	18001.833	18254.018	18086.431

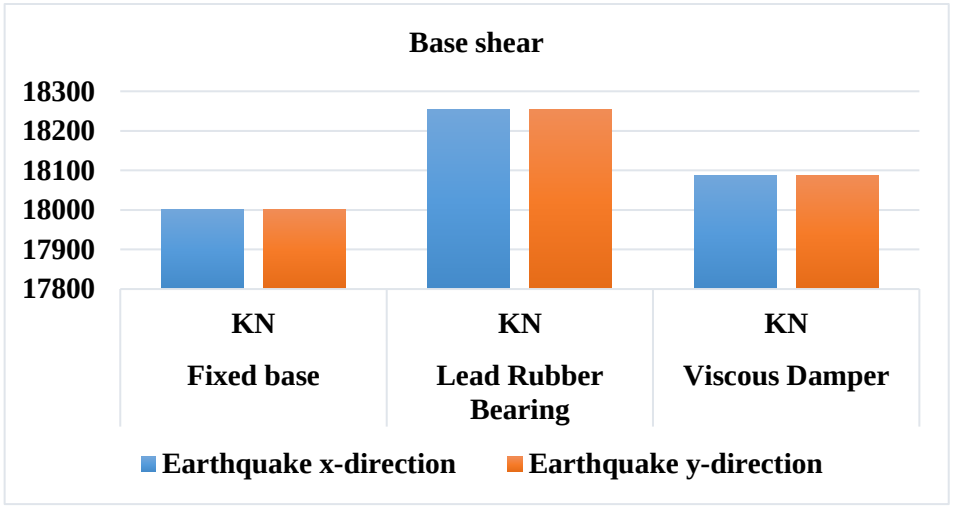

Figure 5. 49 Base shear for the conventional structure, (LRB), and (FVD).

Figure 5.49 above, a building with conventional structure will react to shear as much as a building with a flexible base system when compared with a lead rubber bearing system. The time period shift in the lead rubber bearing will restrict the amount of seismic acceleration delivered to the building. As a result, the building will have much less functional base shear. Because of the varied dynamic response values on

every damper in the (FVD) and (LRBs), various damper framed structures will provide distinct base shear reactions. The fluid viscous damper system structure has the most negligible base shear response. The building with the (LRBs) has a more excellent base-shear response.

5.25 Stiffness models for the conventional structure, (LRB), and (FVD).

The stiffness modal of different levels floors are determined for the conventional structure, (LRB), and fluid viscous damper; as we can see in these different structures models, there is variation stiffness as shown in table 5.14 below.

Table 5. 14 Stiffness models for the fixed base, lead rubber bearing, and fluid viscous damper.

Fixed base	Lead rubber bearing	Fluid viscous damper
Modal stiffness	Modal stiffness	Modal stiffness
KN-m	KN-m	KN-m
5.87704	1.53025	5.8539
6.34048	1.55091	8.13704
16.53128	2.32152	19.54264
48.50986	17.78633	48.27017
61.18379	20.36954	85.49482
141.03889	46.49393	144.51316
145.25121	86.48074	173.86923
225.72781	174.32075	295.18864
337.31374	228.27077	335.69506
458.67677	338.34999	553.11782
489.18288	464.23353	640.43137
696.40978	479.37749	693.00953

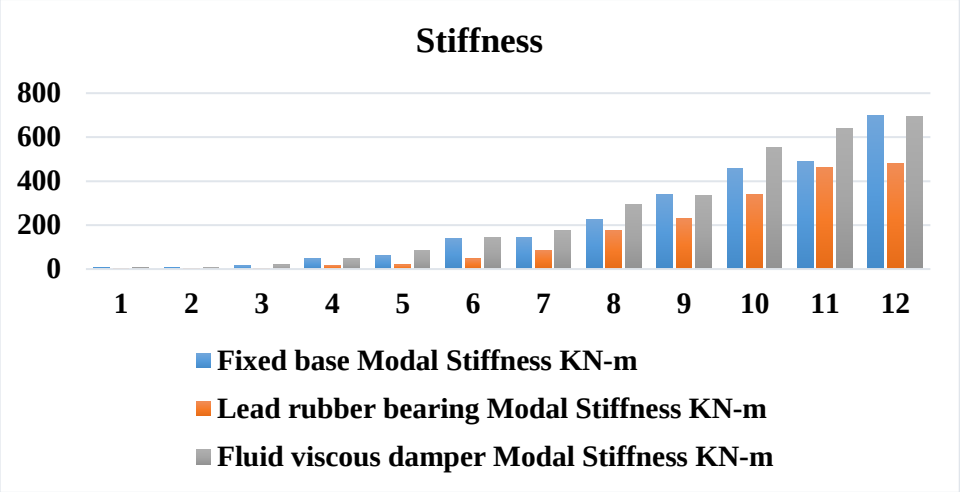

Figure 5. 50 Stiffness models for the fixed base, lead rubber bearing, and fluid viscous damper.

It has been observed that the complexity of the storey of the lead rubber bearing system is a lower value than the fixed base and fluid viscous damper in terms of building length compared to storeys stiffness of the structure shown in figure 5.50 above.

5.26 Comparing results of dampers for building structure systems with lead rubber bearing (LRB) and fluid viscous damper (FVD).

Introduction

Hysteretic systems are created and built to safeguard building integrities, regulate, and avoid building failure by absorption vibration forces and decreasing building deformation. Earthquake absorbers help buildings resist high energy input while limiting detrimental deflection, force, and accelerations to buildings and people. Earthquake dampers are classified into numerous categories. But the case study compared shear, axial force, and displacement for both (LRB), and (FVD).

5.26.1 Storey drift in the x-direction due to earthquake for (LRB) and (FVD).

The earthquake in the x-direction for the (LRBs) and (FVD), structures is used to calculate the inter-drift of different storeys. Table 5.15 is shown below.

Table 5. 15 Storey drift in the x-direction due to earthquake for lead rubber bearing and fluid viscous damper

Storey	H(m)	Lead rubber bearing storey drift	Fluid viscous damper storey drift
		Δi	Δi
12	3.5	16.9494	27.93523
11	3.5	22.72337	38.58832
10	3.5	28.13457	48.77546
9	3.5	30.92085	54.04906
8	3.5	33.96702	59.83095
7	3.5	36.05808	63.70673
6	3.5	36.68399	64.68097
5	3.5	36.40461	63.70673
4	3.5	33.64107	56.54819
3	3.5	30.93168	46.42458
2	3.5	35.25566	39.4143
1	4.5	4398.19374	29.2906927

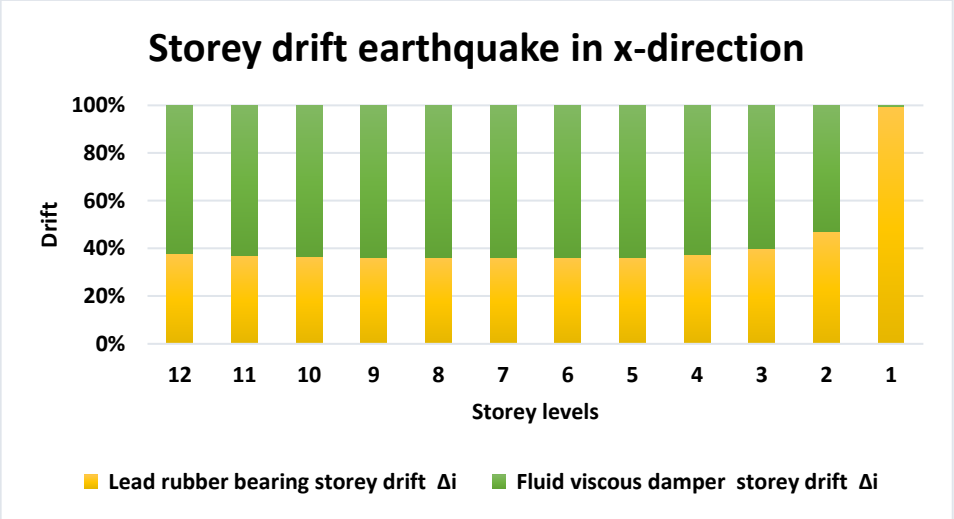

Figure 5. 51 Storey drift in the x-direction due to earthquake (LRB) and (FVD).

The inter-drift of the lead rubber bearing system structure on the first storey increased value 92%. Therefore, the lead rubber bearing is bigger than when compared to fluid viscous damper structure when analyzed of seismic in the x-axis response, as seen in figure 5.51 above.

5.26.2 Storey drift in the y-direction due to earthquake for lead rubber bearing and fluid viscous damper.

Inter-drift of different storeys is determined using earthquake in the y-direction for the lead rubber bearing isolation system and fluid viscous damper buildings shown in table 5.16 below.

Table 5. 16 Storey drift in the y-direction due to earthquake for lead rubber bearing and fluid viscous damper.

Storey	H(m)	Lead Rubber Bearing Storey Drift	Fluid Viscous Damper Storey Drift
		Δi	Δi
12	3.5	1.309313	2.310447
11	3.5	1.535735	3.484924
10	3.5	1.653869	4.486118
9	3.5	1.683402	4.9097
8	3.5	1.72278	5.506566
7	3.5	1.732625	5.872386
6	3.5	1.712936	5.968655
5	3.5	1.565269	5.930147
4	3.5	1.486513	5.21776
3	3.5	1.299468	4.062536
2	3.5	1.279779	2.888059
1	4.5	447.489663	2.07940236

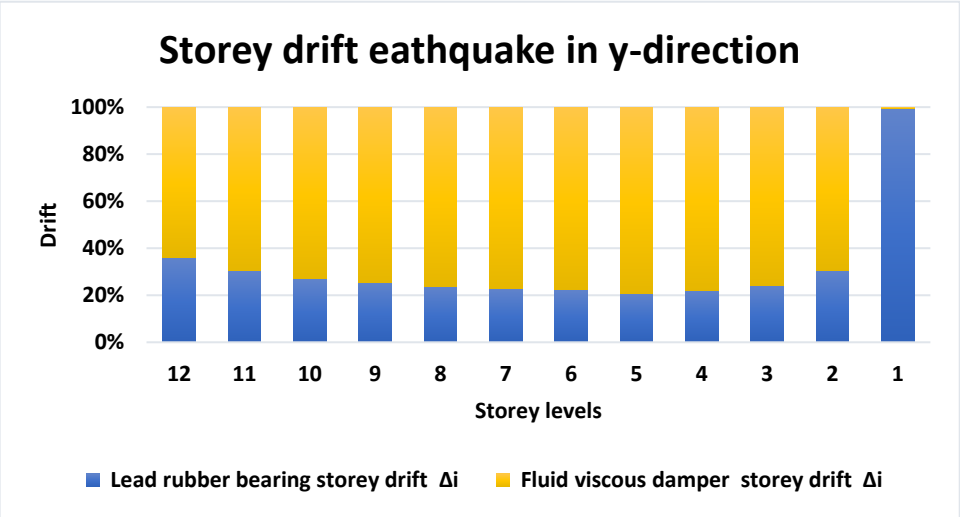

Figure 5. 52 Storey drift in the y-direction due to earthquake for (LRB) and (FVD).

The inter-drift of the lead rubber bearing system structure on the first floor increased the value by 96%. As a result, the lead rubber bearing is larger than the fluid viscous damper structure when analyzed through seismic reaction in the y-axis, as shown in figure 5.52 above.

5.27 Axial-force in the exterior columns for comparing with the lead rubber bearing and fluid viscous damper.

The external-forces acting on the building or frame affect the internal-force with lead rubber bearing system has average greater strength than the steel frame with fluid viscous damper. However, the seismic excitations on structures affect the axial force of the column depending on the component and magnitude of an earthquake. Data table 5.17 with graphs shown below.

Table 5. 17 Axial-force in the exterior columns for comparing with the lead rubber bearing and fluid viscous damper.

Storey	Joints Labels	Frames Labels	Lead rubber bearing axial force (KN)	Fluid viscous damper axial force (KN)
			Exterior column	exterior column
12	637	588-1	199.19	212.76
11	636	587-1	504.29	537.1
10	635	586-1	890.76	948.17
9	616	567-1	1410.98	1502.96
8	615	566-1	2010.84	2142.8
7	614	565-1	2661.03	2837.39
6	595	546-1	3390.98	3617.62
5	594	545-1	4141.11	4418.45
4	593	544-1	4095.41	5221.45
3	574	525-1	5892.32	6214.22
2	573	524-1	7057.91	7181.44
1	572	523-1	8415.314	8004.96

An axial-force is defined as a compression or tension occurring on a frame or a structural part. Tensile-forces are positive; compression forces are negative. The columns are being acted upon by forces of the steel member in the exterior column due to the earthquake with (LRB), and fluid viscous damper.

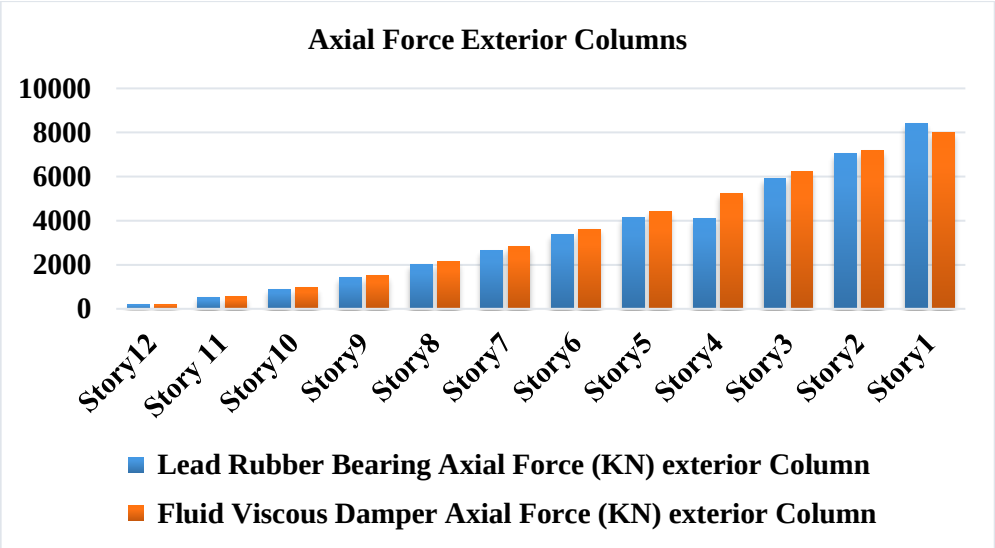

Figure 5. 53 Axial-force in the exterior columns for comparing with the lead rubber bearing and fluid viscous damper.

Figure 5.53 shown above, the axial column force for each floor underground motion with axial force condition. However, the result shows so the external column's axial load on the first floor increases with the lead rubber bearing system has increased value 2% as contrasted to a steel building with fluid viscous damper.

5.28 Axial-force in the interior columns for comparing with the lead rubber bearing and fluid viscous damper.

The interior pressure is determined by the external factors applied load or frame with (LRBs) has almost the same strength ratios as the steel frame with fluid viscous damper. However, the seismic excitations on structures affect the axial force of the column depending on the component and magnitude of an earthquake. Data table-5.18 with graphs are shown below.

Table 5. 18 Axial-force in the interior columns for comparing with the lead rubber bearing and fluid viscous damper.

Storey	Joints Labels	Frames Labels	Lead rubber bearing axial force (KN)	Fluid viscous damper axial force (KN)
			Interior column	Interior column
12	349	321-1	333.82	333.82
11	348	320-1	667.63	667.63
10	347	319-1	1001.45	1001.45
9	328	300-1	1345.31	1345.31
8	327	299-1	1689.16	1689.16
7	326	298-1	2033.01	2033.01
6	307	279-1	2382.2	2382.2
5	306	278-1	2731.4	2731.4
4	305	277-1	3080.59	3080.59
3	281	258-1	3465.68	3465.68
2	280	257-1	3850.68	3850.68
1	279	256-1	4243.77	4243.77

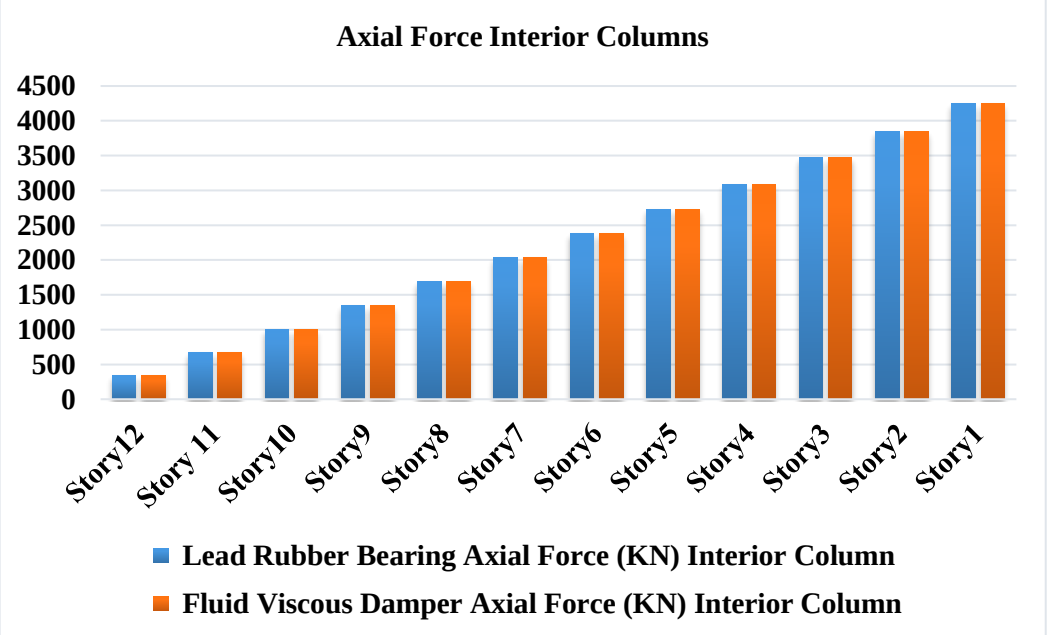

Figure 5. 54 Axial-force in the interior columns for comparing with the lead rubber bearing and fluid viscous damper.

The axial column force for each floor below movement with axial force condition is given in figure 5.54 above. However, the findings indicate that the vertical

force of the interior column it's similar across all levels. There is no difference between the lead rubber bearing system and the steel frame with a fluid viscous damper.

5.28.1 Shear force in the beams for the comparing with the lead rubber bearing and fluid viscous damper.

Table 5.19 shows below, that the shear force of the variation at each of the storeys is determined using special moment frames (in the x-axis), with the (LRB), and fluid viscous damper of the buildings.

Table 5. 19 Shear force in beams for comparing with the lead rubber bearing and fluid viscous damper.

Storey	Diagrams for frame object	Lead rubber bearing shear force (KN)	Fluid viscous damper shear force (KN)
		Beam	Beam
12	1596-W30x148	121.442	134.988
11	1512-W30x148	227.338	246.571
10	1428-W30x148	308.716	333.301
9	1344-W30x173	436.627	471.169
8	1260-W30x173	516.258	556.223
7	1176-W30x173	566.589	610.97
6	1092-W30x191	643.966	694.238
5	1008-W30x191	664.151	714.827
4	924-W30x191	671.877	710.57
3	840-W30x326	887.139	892.971
2	756-W30x326	1052.774	854.389
1	672-W30x326	1232.814	698.917

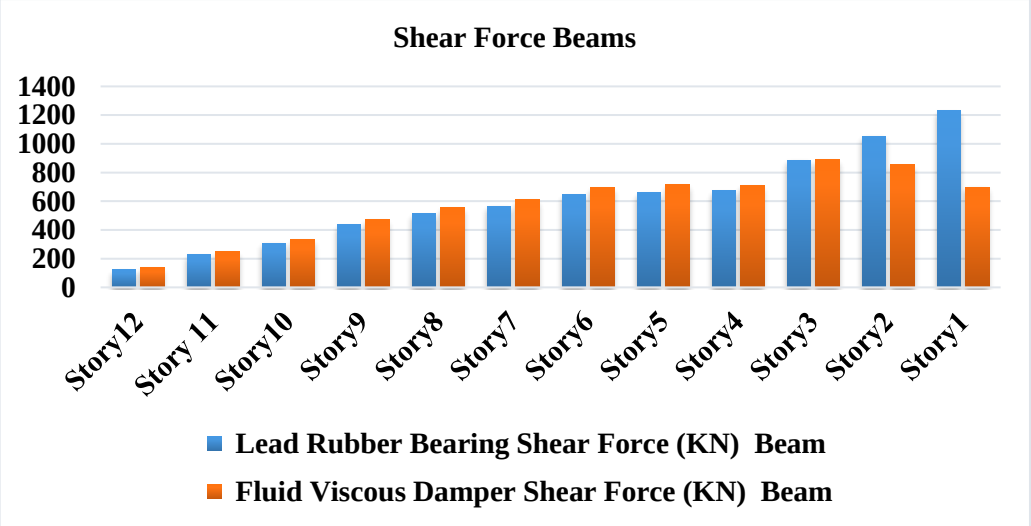

Figure 5. 55 Shear force in the beams for comparing with the(LRB) and (FVD).

The shear-force applies in a diagonal or horizontal axis on a part or frame. The ability to withstand shear forces is required for its design, as is the ability to resist axial forces in Figure 5.55. It demonstrates that installing dampers enhances the member's resilience to the steel member. Therefore, the result indicates that the shear force of the beams on the first floor increases with the lead rubber bearing system has increased value 7% in relation to a steel building with a fluid viscous damper.

5.28.2 Shear force in the exterior column for comparing with the lead rubber bearing and fluid viscous damper.

The earthquake of the special moment frames (in the x-direction) for the (LRBs) and (FVD), of the structures shown in table-5.20 below is used to calculate the shear force in the exterior columns of different at each floor.

Table 5. 20 Shear force exterior column for comparing with the (LRB) and (FVD).

Storey	Diagrams for frame object	Lead rubber bearing shear force (KN)	Fluid viscous damper shear force (KN)
		Exterior column	Exterior column
12	588-W14x311	162.914	193.944
11	587-W14x311	242.724	255.201
10	586-W14x311	351.014	354.69
9	567-W14x398	483.706	487.733
8	566-W14x398	536.865	531.602
7	565-W14x398	605.256	593.986
6	546-W14x426	681.995	670.1
5	545-W14x426	640.946	619.431
4	544-W14x550	876.404	831.798
3	525-W14x550	745.255	715.012
2	524-W14x808	1242.209	915.265
1	523 -W14x808	690.549	567.441

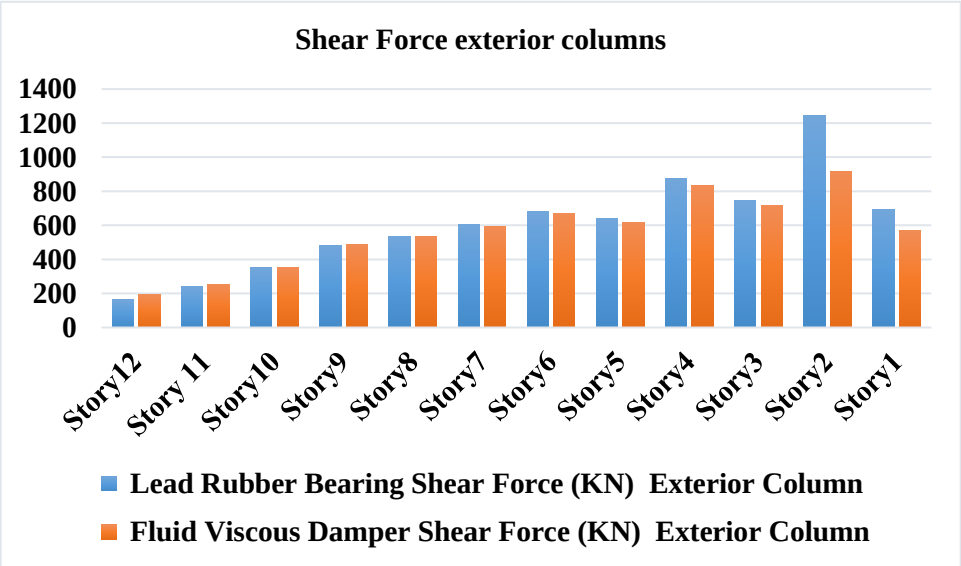

Figure 5. 56 Shear force in the exterior column for comparing with the lead rubber bearing and fluid viscous damper.

Figure 5.56 shown above, the outcome demonstrates which the shear force of the outer columns upon it 1st, 2nd storeys increased with the (LRB), has increased value by 3-5% as compared to the steel frame with fluid viscous damper.

5.28.3 Shear force in the interior column for comparing with the (LRB) and (FVD).

The shear force in the interior columns of specific at each storey is determined by using the earthquake of the special moment frames (in the x-direction) for the lead rubber bearing isolation system and fluid viscous damper of the buildings shown in the table-5.21 below. However, the result demonstrates the effect of the shear force of the internal columns mostly on 2nd storey increases with the lead rubber bearing system has increased value 54% as compared to the steel frame with fluid viscous damper.

Table 5. 21 Shear force in the interior columns for the comparing with the lead rubber bearing and fluid viscous damper.

Storey	Diagrams for frame object	Lead rubber bearing shear force (KN)	Fluid viscous damper shear force (KN)
		Interior column	Interior column
12	327-W14x311	41.291	40.825
11	326-W14x311	6.518	6.562
10	325-W14x311	20.145	19.92
9	306-W14x398	15.053	14.751
8	305-W14x398	11.17	11.3
7	304-W14x398	15.003	15.401
6	285-W14x426	0.045	2.215
5	284-W14x426	32.059	35.662
4	283-W14x550	10.73	29.999
3	264-W14x550	80.151	21.73
2	263-W14x808	203.394	10.531
1	262-W14x808	189.074	214.332

CHAPTER 6

6. CONCLUSION AND RECOMMENDATION

6.1 Conclusion

The comparison study of the three steel project model structures has been conducted designed and analyzed on how they behave against seismic performances when equipped with and without energy dissipation systems.

The fundamental time period of different mode shapes is determined, indicating that the periods of the lead rubber bearing building are larger than the fixed base and fluid viscous damper structures. In particular, the first and second period of the building are determined to be about two times larger than the lead rubber bearing's (LRB). It means that a base isolated structure has a longer time duration than conventional structure, which gives more time for the structure to react during an earthquake.

The storey displacements of the comparison project models, different storeys are calculated using earthquake in the x-direction (SMF) and y-direction (SCBF) structures with conventional structure, with lead-rubber-bearing isolation system (LRB), and with fluid viscous damper. Therefore, the analysis and design for each structural model obtained different displacements. The conventional building and the structure with fluid viscous damper, their values are almost the same percentages of 15% displacement, which occurs on the top storey in the x-axis (SMF), and the bottom storey is 1%. In the y-axis (SCBF) at the top floor ranges from 16-17%. Compared to the lead rubber bearing both directions value, relative same levels displacement occurs at 8% in the x-axis (SMF) and in the y-axis (SCBF) is 8%. However, the displacement at the base isolator (LRB), is less than that at the conventional structure and (FVD),

Because lead rubber bearing in the base isolation has a better control effect on displacement.

When it comes to the storey, drift comparison between different model structures of with lead rubber bearing, fixed base, and with fluid viscous damper, the outcome indicates that the system with lead rubber bearing would raise the bottom storey inter-drift by 92% in the x-axis (SMF) and 95% in the y-axis (SCBF). Meanwhile, for the fixed-based and fluid viscous damper, the values are close, 5% in the x-direction (SMF) and 4% in the y-direction (SCBF). It means that the relatively large storey drift on the ground floor with lead rubber bearing causes excellent flexibility and absorption levels when comparing inter-drift between conventional structure, lead rubber bearing and fluid viscous damper.

In base isolated building with (LRB), storey inter-drift and storey-displacement are decreased to a larger extent due to decreased lateral loads on the structure, and variation in maximum displacement becomes very low against the storeys in base-isolated structures.

The structure with (FVD), inter-drift, storey-acceleration, and storey-displacement to be minimized up to a specific extent due to potential existence of viscous damper's better control effect on displacement.

An axial force tension or compression is used on a cross-section of the structural member. The result is so the exteriors axial force column on the first floor increases 2% as the (LRBs) compared to the steel frame with a fluid viscous damper. On the other hand, the first floor is always the same as the third floor.

The shear reaction force on an element or frame is perpendicular or horizontal. The ability to withstand shear forces is more essential than the ability to resist axial forces in its design. However, the shear force of the variation at each of the storeys is determined using special moment frames (in the x-axis), the (LRBs), and the fluid viscous damper of the structural building. Therefore, the resultant shear force of the beams on the first floor increases 7% as the (LRBs), compared to the steel frame with a fluid viscous damper.

6.2 Recommendation.

It would be very useful to me to conduct more research studies and participate in practical experiments in the future relating to the behaviors of buildings in modern structural design and implement effective techniques to minimize the severity of earthquakes and their tragic and economic consequences. To meet this challenge, I would recommend future structural engineering students in every university have access to a seismic lab possessing earthquake simulator shake tables for seismic design exploratory studies engineering. These devices are equipped of producing motion of the movement of the ground while in a seismic, allowing for control and test of buildings subjected to earthquake. New concepts, techniques, designing, planning, and implementing to all types of seismic isolators will be conducted in the lab by scaling and testing all the structural models in question there in the lab before implementation on actual structures take place. The outcome would be very significant to the students implementing their experiments in a practical manner.

REFERENCES

[1] AISC Committee. "Specification for structural steel buildings (ANSI/AISC 360-10)." *American Institute of Steel Construction, Chicago-Illinois* (2010).

[2] He, Haoxiang, Xiaobing Wang, and Xiaofu Zhang. "Energy-dissipation performance of combined low yield point steel plate damper based on topology optimization and its application in structural control." *Advances in Materials Science and Engineering* 2016 (2016).

[3] Silwal, Baikuntha, Robert J. Michael, and Osman E. Ozbulut. "A superelastic viscous damper for enhanced seismic performance of steel moment frames." *Engineering Structures* 105 (2015): 152-164.

[4] Naeim, Farzad, and James M. Kelly. *Design of seismic isolated structures: from theory to practice*. John Wiley & Sons, 1999.

[5] Taylor, Douglas, and Philippe Duflot. "Fluid viscous dampers used for seismic energy dissipation in structures." *Proceedings of the 12th European Conference on Earthquake Engineering*. 2002.

[6] Taylor, Dauglas P., and Miclhael C. Constantinou. "Fluid dampers for applications of seismic energy dissipation and seismic isolation." *página web www. taylordevices. com/dampers. htm* (1996).

[7] Duflot, Philippe, and Eur Rep. "Fluid Viscous Dampers to reduce Wind-induced Vibrations in Tall Buildings."

[8] Soong, Tsu T., and Michalakis C. Costantinou, eds. *Passive and active structural vibration control in civil engineering*. Vol. 345. Springer, 2014.

[9] Lin, A. N., and H. W. Shenton III. "Seismic performance of fixed-base and base-isolated steel frames." *Journal of engineering mechanics* 118.5 (1992): 921-941.

[10] Cancellara, Donato, Fabio De Angelis, and Mario Pasquino. "A novel seismic base isolation system consisting of a lead rubber bearing in series with a friction

slider. Part I: nonlinear modeling of the system." In Applied Mechanics and Materials, vol. 256, pp. 2185-2192. Trans Tech Publications Ltd, 2013.

[11] Somwanshi, Minal Ashok, and Rina N. Pantawane. "Seismic Analysis of Fixed Based and Base Isolated Building Structures." International Journal of Multidisciplinary and Current Research 3 (2015): 2321-3124.

[12] Win, Nwe Nwe, and Zaw Min Htun. "Seismic Performance Comparison of Fixed Base and Isolated Base Steel Multi-Storey Building." American Scientific Research Journal for Engineering, Technology, and Sciences (ASRJETS) 29.1 (2017): 348-370.

[13] Ras, Abdelouahab, et al. "Dissipative capacity analysis of steel building using viscous bracing device." Fourth International Joint Conference on Advances in Engineering and Technology, AET, NCR, December. 2013.

[14] Miyamoto, H. Kit, and Amir SJ Gilani. "Response of structures with viscous dampers subjected to large earthquakes." *Structures Congress 2013: Bridging Your Passion with Your Profession*. 2013.

[15] Lee, David, and Douglas P. Taylor. "Viscous damper development and future trends." *The Structural Design of Tall Buildings* 10.5 (2001): 311-320.

[16] Chaudhary, Budhi Ram, Suman Devkota, and Gurpreet Singh. "A Review Paper on Comparative Study of Fixed Base, Base Isolation & Damper System in RC Building." (2019).

[17] Code, Uniform Building. "Uniform building code." *International Conference of Building Officials, Whittier, CA*. 1997.

[18] American Society of Civil Engineers (ASCE). "ASCE Standard–ASCE/SEI 7-16: Minimum Design Loads for Buildings and Other Structures." New York: ASCE, 2016.

[19] ASCE. "Minimum design loads for buildings and other structures." American Society of Civil Engineers, 2005.

[20] Oyen, P. E., and J. C. Parker. "Seismic rehabilitation of extreme soft-story school building with friction dampers using the ASCE 41 standard." *Improving the Seismic Performance of Existing Buildings and Other Structures*. 2010. 949-954.

[21] America, C. S. I. "SAP2000 v. 22.1. 0." *Computers & Structures Inc, Berkeley, CA* (2019).

[22] Center, P. E. E. R. "PEER ground motion database." *PEER NGA-West2 Database* 3 (2013).

[23] Symans, M. D., et al. "Energy dissipation systems for seismic applications: current practice and recent developments." *Journal of structural engineering* 134.1 (2008): 3-21.

[24] Heysami, Alireza. "Types of dampers and their seismic performance during an earthquake." *Current world environment* 10.Special-Issue1 (2015): 1002-1015.

[23] Battiato, Lisa A., and Chet E. Robinson. "GEOCON WEST, INC." *APN* 380 (2014): 250-003.

APPENDIX

Appendix A. Design criteria determination

Story Drift Limit (12.2, ASCE 7-10)

U1 Direction:
Risk Category I
Special Moment Frames => A= (0.025) hx
U2 Direction:
Special Concentric Braced Frames =>A-0.025) hx

Seismic Design Manual (AISC 341-05)
Expected Strength / Minimum Strength Ratios (Table 1-6-1, AISC 341-05)
U1 Direction: Special Moment Frames
Moment Frame Girders: A992, Grade 50 => Ry= 1.1, Rt= 1.1
Other Braces (HSS): A992, Grade 50 => Ry= 1.1, Rt= 1.1
U2 Direction: Special Concentrically Braced Frames

Others WF Shapes, WT Shapes: A992, Grade 50 => Ry= 1.4, Rt= 1.3
(Columns and beams)

Appendix B. Response spectrum analysis calculations

Model Response Spectrum Analysis
Combined Model Mass $\geq$ 90% (12.9, ASCE 7-10)

Scaling of Response Spectrum
(U1 Direction, SMF)

R = 8 (Table 12.2-1, ASCE 7-10)

Ω_0 = 3

Cd = 5.5 Risk Category = I => Ie = 1.0 (Table 1.5-2, ASCE 7-10)

FORCE: Divide by R/Ie (12.9.2, ASCE 7-10)

Ie/R = 0.125

DEFELECTION: Divide by R/Ie and Multiply by Cd/Ie

(Ie/R)(Cd/Ie) = (Cd/R) = 0.6875

(U2 Direction, SCBF)

R = 6 (Table 12.2-1, ASCE 7-10)

Ω_0 = 2

Cd = 5 Risk Category = I => Ie = 1.0 (Table 1.5-2, ASCE 7-10)

FORCE: Divide by R/Ie (12.9.2, ASCE 7-10)

Ie/R = 0.1667

DEFELECTION: Divide by R/Ie and Multiply by Cd/Ie

(Ie/R)(Cd/Ie) = (Cd/R) = 0.8333

For Earthquake Design Classes D to F, the Reliability Ratio,

Regarding buildings allocated to Earthquake Design Class D, E, or F, must exceed 1.3 unless one of the two requirements listed below is satisfied, in which case is allowed to be treated as 1.0:

Seismic Load Reduction Factor

(U1- SMF)

R = Response modification factor = **8** Scale Factor = I*g / R

I = Occupancy factor = **1** 1*9.810/8 = **1.22625**

g = Acceleration due to gravity

(U2- SCBF)

R = Response modification factor = **6** Scale Factor = I*g / R

I = Occupancy factor = **1** 1*9.810/6 = **1.635**

g = Acceleration due to gravity

ASCE 7-16

The study must contain a significant set of possible to generate a combined modeling mass participation with a minimum 90% of actual mass within every orthogonal horizontal reaction axis addressed either by system.

Fx or Fy of RS Max >= 0.85 x Calculated base shear (Ex or Ey).

Along x axis = (Rs Max / Ex) x 100 = 85% above

Along y axis = (Rs Max / Ey) x 100 = 85% above

(Rescaling)

(I*g/R) x 0.85 x static base shear / RS base shear

Modal Participating Mass Ration = 90% Above

Base Reaction = 85% above

The Parameters that define the seismic analysis shape are:

- Risk classification **= I** **(ASCE 7-16, Table 1.5-1)**
- Factor of significance, **I = 1** **(ASCE 7-16, Table 1.5-2)**
- Soil Site type **= C** **(ASCE 7-16 Table 11.4-3)**
- Spectral Accel, **Ss = 2.29** **(ASCE 7-16, Table 11.4-2)**
- Spectral Accel, **S_1 = 0.869** **(ASCE 7-16, Table 11.4-2)**
- Long. Trans. Period, **T_L = 8**
- Structure Height, **hn = 43m**
- EarthQ-X Direction Seismic Resist. System = **C1** **(U1-SMF)**
- EarthQ-Y Direction Seismic Resist. System = **B2** **(U2-SCBF)**

(**ASCE 7-16 Table 12.2-1)**

Procedure Calculation:

Coefficient values of Site:

Fa = 1.200 (ASCE 7-16, Table 11.4-1)

Fy = 1.400 (ASCE 7-16, Table 11.4-2)

Maximum (RSA) for short and 1-Second Periods:

SMS = **2.748g** (SMS = Fa* Ss) (ASCE 7-16, Equ 11.4-1)

SM1 = **1.2166g** (SM1 = Fv* S1) (ASCE 7-16, Equ 11.4-2)

Design (RSA) for short and 1-Second Periods:

SDS = **1.832** (SDs = 2/3*SMs) (ASCE 7-16, Equ 11.4-3)

SD1 = **0.8111** (SD1= 2/3*SM1) (ASCE 7-16, Equ 11.4-4)

Fundamental period (Earth Q-X):

Period-Coefficient, **CT** = **0.028** (ASCE 7-16, Table 12.8-2)

Period-Exponent, **X** = **0.80** (ASCE 7-16, Table 12.8-2)

Approx.-Period, **Ta** = **0.56745 sec**, (ASCE 7-16) Ta = CT*hn^(x)

Upper-Limit-Coef, **Cu** = **1.400** (ASCE 7-16, Table 12.8-1)

Period-Max, **T(max)** = **0.79443 sec**, (ASCE 7-16, Table) T(max) = Cu*Ta

Fundament. Period, **T** = **0.56745 sec**, (ASCE 7-16, Table) T = Ta <= Cu*Ta

Fundamental period (Earth Q-Y):

Period-Coefficient, **CT** = **0.030** (ASCE 7-16, Table 12.8-2)

Period-Exponent, **X** = **0.75** (ASCE 7-16, Table 12.8-2)

Approx.-Period, **Ta** = **0.504 sec**, (ASCE 7-16) Ta = CT*hn^(x)

Upper-Limit-Coef, **Cu** = **1.400** (ASCE 7-16, Table 12.8-1)

Period-Max, **T(max)** = **0.706 sec**, (ASCE 7-16, Table) T(max) = Cu*Ta

Fundament-Period, **T** = **0.504 sec**, (ASCE 7-16, Table) T = Ta <= Cu*Ta

Coefficients and parameters for earthquake design:

Response-Mod.-Coef, **EX=R = 8 , EY=R = 6** (ASCE 7-16, Table 12.2-1)

Overstrength-Factor, **EX=Ω = 3 , EY=Ω = 2** (ASCE 7-16, Table 12.2-1)

Defl. Amplification-Factor, **EX=Cd = 5.5 , EY=Cd = 5**
(ASCE 7-16, Table 12.2-1)

Earth Q-X

Cs = **0.229** [Cs = SDs/(R/I),] (ASCE 7-16, Equ 12.8-2)

Cs-(max) = **0.17867** For T<= TL, CS (max) = SD1/(T*(R/I)),

CS-(min) = **0.0543** [CS (min) = 0.5*S1/(R/I),] (ASCE 7-16, Equ 12.8-5)

Use=Cs = **0.17867** **[**Cs (min) <= Cs <= Cs (min)]

Earth Q-Y

Cs = **0.3053** [Cs = SDs/(R/I),] (ASCE 7-16, Equ 12.8-2)

Cs-(max) = **0.2682** For T<= TL, CS (max) = SD1/(T*(R/I)),

CS-(min) = **0.0724** [CS (min) = 0.5*S1/(R/I),] (ASCE 7-16, Equ 12.8-5)

Use=Cs = **0.2682** **[**Cs (min) <= Cs <= Cs (min)]

Earthquake base shear:

Vx = 109919.776 KN, [V = Cs*W =$\sum Fi$,] (ASCE 7-16, Section 12.8-1)

VY =164999.631 KN, [V = Cs*W =$\sum Fi$,] (ASCE 7-16, Section 12.8-1)

Seismic Shear Vertical Distribution:

Distribution Exponent, **k is equal 1.0 k** = 1 for [T<=0.5 sec., k = 2 for T>=2.5 sec].

k = [(2-1)*(T-0.5)/(2.5-0.5)+1, for 0.5 sec. < T < 2.5 sec].

Structure Weight Distribution:		
No. of Seismic Levels =	12	
Seismic Level x	Height, hx (m.)	Weight, Wx (KN)
12	43.000	51541.332
11	39.500	51541.332
10	36.000	51541.332
9	32.500	51541.332
8	29.000	51541.332
7	25.500	51541.332
6	22.000	51541.332
5	18.500	51541.332
4	15.000	51541.332
3	11.500	51541.332
2	8.000	51541.332
1	4.500	51541.332
Total Weight, W= $\sum wx$=		618495.98

Assign Area Section two way
Dead = 4.5 KN/m
Live = 2 KN/m

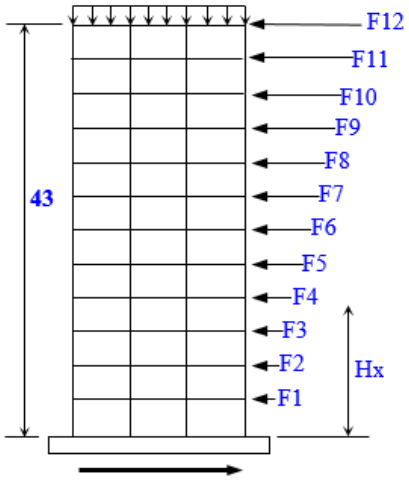

VX = Cs*W = $\sum Fi$ = **109919.776 KN**

VY = Cs*W = $\sum Fi$ = **164999.631 KN**

Lateral Force at Any Level: Fx = Cvx*Vx, (**ASCE 7-16 Section 12.8.3, Eqn. 12.8-11**)

Lateral Force at Any Level: FY = Cvx*Vy, (**ASCE 7-16 Section 12.8.3, Eqn. 12.8-11**)

Vertical Distribution Factor: C_{vx} = Wx*h^k/(ΣWx *h_{i^k}),

(**ASCE 7-16 Section 12.8.3, Eqn. 12.8-12**)

Seismic Level x	Weight, Wx (KN)	hx^k (m.)	Wx*h^k (m-KN)	Cvx (%)	Shear, Fx (KN)	Shear, Fy (KN)
12	51262.096	43	2204270.128	0.150866 2	1381.1762 1	24892.8631 5
11	51263.096	39.5	2024892.29	0.138589	1268.6799	22867.1459
10	51264.096	36	1845507.45	0.126311	1156.1310	20841.3496
9	51265.096	32.5	1666115.62	0.114033	1043.5294	18815.4743
8	51266.096	29	1486716.78	0.101754	931.87525	16789.5200
7	51267.096	25.5	1307310.94	0.089475	819.16835	14763.4866
6	51268.096	22	1127898.11	0.077196	706.40879	12737.3742
5	51269.096	18.5	948478.276	0.064917	594.59658	10711.1826
4	51270.096	15	769051.44	0.052636	481.73169	8684.91208
3	51271.096	11.5	589617.604	0.040355	369.81415	6658.56246
2	51272.096	8	410176.768	0.028074	256.84394	4632.13379
1	51273.096	4.5	230728.932	0.015792	144.82107	2605.62608
Σ =	615211.15		14610764.3	1	109919.77	164999.631

Structure Story Deflections: EarthQ-X		
	No. of Seismic Levels =	12

Seismic Level x	Height (m), hx	Deflect. (m) δxe	Allowable Drift, δa	Drift Check (δxe <= δa)
12	43.000	0.0581	0.0875	O.K.
11	39.500	0.0556	0.0875	O.K.
10	36.000	0.0522	0.0875	O.K.
9	32.500	0.0476	0.0875	O.K.
8	29.000	0.0425	0.0875	O.K.
7	25.500	0.0367	0.0875	O.K.
6	22.000	0.0306	0.0875	O.K.
5	18.500	0.0246	0.0875	O.K.
4	15.000	0.0184	0.0875	O.K.
3	11.500	0.0125	0.0875	O.K.
2	8.000	0.0075	0.0875	O.K.
1	4.500	0.0032	0.1125	O.K.

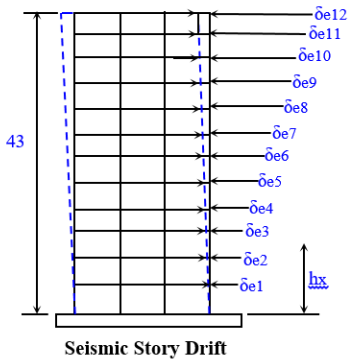

Seismic Story Drift

Amplified Elastic Story Deflection: **$\delta_x = \delta_{xe} * C_d / I$**, ASCE 7-10 Eqn. 12.8-15, page 92

Amplified Story Drift: **$\Delta x = \delta x - \delta(x-1)$,** ASCE 7-10 Figure 12.8-2, page 93

Allowable Story Drift: **$\Delta a = 0.025 h_{sx} / \rho$ (m)** ASCE 7-10 Table 12.12-1

Story Height: **hsx = hx - h(x-1)**

Where:

Cd = 5.5 Steel special moment frames (SMF)

Ie = 1.0 buildings with risk category I.

ρ = 1.0

Seismic Level x	Story Height hsx (m.)	Amplified Deflect., δx (m.)	Amplified Drift, Δx (m.)	Amplified Drift Ratio Δx/(hsx*12)	Allowable Drift, Δa (m.)	Allowable Drift Ratio Δa/(hsx*12)
12	3.50	0.31955	0.01375	0.0003273	0.0875	0.0020833
11	3.50	0.3058	0.0187	0.0004452	0.0875	0.0020833
10	3.50	0.2871	0.0253	0.0006023	0.0875	0.0020833
9	3.50	0.2618	0.02805	0.0006678	0.0875	0.0020833
8	3.50	0.23375	0.0319	0.0007595	0.0875	0.0020833
7	3.50	0.20185	0.03355	0.0007988	0.0875	0.0020833
6	3.50	0.1683	0.033	0.0007857	0.0875	0.0020833
5	3.50	0.1353	0.0341	0.0008119	0.0875	0.0020833
4	3.50	0.1012	0.03245	0.0007726	0.0875	0.0020833
3	3.50	0.06875	0.0275	0.0006547	0.0875	0.0020833
2	3.50	0.04125	0.02365	0.0005630	0.0875	0.0020833
1	4.50	0.0176	0.0176	0.0003259	0.1125	0.0020833

Where:

Cd = 5 Steel special concentrically braced frames (SCBF)

Ie = 1.0 buildings with risk category I.

ρ = 1.0

Structure Story Deflections: EarthQ-Y		
	No. of Seismic Levels =	12

Seismic Level x	Height (m), hx	Deflect.(m) δxe	Allowable Drift, Δa	Drift Check (δxe <= Δa)
12	43.000	0.0041	0.0875	O.K.
11	39.500	0.0039	0.0875	O.K.
10	36.000	0.0036	0.0875	O.K.
9	32.500	0.0032	0.0875	O.K.
8	29.000	0.0028	0.0875	O.K.
7	25.500	0.0024	0.0875	O.K.
6	22.000	0.0021	0.0875	O.K.
5	18.500	0.0017	0.0875	O.K.
4	15.000	0.0013	0.0875	O.K.
3	11.500	0.001	0.0875	O.K.
2	8.000	0.0006	0.0875	O.K.
1	4.500	0.0003	0.1125	O.K.

Seismic Level x	Story Height hsx	Amplified Deflect., δx	Amplified Drift, Δx	Amplified Drift Ratio	Allowable Drift, Δa	Allowable Drift Ratio
	(m.)	(m.)	(m.)	Δx/(hsx*12)	(m.)	Δa/(hsx*12)
12	3.50	0.0205	0.001	2.38095E-05	0.0875	0.002083333
11	3.50	0.0195	0.0015	3.57143E-05	0.0875	0.002083333
10	3.50	0.018	0.002	4.7619E-05	0.0875	0.002083333
9	3.50	0.016	0.002	4.7619E-05	0.0875	0.002083333
8	3.50	0.014	0.002	4.7619E-05	0.0875	0.002083333
7	3.50	0.012	0.0015	3.57143E-05	0.0875	0.002083333
6	3.50	0.0105	0.002	4.7619E-05	0.0875	0.002083333
5	3.50	0.0085	0.002	4.7619E-05	0.0875	0.002083333
4	3.50	0.0065	0.0015	3.57143E-05	0.0875	0.002083333
3	3.50	0.005	0.002	4.7619E-05	0.0875	0.002083333
2	3.50	0.003	0.0015	3.57143E-05	0.0875	0.002083333
1	4.50	0.0015	0.0015	2.778E-05	0.1125	0.002083

Appendix C. ASCE 7-05 wind-load calculations

Wind Properties.

Two main wind directions: **θ = 0º and θ = 90º.**

The **Basic Design Wind Speed, V (mph)**, corresponds to a 3-second gust speed at 33' above ground in Exposure Category "C" and is associated with an annual probability of 0.02 of being equaled or exceeded (50-year mean recurrence interval).

1. Wind Coefficients.

- Wind Speed = **70 mph**
- Exposure Type = **C**
- Importance Factor = **1**
- Topographical Factor, Kzt = **1**
- Gust Factor = **0.85**
- Directionality Factor, Kd = **0.85**

Surface Roughness Categories for the purpose of assigning **Exposure Category** are defined as follows:
Surface Roughness "B":
Urban and suburban areas, wooded areas or other terrain with numerous closely spaced obstructions having the size of single family dwellings or larger.
Surface Roughness "C":
Open terrain with scattered obstructions having heights generally < 30 ft. This category includes flat open country, grass lands, and all water surfaces in hurricane prone regions.
Surface Roughness "D":
Flat, unobstructed areas and water surfaces outside hurricane prone regions. This category includes smooth mud flats, salt flats, and unbroken ice.

Exposure Categories are defined as follows:
Exposure "B":
Exposure B shall apply where the ground surface roughness condition, as defined by Surface Roughness B, prevails in the upwind direction for a distance of at least 2600 ft. or 20 times the building height, whichever is greater.
Exception: For buildings whose mean roof height <= 30 ft., the upwind distance may be reduced to 1500 ft.
Exposure "C":
Exposure C shall apply for all cases where exposures B and D do not apply.
Exposure "D":
Exposure D shall apply where the ground surface roughness, as defined by Surface Roughness D, prevails in the upwind direction for a distance >= 5,000 ft. or 20 times the building height, whichever is greater. Exposure D shall extend into downwind areas of Surface Roughness B or C for a distance of 600 ft. or 20 times the height of the building, whichever is greater.

2. Exposure and Pressure Coefficients

- Exposure from Extents of Rigid Diaphragm

3. Wind Exposure Parameters

- Wind Direction Angles
- Windward Coeff, Cp = **0.8**
- Leeward Coeff, Cp = **0.5**
- Case **(ASCE 7-05 Fig. 6-9) = select create all cases.**
- E1 Ration **(ASCE 7-05 Fig. 6-9).**
- E2 Ration **(ASCE 7-05 Fig. 6-9).**

If the structure is "rigid", then the minimum of either the calculated value of 'G' for "rigid" structures or 0.85 is used. If the structure is "flexible" then the calculated value of 'G' is used.

Wind Directionality Factor, Kd (Table 6-4)

Structure Type	Kd
Buildings	
Main Wind-Force Resisting System	0.85
Components and Cladding	0.85

Note: this factor shall only be applied when used in conjunction with load combinations specified in Sect. 2.3 and 2.4. Otherwise, use Kd = 1.0.

The **Topographic Factor, Kzt**, accounts for effect of wind speed-up over isolated hills and escarpments (**Sect. 6.5.7** and **Fig. 6-4**).
Kzt = (1+K1*K2*K3)^2 (Eq. 6-3), where:
H = height of hill or escarpment relative to the upwind terrain, in feet.
Lh = Distance upwind of crest to where the difference in ground elevation is half the height of hill or escarpment, in feet.
K1 = factor to account for shape of topographic feature and maximum speed-up effect.
K2 = factor to account for reduction in speed-up with distance upwind or downwind of crest.
K3 = factor to account for reduction in speed-up with height above local terrain.
x = distance (upwind or downwind) from the crest to the building site, in feet.
z = height above local ground level, in feet.
The effect of wind speed-up shall not be required to be considered (Kzt = 1.0) when H/Lh < 0.2, or H < 15' for Exposures 'C' and 'D', or H < 60' for Exposure 'B'.

Structures which have a natural frequency, f >= 1 Hz are considered "rigid".
Structures which have a natural frequency, f < 1 Hz are considered "flexible".

Determination of Gust Effect Factor, G:

Structures which have a natural frequency, f >= 1 Hz are considered "rigid".
Structures which have a natural frequency, f < 1 Hz are considered "flexible".

Flexible? No f >=1 Hz.

1: Simplified Method for Rigid Structure

The **Gust Effect Factor, G**, for rigid structures may be simply taken as **0.85** for all structure exposure conditions.

G = **0.85**

Parameters Used in Both Item #2 and Item #3 Calculations (from Table 6-2):

a^ = **0.105**

b^ = **1.00**

a(bar) = **0.154**

b(bar) = **0.65**

c = **0.20**

l = **500** ft.

e(bar) = **0.200**

z(min) = **15** ft.

Terrain Exposure Constants (Table 6-2)

Exposure	α	zg(ft)	α^	b^	α(bar)	b(bar)	c	l (ft)	ε	z(min)
B	7.0	1200	1/7	0.84	1/4.0	0.45	0.30	320	1/3.0	30
C	9.5	900	1/9.5	1.00	1/6.5	0.65	0.20	500	1/5.0	15
D	11.5	700	1/11.5	1.07	1/9.0	0.80	0.15	650	1/8.0	7

Note: z(min) = minimum height used to ensure that the equivalent height z(bar) is greater of 0.6*h or z(min). For buildings with h<= z(min), z(bar) shall be taken as z(min).

Calculated Parameters Used in Both Rigid and/or Flexible Structure Calculations:

z(bar) = **84.60** = 0.6*h , but not < z(min) , ft.

Iz(bar) = **0.171** = c*(33/z(bar))^(1/6) , Eq. 6-5

Lz(bar) = **603.59** = l*(z(bar)/33)^(e(bar)) , Eq. 6-7

gq = **3.4** (3.4, per Sect. 6.5.8.1)

gv = **3.4** (3.4, per Sect. 6.5.8.1)

gr = **4.237** = (2*(LN(3600*f)))^(1/2)+0.577/(2*LN(3600*f))^(1/2) , Eq. 6-9

Q = **0.846** = (1/(1+0.63*((B+h)/Lz(bar))^0.63))^(1/2) , Eq. 6-6

2: Calculation of G for Rigid Structure

G = **0.854** = 0.925*((1+1.7*gq*Iz(bar)*Q)/(1+1.7*gv*Iz(bar))) , Eq. 6-4

3: Calculation of Gf for Flexible Structure

The **Gust Effect Factor, Gf**, for a flexible structure as calculated from Eqn 6-8. Note: calculations below are applicable only for "flexible" structures which have a natural frequency, f < 1 hz.

b = **0.050** Damping Ratio

Ct = **0.020** Period Coefficient

T = **0.818** = Ct*h^(3/4) , sec. (Period)

f = **1.222** = 1/T , Hz. (Natural Frequency)

Appendix D. Lead rubber bearing calculations

Parameters seismic properties of the subject structure according to UBC-97

Seismic Source Type	C	TABLE 16-U
Seismic Zone Coefficient, (Z)	0.3	TABLE 16-I
Distance to Known Source Fault (km)	5km	TABLE 16-S
Soil Profile Type	Sc	TABLE 16-J
Near Fault Coefficient, (NA)	1	TABLE 16-S
Near Fault Coefficient, (NV)	1	TABLE 16-T
Seismic Coefficient, (CA)	0.33	TABLE 16-Q
Seismic Coefficient, (CV)	0.45	TABLE 16-R
MCE Behavior Coefficient, (MM)	1.5	TABLE A-16-D
Effective Damping Bd or Bm (10%)	1.2	TABLE 16-C

- **Numerical Application :**

Maximum Vertical Load Column Support, W = 4243.78 KN

Natural vibration period of the structure: 2.60 s

$T_D \geq 3 \times T_{ENCASTRE} = 3 * 2.60 = 7.8$, $T_D = 4.0$ s Selected

- **Lead rubber bearing system**

Calculation of effective horizontal stiffness

$D_D = (g \times CvD \times T_D) / (B_D \times 4\pi^2) = (9.81*0.33*4) / (1.2*4\pi^2) = 0.2734$

(Percentage of damping 10%)

$D_m = (g \times C_{VM} \times T_M)/(B_M \times 4\pi^2) = (9.81*0.45*4) / (1.2*4\pi^2) = 0.3727$

(Percentage of damping 10%)

Effective stiffness of the isolator

$K_H = K_{eff} = (W/g) \times [(2\pi / T_D)]^2 = (4243.78 /9.81) * (2\pi / 4)^2 = 1067.39$ KN/m

Energy dissipated per cycle at the specified displacement (Wd)

$W_D = 2\pi \times K_{eff} \times (d_D)^2 \times \beta_{eff} = (2\pi)*(1067.39)*(0.2734)^2*(0.01) = 5.01$ KNm

Force at zero displacement under cyclic loading

$Q_D = W_D / (4 \times d_D) = (5.01) / (4*0.2734) = 4.58$ KNm

Post yield stiffness of the isolator

$K_d = Keff - (Qd / d_d) = 1067.39 - (4.58 / 0.2734) = 1050.64$ KN/m

- **Yield displacement**

$D_y = Q_d / (9 \times K_d) = 4.58 / (9*1050.64) = 4.8436E\text{-}4$ m

- **Yield force**

$F_y = (K_U \times K_d)$

$K_U = 10 \times K_d$

Fy = 10 x 1050.64 x 4.8436E-4

Fy = 5.088 kN

- **Maximum force**

$Fm = QD + Kd\ d_D$

Fm = 4.58 + 1050.64 x 0.2734

Fm = 291.825 kN

Ku = Fy / Dy = 5.088 / 4.8436E-4

Ku = 10504.58 kN/m

- **Check for Keff**

$Keff = Fm / d_D = 291.825 / 0.2734 = 1067.39$ KN/m

- **Rigidity main core of (LRB).**

$K_{pb} = Q_d / d_D = 4.58 / 0.2734 = 16.75$ KN

- **Stiffness of rubber in lead rubber bearing**

$K_{rub} = K_d = K_H - K_{pb} = 1067.39 - 16.75 = 1050.64$

- **Total thickness of lead rubber bearing**

$tr = d_D / \Upsilon = 0.2734 / 0.5 = 0.5468$ m

Where Υ is the design shear strain which is 0.5 (as per T.K. Dutta).

- **Diameter of lead rubber bearing**

$$D_{bearing} = \sqrt{\frac{Krtr}{400\pi}} = \sqrt{\frac{1050.64\ x\ 0.5468}{400\pi}} = 0.67614\ m$$

Where,

$D_{bearing}$ = Diameter of (LRB)

tr= Total (LRB) thickness.

- **Calculation of totally ultimate load (AL).**
- **D_{pb}= LRB's lead core dimension**

$$Dpb = \sqrt{\frac{4Qd}{\pi\sigma pb}} = \sqrt{\frac{4x4.58}{\pi x11000}} = 0.023025\ m$$

Where,

σpb = It is estimated that the total yield stress in lead is 11 pa.

- **LRB Lead core zone**

$$Apb = \frac{\pi}{4} x\ (Dpb)^2 = \frac{\pi}{4} x\ (0.023025\ )^2 = 4.16379E - 4\ m^2$$

- **Diameter of Force Free Section**

$D_{ff} = D_{bearing} - 2t = 0.67614 - 2x0.01 = 0.65614\ m$

Where t is the single layer thickness which is 0.01 m

- **Force Free Area**

$A_{ff} = \frac{\pi}{4} x\ (Dff)^2 = \frac{\pi}{4} x\ (0.65614)^2 = 0.338129\ m$

- **Totally Loaded surface Area**

AL = Force-free zone – Lead-core zone

$AL = 0.338129\ - 4.16379E - 4\ = 0.337713\ m^2$

- **Forece-Free Zone Diameter**

$C_f = [\pi\ t\ D_{ff}\ ] = [\pi\ x\ 0.01\ x\ 0.65614\ ] = 0.02061$ m

- **Shap-Factor**

$$Si = \frac{\text{Load Area}}{\text{Circumference of force free}} = \frac{0.337713}{0.02061} = 16.38588$$

- **Total Height of Lear Rubber Bearing**

Height = (Num x t) + (Num-1)ts + 2tap

$\text{Number} = \frac{0.2}{t} = \frac{0.2}{0.01} = 20$

Height = (20 x 0.01) + (20-1) 0.003 + 2 x 0.04 = 0.337 m

Where, The number-rubber-layer

t is the single-layer-thickness which is 0.01 m

ts is the thickness of steel lamination which is 0.003m

tap is the laminated anchor plate thickness which is 0.04 m

- **Lateral Rigidity Bearing**

$$K_b = \left[\frac{G\ Ar}{H}\right] = [\frac{1000\ x\ 0.337713}{0.337}] = 1002.116\ KN/m$$

Shear-Modulus (G), (ranging between 0.4 and 1.1 Mpa) Using 1 Mpa

Rubber-Layer-Area (Ar) = 0.337713 m2

Height of LRB = 0.337 m

Vertical Overall Bearing

$$Kv = \frac{6GSi^2 Ar\ K}{(6GSi^2+K)H} = \frac{6x1000x11^2x\ 0.337713\ \ x\ 2000x10^3}{(6x1000x11^2+\ 2000x10^3)x0.337} =$$

$$533.775\ E3\ KN/m$$

The main isolator parameters used in the building are specified in the table

Rotary Limitation 1	1 KN/m
U1 – Effective-Stiffness (kN/m)	1067391.17
U2 – Effective-Stiffness (kN/m)	1067.39
U2 – Stiffness (kN/m)	1050.64
U2 – Yield Strength (kN)	5.088
U2 – Distance from End-J	4.8436E-4
U2 – Post Yield Stiffness Ratio (Kd/Ku)	0.1
U3 – Effective stiffness (kN/m)	1067.39
U3 – Stiffness (kN/m)	1050.64
U3 – Yield Strength (kN)	5.088
U3– Distance from End-J	4.8436E-4
U3 – Post Yield Stiffness Ratio (Kd/Ku)	0.1

Rubber isolator parameters to be used in the subject structure.

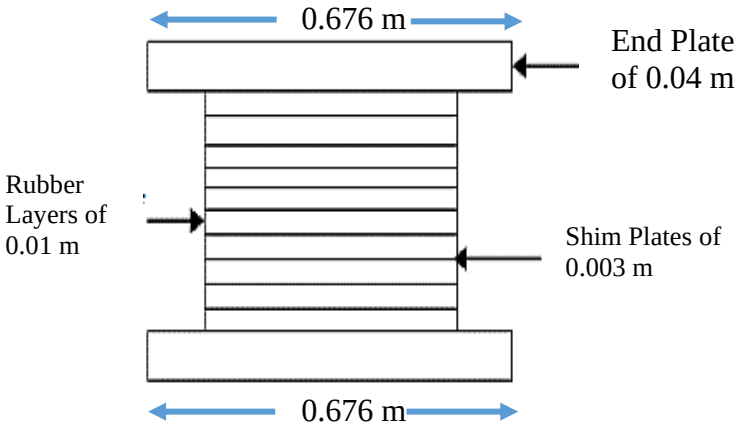

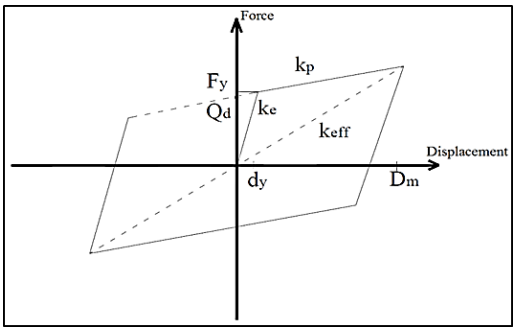

Appendix E. Fluid viscous damper calculations

1) Ratio of successive Displacement

$$X1/X2 = \ 0.12834/0.12285 = 1.0447 \qquad (3\text{-}26)$$

2) Logarithmic Decrement

$$\delta = \ln\left(\frac{X1}{X2}\right) = (1.0447) = 0.0437$$

$$\xi = \delta/\sqrt{((2\pi)\text{^}2\ )} = \ 0.0437/\sqrt{((2\pi)\text{^}2 + 0.0437)} = 0.00695$$

$$Wd = 2\pi/Td = \ 2\pi/0.2s = 31.42\ rad/s$$

$$Wd\ = Wn\sqrt{1-(\xi)^2}$$

$$Wn = Wd/\sqrt{(1-(\xi)\text{^}2\ )}\ = 31.42/\sqrt{(1-(0.00695)\text{^}2\ )} = 31.42\ rad/s$$

$$Wn = \ Wd$$

$$Wn = \sqrt{(K/m)} \quad K = (Wn)\text{^}2.m\ = (31.42)\text{^}2.5225.5 = 5158.699\ E3\ KN/m$$

$$\xi = C/Cc \qquad\qquad C = \ \xi cc = \ \xi 2\sqrt{Km}$$

$$= (0.00695)x2\sqrt{((5158.699\ E3)(5225.5)\ )} = 2282.17\ (KN.s)/m$$

The result properties of fluid viscous damper

A damper is a component that is attached to a building to lessen its earthquake effect. In Sap2000 the (FVD), element is assigned to the structure in the form of V or V inverse like chevron bracing throughout the height of the structure at two sides Central of the structure.

Stiffness	5158.699 E3 KNm
Damping-Coefficient	2282.17 (KN. s)m
Velocity-Exponent	0.3

Appendix F. Nominal compressive strength members design

1st floor Columns connection with brace member size:

Select: W14x808

Member Properties:		
A	0.152903	m^2
d	0.57912	m
bf	0.47244	m
tw	0.094996	m
tf	0.130048	m
rt	0.13081	m
d/Af	0.24	
lx	0.00665970448093	m^4
sx	0.022942	m^3
rx	0.20828	m
ly	0.0022934351573	m^4
sy	0.009734	m^3
ry	0.122428	m
j	0.00076586582384	m^4
cw	10998.2	m^6
K_{des}	0.145034	m
K1	0.0635	m

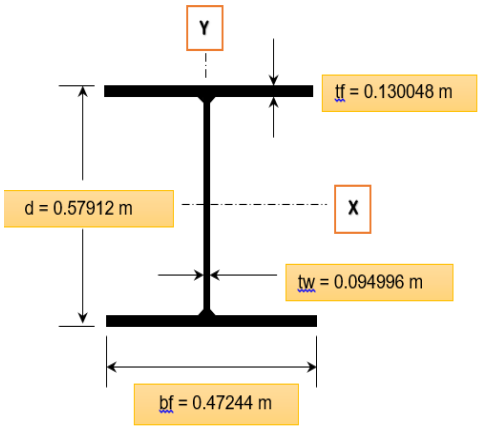

Table Summarize of Results Ground floor checking column brace					
Axial Compression		X-axis Bending		Y-axis Bending	
Kx*Lx/rx	14.043595	Lc	1.933084 m	fby	1.5952332 KN/m
Ky*Ly/ry	23.891594	Lu	241.545893 m	Fby	258.75 KN
Cc	106.9720	Lb/rt	34.40	Mry	0.209889 KNm
fa	16569.00126 KN	fbx	0.00 KN	X-axis Euler Stress	
Fa	12.5294045 KN	Fbx	0.997578 KNm	F'ex	36.26302724 KN/m
Pa	1.915784 KN/m	Mrx	0.022886 KNm	Y-axis Euler Stress	
Stress Ratio		S.R.	1.33	F'ey	12.5294044 KN/m

Column Section: W14x500

Member Properties:		
A	0.0948385	m^2
d	0.49784	m
bf	0.4318	m
tw	0.055626	m
tf	0.0889	m
rt	0.120142	m
d/Af	0.33	
sx	0.0137324	m^3
rx	0.189992	m
sy	0.00555521	m^3
ry	0.112522	m
j	0.000213942952964	m^4
cw	4749.8	m^6
K_{des}	0.10414	m
K1	0.0587375	m

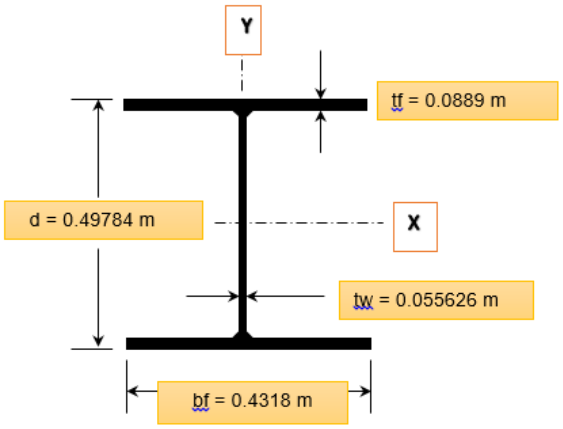

Table Summarize of Results floors checking column brace					
Axial Compression		X-axis Bending		Y-axis Bending	
Kx*Lx/rx	11.9742	Lc	1.766797 m.	fby	2.79521386 KN/m
Ky*Ly/ry	20.218268	Lu	175.669741 m	Fby	258.75 KN
Cc	107.00	Lb/rt	29.13219	Mry	0.1197842 KNm
fa	26713.30736 KN	fbx	0.00 KN	X-axis Euler Stress	
Fa	17.495789 KN	Fbx	1.39104 KNm	F'ex	49.880234 KN/m
Pa	1.6592744 KN/m	Mrx	1.592E-3 KNm	Y-axis Euler Stress	
Stress Ratio		S.R.	1.52	F'ey	17.495757 KN/m

Column Section: W14x426

Member Properties:		
A	0.080645	m^2
d	0.47498	m
bf	0.42418	m
tw	0.047752	m
tf	0.077216	m
rt	0.117856	m
d/Af	0.37	
sx	0.0115693	m^3
rx	0.184404	m
sy	0.00463754	m^3
ry	0.110236	m
j	0.000137772602006	m^4
cw	3657.6	m^6
K_{des}	0.092202	m
K1	0.053975	m

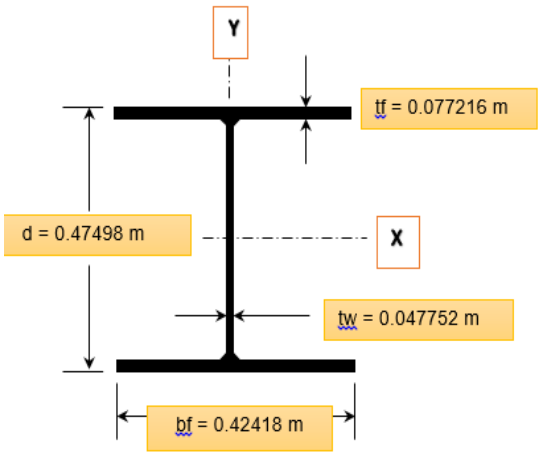

Column Section: W14x311

Table Summarize of Results floors checking column brace					
Axial Compression		X-axis Bending		Y-axis Bending	
Kx*Lx/rx	12.33704	Lc	1.735618 m.	fby	3.3483269 KN/m
Ky*Ly/ry	20.63754	Lu	156.6784 m.	Fby	258.75 KN
Cc	107.00	Lb/rt	29.697257	Mry	0.0999996 KNm
fa	31414.8428 KN	fbx	0.00 KN	X-axis Euler Stress	
Fa	16.792157 KN	Fbx	1.338609 KNm	F'ex	46.9892519 KN/m
Pa	1.3542035 KN/m	Mrx	1.291E-3 KNm	Y-axis Euler Stress	
Stress Ratio		S.R.	1.80	F'ey	16.792089 KN/m

Member Properties:		
A	0.05896762	m^2
d	0.43434	m
bf	0.41148	m
tw	0.035814	m
tf	0.057404	m
rt	0.1143	m
d/Af	0.47	
sx	0.00829185	m^3
rx	0.174752	m
sy	0.00326103	m^3
ry	0.10668	m
j	0.000056607473936	m^4
cw	2258.06	m^6
K_{des}	0.072644	m
K1	0.0492125	m

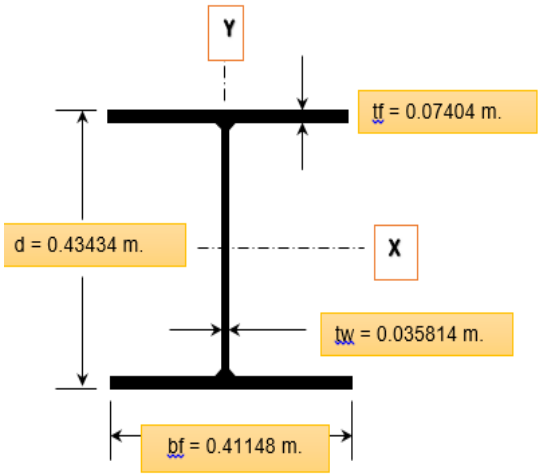

This Table Summarize of Results floors checking column brace					
Axial Compression		X-axis Bending		Y-axis Bending	
Kx*Lx/rx	13.01845	Lc	1.683654 m.	fby	4.7616857 KN/m
Ky*Ly/ry	21.325459	Lu	123.3426 m.	Fby	258.75 KN
Cc	107.00	Lb/rt	30.62117	Mry	0.070315959 KNm
fa	42963.40941 KN	fbx	0.00 KN	X-axis Euler Stress	
Fa	15.72620422 KN	Fbx	1.259049 KNm	F'ex	42.1990007 KN/m
Pa	0.9273368 KN/m	Mrx	8.699E-4 KNm	Y-axis Euler Stress	
Stress Ratio		S.R.	2.70	F'ey	15.72620277 KN/m

Table 5. 9th, 10th and 11th floor checking column

CURRICULUM VITAE

Publications

[1]https://www.researchgate.net/publication/349831081_Carsharing_system_and_its_impact_to_the_environment/stats